# Review of Hot-Wire Anemometry Techniques and the Range of their Applicability for Various Flows

**P.C. Stainback**
*Distingushied Research Associate*
*NASA Langley Research Center*
*Hampton, VA 23681*

**and**

**K.A. Nagabushana**†
*Research Associate*
*Old Dominion University Research Foundation*
*Norfolk, VA 23508*

## ABSTRACT

**A review of hot-wire anemometry was made to present examples of past work done in the field and to describe some of the recent and important developments in this extensive and ever expanding field. The review considered the flow regimes and flow fields in which measurements were made, including both mean flow and fluctuating measurements. Examples of hot-wire measurements made in the various flow regimes and flow fields are presented. Comments are made concerning the constant current and constant temperature anemometers generally in use and the recently developed constant voltage anemometer. Examples of hot-wire data obtained to substantiate theoretical results are presented. Some results are presented to compare hot-wire data with results obtained using other techniques. The review was limited to wires mounted normal to the flow in non-mixing gases.**

## NOMENCLATURE

| | |
|---|---|
| $a_1 - a_4$ | **constants in equation (47)** |
| $a$ | **speed of sound** |
| $A, B$ | **constants in equation (24)** |
| $A_1 - A_3$ | **constants in equation (18)** |
| $b_1 - b_3$ | **order of $q$ in equation (47)** |
| $B_1 - B_5$ | **constants in equation (19)** |
| $A'(T_o)$ | $Lk_t$ |
| $A'_w$ | **overheat parameter** $\frac{1}{2}\left(\partial \log R_w / \partial \log I\right)_h$ |
| $B'(T_o)$ | $2L\sqrt{\pi k_t c_p r_w}$ |
| $c_p$ | **specific heat at constant pressure** |
| $c_v$ | **specific heat at constant volume** |
| $c_w$ | **specific heat of wire** |
| $d$ | **wire diameter of mesh** |
| $d(\ )/dt$ | **rate of change of quantity ( ) with respect to time** |
| $d_c$ | **diameter of cylinder** |
| $d_i$ | **diameter of jet** |
| $d_w$ | **diameter of wire** |
| $e'$ | **instantaneous voltage across the wire** |
| $E$ | **mean voltage across the wire** |
| $E_{out}$ | **anemometer output voltage** |
| $E'$ | **finite-circuit parameter** $(1 - e)/(1 + 2A'_w e)$ |
| $f$ | **frequency** |

† **Currently Engineer at Computer Science Corporation, Laurel, MD 20707**
**Also, Consulting Research Engineer at Advanced Engineering, Yorktown, VA 23693**

$F$ dimensionless frequency

$F_{11}$ true one-dimensional spectral density

$F_M$ measured one-dimensional spectral density

$F_{trf}$ turbulence reduction factor

$Gr$ Grashof Number

$h$ coefficient of heat transfer

$h_w$ height above wire shock generator to probe

$h_{w,s}$ height above shock generator, immediate postshock value

$I$ current

$k$ thermal conductivity of air evaluated at subscript temperature

$k_1$ wave number in the flow direction

$Kn$ Knudsen number

$L$ characteristic length

$m$ mean mass flow

$m_t$ $\P \log m_t / \P \log T_o$

$M$ Mach number

$M_m$ mesh size

$n$ exponent for mass flow in equations (16) & (17)

$n_t$ $\P \log k_t / \P \log T_o$

$Nu$ Nusselt number evaluated at subscript temperature

$p$ mean static pressure

$p_o$ mean total pressure

$P$ electrical power to the hot-wire

$Pr$ Prandtl number

$q$ sensitivity ratio, $S_u / S_{T_o}$

$q_\infty$ dynamic pressure

$Q$ forced convective heat transfer

$r$ sensitivity ratio, $S_m / S_{T_o}$

$r_d$ radial distance in cylinderical polar co-ordinate

$r_p$ distance of virtual source of jet from origin

$r_w$ radius of wire

$r'$ $r_p - r_d$

$R$ resistance

$Re$ Reynolds number based on viscosity evaluated at subscript temperature and wire diameter

$R_{mT_o}$ mass flow - total temperature correlation coefficient, $\overline{m' T_o'} / \tilde{m} \tilde{T}_o$

$R_{uT_o}$ velocity - total temperature correlation coefficient, $\overline{u' T_o'} / \tilde{u} \tilde{T}_o$

$R_{rT_o}$ density - total temperature correlation coefficient, $\overline{r' T_o'} / \tilde{r} \tilde{T}_o$

$R_{ur}$ velocity - density correlation coefficient, $\overline{u' r'} / \tilde{u} \tilde{r}$

$R_{xx}$ normalized auto-correlation function

$s$ sensitivity ratio, $S_r / S_{T_o}$

$S$ sensitivity of hot-wire to the subscript variable

$t$ time

$T$ temperature

$T_f$ $(T_w + T_o)/2$

$u,v,w$ velocity in $X$, $y$ and $Z$ directions respectively

$u_t$ frictional velocity

$x$ distance in the flow direction

$x_o$ virtual origin of the wake

$x_w$ distance along the length of wire

$y$ distance normal to the flow direction

$a$ $\left(1 + \frac{g-1}{2} M^2\right)^{-1}$

$a_1$ linear temperature - resistance coefficient of wire

$b$ $a(g-1)M^2$

$b_1$ second degree temperature - resistance coefficient of wire

$d$ boundary layer thickness

$d^*$ displacement thickness for Blasius flow

$e$ finite circuit factor, $(\P \log I_w / \P \log R_w)_s$

$e_f$ finite circuit factor with fluid conditions held constant while the hot-wire conditions change, $\partial \log I_w / \partial \log R_w$

$h_y$ transformed co-ordinate distance normal to body

$h$ recovery temperature ratio, $T_{adw} / T_o$

$q$ temperature parameter, $T_w / T_o$

$q_1$ angle between plane sound wave and axis of probe

$l$ mean free path

$m$ absolute viscosity

$g$ specific heat ratio, $c_p / c_v$

$r$ density

$t$ time lag

$t_w$ temperature loading parameter, $(T_w - T_{adw})/T_o$

$t_{wr}$ temperature parameter, $(T_w - T_{adw})/T_{adw}$

$t_{wall}$ shear stress at the wall

$f'$ normalized fluctuation voltage ratio, $\left(e'/E\right) / S_{T_o}$

**Subscript**

| | |
|---|---|
| *adw* | adiabatic wall condition |
| *adw,c* | adiabatic wall temperature, continuum flow condition |
| *adw,f* | adiabatic wall temperature, free molecular flow condition |
| *B* | due to buoyancy effect |
| *C* | constant current anemometer |
| *e* | edge condition |
| *eff* | effective velocity |
| *f* | film condition |
| *h* | $M$ and $Re_t$ are constant as $Q$ varied |
| *o* | total condition |
| *ref* | reference condition |
| *s* | electrical system untouched as $M$ and $Re_t$ varied |
| *s* | sound source |
| *sc* | settling chamber |
| *t* | evaluated at total temperature |
| *T* | constant temperate anemometer |
| *w* | wire condition |
| ∞ | free stream or static condition |

**Superscript**

| | |
|---|---|
| ' | instantaneous |
| ~ | RMS |
| ¯ | mean |

## INTRODUCTION

Comte-Bellot[1] noted that the precise origin of hot-wire anemometry cannot be accurately determined. One of the earlier studies of heat transfer from a heated wire was made by Boussinesq[2] in 1905. The results obtained by Boussinesq were extended by King[3] and he attempted to experimentally verify his theoretical results. These earlier investigations of hot-wire anemometry considered only the mean heat transfer characteristics from heated wires. The first quantitative measurements of fluctuations in subsonic incompressible flows were made in 1929 by Dryden and Kuethe[4] using constant current anemometry where the frequency response of the wire was extended by the use of a compensating amplifier. In 1934 Ziegler[5] developed a constant temperature anemometer for measuring fluctuations by using a feedback amplifier to maintain a constant wire temperature up to a given frequency.

In the 1950's, Kovasznay[6,7] extended hot-wire anemometry to compressible flows where it was found experimentally that in supersonic flow the heated wire was sensitive only to mass flow and total temperature. Kovasznay developed a graphical technique to obtain these fluctuations, which is mostly used in supersonic flow. In subsonic compressible flows the heat transfer from a wire is a function of velocity, density, total temperature, and wire temperature. Because of this complexity, these flow regimes were largely bypassed until the 1970's and 1980's when attempts were made to develop methods applicable[8] for these flows. In recent years there were several new and promising developments in hot-wire anemometry that can be attributed to advances in electronics, data acquisition/reduction methods and new developments in basic anemometry techniques.

Previous reviews, survey reports, and conference proceedings on hot-wire anemometry are included in references 1,9-20. Several books[21-24] have been published on hot-wire anemometry and chapters[25-30] have been included in books where the general subject matter was related to anemometry.

This review considers the development of hot-wire anemometry from the earliest consideration of heat transfer from heated wires to the present. Although mean flow measurements are considered, the major portion of the review addresses the measurement of fluctuation quantities. Examples of some of the more important studies are addressed for wires mounted normal to the flow in non-mixing gases. The present review attempts to bring the development of hot-wire anemometry up to date and note some of the important, recent developments in this extensive and ever expanding field.

## FLOW REGIMES AND FLOW FIELDS

Based on the applicable heat transfer laws and suitable approximations, hot-wire anemometry

can be conveniently divided into the following flow regimes:

1. Subsonic incompressible flow
2. Subsonic compressible, transonic, and low supersonic flows
3. High supersonic and hypersonic flows

Within each of these major flow regimes are the following sub-regimes:

1. Continuum flow
2. Slip flow
3. Free molecular flow

In subsonic incompressible flow the heat transfer from a wire is a function of mass flow, total temperature and wire temperature. Since density variations are assumed to be zero, the mass flow variations reduce to velocity changes only. The non-dimensional heat transfer parameter, the Nusselt number, is usually assumed to be a function of Reynolds and Prandtl numbers and under most flow conditions the Prandtl number is constant. Evidence exist which indicate that $Nu_t$ is also a function of a temperature parameter[6]. In subsonic compressible, transonic and low supersonic flows the effects of compressibility influence the heat transfer from a wire. For these conditions the heat transfer from the wire is a $f(u, r, T_o, T_w)$ and $Nu_t = f(Re_t, M, q)$. In high supersonic and hypersonic flows a strong shock occurs ahead of the wire and the heat transfer from the wire is influenced by subsonic flow downstream of the shock. Because of this, it was found experimentally that $Nu_t = f(Re_t, q)$ only, and the heat transfer from the wire is again a function of mass flow, total temperature, and wire temperature.

In continuum flow the mean free path of the particles is very much less than the diameter of the wire and conventional heat transfer theories are applicable. Where the diameter of the wire approaches a few mean free paths between the particles, the flow does not behave as a continuum, but exhibits some effects of the finite spacing between the particles. These effects have been studied[31,32] by assuming a finite velocity and a temperature jump at the surface of a body. This gas rarefaction regime was noted as slip flow. In free molecular flow the fluid is assumed to be composed of individual particles and the distance between the particles is sufficiently large that their impact with and reflection from a body is assumed to occur without interaction between the particles. Free molecular flow is theoretically studied[33] using the concepts of kinetic theory[34].

Figure 1 presents a plot of Mach number vs. Reynolds number for lines of constant Knudsen number where $d_w$ = 0.00015 inch and for flow conditions where $1.5 \leq p_o$, psia $\leq 150$. Baldwin noted[35] that the continuum flow regime existed for $Kn < 0.001$ and slip flow conditions existed for $0.001 \leq Kn \leq 2.0$. Other references suggest that slip flow conditions were attained only for $Kn > 0.01$. Even using the larger value of $Kn$ for the slip flow boundary, (i.e., $Kn > 0.01$) a 0.00015 inch wire operated at low Mach numbers and at atmospheric conditions is near the slip flow boundary. If the total pressure is decreased or the wire diameter reduced, the value of $Kn$ would be shifted farther into the slip flow regime. Free molecular flow conditions are generally assumed to exist for $Kn > 2.0$. Figure 1 can be used to delineate approximate values for $M$ and $Re_t$ for the various sub-regimes.

Various applications of hot-wire anemometry and the approximate level of velocity functuations are:

| Types of Flows | Approximate[29] $\tilde{u}/u$ |
|---|---|
| 1. Freestream of wind tunnels[36,37] | 0.05% |
| 2. Down stream of screens and grids[25,38] | 0.20 - 2.00 % |
| 3. Boundary layers[39-42] | 3.0 - 20.0 % |
| 4. Wakes[43,44] | 2.0 - 5.0 % |
| 5. Jets[45-47] | Over 20.0 % |
| 6. Flow downstream of shocks[48] | |
| 7. Flight in Atmosphere[49] | |
| 8. Rotating Machinery[50,51] | |
| 9. Miscellaneous[52-56] | |

## TYPES OF ANEMOMETERS

The two types of anemometers primarily used are the constant current anemometer (CCA) and the constant temperature anemometer (CTA).

A constant voltage anemometer (CVA) is presently under development[57]. Even though these three anemometers are described as maintaining a given variable "*constant*", none of these strictly accomplish this. The degree of non-constancy for the CCA is determined by the finite impedance of its circuit[58]. The constancy of the mean wire temperature for a CTA at high frequencies is limited by the rate at which the feedback amplifier can detect and respond to rapid fluctuations in the flow. The CVA maintains the voltage across the wire and leads constant rather than across the wire[57]. The non-constancy effects in the CCA and the CVA can be accounted for by calibration of the CCA[58] and by knowing the lead resistance in the CVA.

The heat balance for an electrically heated wire, neglecting conduction and radiation is:

*Heat Stored = Electrical Power In - Aerodynamic Heat Transfer Out*

$$\frac{dc_w}{dt} T_w = P - Q \qquad (1)$$

$$\frac{dc_w}{dt} T_w = I^2 R_w - p\, L d_w h\left(T_w - T_{adw}\right) \qquad (2)$$

If the heat storage term is properly compensated, then equation (2) becomes:

$$I^2 R_w = p\, L d_w h\left(T_w - T_{adw}\right) \qquad (3)$$

The measurement of fluctuations in a flow requires a sensor, in this case a wire, with a time response up to a sufficiently high frequency. The time constant of even small wires are limited and the amplitude response of these wires at higher frequencies decreases with frequency. Therefore, some type of compensation must be made for the wire output. There are two methods for accomplishing this. Earlier approaches utilized a constant current anemometer with a compensating amplifier that had an increase in gain as the frequency increased[4]. An example of the roll off in the frequency of the wire, the gain of the amplifier and the resulting signal is shown schematically in figure 2. In principle, the output from the wire can be compensated to infinite frequencies. However, as the frequency increases, the noise output from the compensating amplifier will equal and ultimately exceed the wire output, which limits the gain that can be obtained. A schematic diagram of a CCA is presented in figure 3.

The constant temperature anemometer uses a feedback amplifier to maintain the average wire temperature and wire resistance constant {i.e., $dT_w/dt = 0$ in equation (2)}, within the capability of the amplifier. The practical upper frequency limit for a CTA is the frequency at which the feedback amplifier becomes unstable. A schematic diagram of a CTA is presented in figure 4. A third anemometer, presently under development[57], is the constant voltage anemometer. This anemometer is based on the alterations of an operational amplifier circuit and does not have a bridge circuit. A schematic diagram of a CVA is presented in figure 5.

The upper frequency response of a CCA is generally accepted to be higher than that of a CTA. There is some evidence that the frequency response of the CVA might equal or exceed that of the CCA. The fluctuation diagram technique described by Kovasznay is usually used with a CCA to obtain data at supersonic speeds. This technique depends on the sensitivity of the wire being a function of wire temperature or overheat and the frequency response of the wire being assessable to compensation to almost zero overheat. This technique has limited application for a CTA, since at low overheats, the frequency response of the anemometer approaches the frequency response of the wire[25].

An example of the difference between the fluctuation diagrams obtained[59] using a CTA and a CCA is presented in figure 6. The intersection of the diagram with the vertical axis at $S_{ru}/S_{T_o} = 0$ represents the total temperature fluctuation and the data show that the CTA cannot be used to measure these fluctuations. The reason for this is illustrated in figure 7a where the total temperature spectra at low overheats for the two anemometers are presented. In these cases the spectrum obtained with the CTA was attenuated at a frequency that was about two orders of magnitude less than for the CCA. At high overheats the two mass flow spectra were more nearly equivalent (figure 7b). However, in reference 60 the output of a laser was modulated and used to heat a wire to

check the frequency response of a CTA. It was shown that the frequency response was essentially unchanged down to an overheat of 0.07.

The CTA can be used to make measurements in supersonic flows by using two wires. For these flows the CTA is operated with two wires having different but high overheats, digitizing the voltages and using two equations to obtain $m'$, $T_o'$ and $m'T_o'$ as a function of time[61]. Then statistical techniques can be used to obtain quantities of interest. In general, the CTA is more suitable for measuring higher levels of fluctuations than a CCA[25]. It remains to be determined how the CVA will compare with the CCA and CTA. At present it appears that the CVA has a higher signal to noise ratio than either CCA or CTA. Additional advantages and disadvantages of the CCA versus the CTA are described in references 1, 29, 57, 62 and 63.

At low speeds a linearizer is often used to convert the non-linear relationship between wire voltage and velocity to a linear relationship. There are two types of linearizers in use; the logarithmic and the polynomial. A linearizer makes it possible to directly relate the measured voltage to the velocity. However, the linearization process does not result in better measured quantities[25].

## LIMITATIONS OF HOT-WIRE ANEMOMETRY

Most of the data obtained using hot-wire anemometry is limited to small perturbations. There are cases, however, where this linearization of the anemometry equation is not accurate and non-linear effects can influence both the mean[47] and fluctuating[25] voltages. Since high level fluctuations can influence the mean voltage measured across the heated wire, it is important to calibrate probes in flows with low levels of fluctuations.

Because of the mass associated with the wire supports, there can be a significant amount of heat loss from the wire due to conduction to the relatively cold supports. This heat loss results in a spanwise temperature distribution along the wire that, in turn, causes a variation of heat transfer from the wire[12,21,64] along its length. In order to compare the heat transfer results from one wire or probe with another, the heat transfer rates must be corrected for these losses. However, computation of fluctuation quantities requires that the uncorrected values of the heat transfer rates be used. An example of the temperature distribution along a wire and its mean temperature[21] is shown in figure 8. The finite length of the wire and its attendant temperature and heat transfer distribution influences the level of the spectra (especially at higher frequencies), correlations, and phase relationships between sensors[25,65].

The spacial resolution of a wire is limited by the length of the wire and the size of the smallest scales of fluctuations in the flow. If the length of the wire is larger than the smallest scale, the resultant magnitude of the spectra will be attenuated at the higher frequencies. The length of the wire with respect to the size of turbulence can have an effect on the measurements of fluctuation intensity, space and time correlations, and the turbulence scales and micro scales[66-68]. Additional spacial resolution problems encountered near walls were discussed in references 69 and 70. Proximity to walls of wind tunnels or to surfaces of models can introduce errors in measurements due to increased heat transfer from the wire due to conduction to the relatively cold walls[21,25]. An example of the effect of wire length on normalized spectra is presented in figure 9. The spacial resolution of multi-wire probes is further limited by the distance between the wires. The hot-wire probe intrusion into the flow can cause severe disturbance in certain flows. Examples are flows with large gradient such as boundary layers and vortices. Because of the above, hot-wire anemometry has limited resolution in space, time, and amplitude[29].

A severe problem is encountered in hypersonic flows when the gas is air. At higher Mach numbers the total temperature must be high enough to prevent liquefaction of air in the test section. There is a maximum recommended operating temperature for each wire material. These two facts places severe limitations on the maximum overheat at which wires can be operated. For example, the maximum recommended operating temperature for Platinum-10% Rhodium wire is 1842°R. For a $M$ = 8 wind tunnel, the total temperature required can be as high as 1360°R.

Using a recovery temperature ratio of 0.96, the maximum values for $t_w$ is 0.394 and $q_{max}$ = 1.354. If gas rarefaction effects are experienced and $h$ is greater than one, then the problem is even more severe. For $h$ = 1.1 the maximum value for $t_w$ under the above conditions is 0.254. The above values for $t_w$ are based on the average temperature for the wire. For small $L/d_w$ wires the limitation on $t_w$ would be greater due to higher temperatures at the mid-portion of the wire. The total temperature at low pressures where $h$ could be larger need not be as high as those at higher pressures, however, the constraint of constant total temperature during the calibration process limits the amount that $T_o$ can be reduced. (Also see ref. 71-76).

## PROBE PRE-CALIBRATION PROCEDURE

Once a probe is constructed, the following procedure should ensure accurate and reliable measurements. First, the probe should be operated at the maximum $q_\infty$ and $T_w$ that will be used during the proposed test. This is done to pre-stress and pre-heat the wire to ensure that no additional strain will be imposed on the wire during the test that could alter its resistance. For supersonic and high $q_\infty$ subsonic flows, the wires should also be checked for strain gaging, that is, stresses generated in the wire due to its vibration. Note, for testing in flows having high values of $q_\infty$, the wires should have slack to reduce the stress in the wires and to help eliminate strain gaging. If strain gaging is significant the wire should be replaced. During this pre-testing many wires will fail due to faulty wires or manufacturing techniques, but it is better that the wires fail in pre-testing rather than during an actual test.

A temperature-resistance relationship for wires is usually requires to compute the heat transfer rate from the heated wires. It is generally recommended that the following equation, which is a second degree equation in $\Delta T$, be used:

$$\frac{R}{R_{ref}} = 1 + a_1\left(T_w - T_{ref}\right) + b_1\left(T_w - T_{ref}\right)^2 \qquad (4)$$

After the wires have been pre-stressed and pre-heated, they should be placed in an "*oven*" and the wires calibrated to determine the values for $a_1$ and $b_1$. Once this calibration has been completed, the probes can be placed in a facility for mean flow calibration over the appropriate ranges of velocity, density, total temperature and wire temperature.

## STATISTICAL QUANTITIES

Data obtained using hot-wire anemometry are typically reduced to statistical quantities. Over the past few years the analysis of random data has been developed to a very high degree[77-79]. This plus the rapid developments in electronics (i.e., the A/D converters and high speed computers), have made it possible to obtain almost any statistical quantity of interest within the error constraints of the heated wire. Much of this is due to the fact that the digital processing of data can be used to obtain many quantities that are difficult or impossible to obtain using analog data reduction techniques.

Many types of single point and multi-point statistical quantities can be obtained using hot-wire anemometry[80-83]. It is routine to measure mean flow and RMS values, histograms and the higher order moments of skewness and kurtosis, auto correlation, and one dimensional spectra. Measurements of multi-point statistical quantities include cross correlations, two-point histograms and higher order two-point moments, cross spectra, and coherence functions. Attempts were made to measure higher moments up to eighth order[81].

These measurements can be used in various ways to evaluate many characteristics of the flow such as scales, decay rate, energy content etc[25]. The coherence function is a useful statistical quantity that can be used to evaluate various properties of a flow[84]. It can often be used to determine the predominant sound propagating angle and to determine the dominant mode present in a fluctuating flow field[85,86].

A few examples of statistical quantities that were measured using hot-wire anemometry are presented in figures 10-13. Integral and micro time and length scales of a flow can be determined from autocorrelation functions such as the one presented in figure 10. The higher moments of skewness and kurtosis (figure 11a-b) can be used to determine if

the fluctuations are Gaussian. For a Gaussian distribution the value of the skewness parameter is zero and for the kurtosis the value is 3. Figure 11 shows that both of these moments indicate that the mass flow and total temperature fluctuations are Gaussian over most of the thickness of the boundary layer. The value of third order auto-correlation function, such as the one shown in figure 12, can be used to support turbulent flow theories. An example of space-time correlations measured in a turbulent boundary [59,87] is presented in figure 13. The peak of these correlations at $t \neq 0$ indicate the presence of convection. The calculation of the convection velocity, obtained by dividing the separation distance by the time at which the individual curves peaks, indicates that there was no significant variation of the convective velocity over the spacings used. An example of normalized spectra measured downstream of a grid[88] is presented in figure 14 and show the increased attenuation of high frequency disturbances with increased distance downstream from the grid. (Also see ref. 89-92).

## GENERAL HEAT TRANSFER RELATIONSHIPS

The heat transfer from a wire under the limits of the present report (i.e., the wires mounted normal to flow in non-mixing gases) is[29]:

$$Q = f(u, m, r, c_p, T_w, T_{adw}) \qquad (5)$$

if the fluid properties of $m$, $c_p$, and $k$ are based on $T_o$, then the above equation becomes:

$$Q = f(u, r, T_w, T_o) \qquad (6)$$

Since $T_{adw} = hT_o$ and $h = f(Kn, M) = f(u, r, T_o)$. For incompressible continuum flows equation (6) reduces to:

$$Q = f(m, T_o, T_w) \qquad (7)$$

Unless noted, the total temperature will be used throughout this report to evaluate $m_t$, $c_p$, and $k_t$ where as $r$ will be based on $T_\infty$.

For a wire with a given $L/d_w$ the Nusselt number can be expressed[25] in terms of other dimensionless parameters as:

$$Nu_t = f\left(Re_t, Pr, Gr, \frac{T_w - T_{adw}}{T_o}, \frac{u^2}{c_p(T_w - T_{adw})}\right) \qquad (8)$$

and can be written as follows to show the effects of compressibility:

$$Nu_t = f\left(Re_t, Pr, Gr, M_\infty, \frac{T_w - T_{adw}}{T_o}\right) \qquad (9)$$

For relatively constant temperatures, $Pr$ = constant and if $Gr < Re^3$, buoyancy effects will be small and $Gr$ can be neglected. These approximations lead to:

$$Nu_t = f(Re_t, M_\infty, t_w) \qquad (10)$$

## MEAN FLOW MEASUREMENTS

### SUBSONIC INCOMPRESSIBLE - CONTINUUM FLOW

#### Theoretical Considerations

The functional relationship between the power to the wire or the heat transfer from the wire and the mean flow variables are required to determine the so called "*static*" calibration of the wire from which the sensitivities to the various flow variables can be obtained in order to calculate the fluctuations. Because of this the mean flow results and probe mean flow calibration procedure are considered together.

The first attempt to obtain a theoretical solution for the heat transfer from a heated wire mounted normal to the flow was carried out by Boussinesq[2]. The equation that he obtained is:

$$Q = L\left(2\sqrt{p k_t c_p r u r_w}\right)(T_w - T_{adw}) \qquad (11)$$

Equation (11) can be expressed in terms of non-dimensional quantities as follows:

$$Nu_t = \sqrt{\frac{2}{p}}\sqrt{PrRe_t} \qquad (12)$$

**King re-analyzed the problem of heat transfer from a heated wire and obtained the following relationship:**

$$Q = L\left(k_t + 2\sqrt{p\,k_t c_p r u r_w}\right)\left(T_w - T_{adw}\right) \qquad (13)$$

**or in terms of non-dimensional quantities:**

$$Nu_t = \frac{1}{p} + \sqrt{\frac{2}{p}}\sqrt{PrRe_t} \qquad (14)$$

**From equation (11) and (13) it can be seen that the only difference between Boussinesq's and King's results is the inclusion of the additional term $k_t$ in King's result that attempts to account for the effects of natural convection. At "high" values of Reynolds number the two results are essentially equal.**

**Using equation (3), equation (13) can be expressed as:**

$$P = \left[A'(T_o) + B'(T_o)\sqrt{m}\right]\left[T_w - T_{adw}\right] \qquad (15)$$

**where $A'(T_o)$ and $B'(T_o)$ are based on King's results. However, the quantities $A'$ and $B'$ are usually determined for a given wire by direct mean flow calibration. Often the exponent for the mass flow term is determined from a curve fit to the data. The values for the exponent can range[25] from 0.45 to 0.50.**

**For a CTA, equation (15) can be generalized to:**

$$\frac{E^2}{\left(R_w - R_{adw}\right)} = A_T(T_o) + B_T(T_o)m^n \qquad (16)$$

**where $A_T(T_o) = \dfrac{R_w A'(T_o)}{a_1 R_{ref}}$ and $B_T(T_o) = \dfrac{R_w B'(T_o)}{a_1 R_{ref}}$.**

**For a CCA:**

$$\frac{I^2 R_w}{\left(R_w - R_{adw}\right)} = A_C(T_o) + B_C(T_o)m^n \qquad (17)$$

**where $A_C(T_o) = A'(T_o)/a_1 R_{ref}$ and $B_C(T_o) = B'(T_o)/a_1 R_{ref}$. Therefore, if wires operated with a CTA or a CCA are calibrated over a range of $m$ and $T_o$, equations (16) and (17) indicate that the calibration curves will be straight lines if the left hand side of the equation is plotted as a function of $m^n$. In general, the slopes, $B$, and intercepts, $A$, will be functions of the total temperature. If the total temperature is constant, $A$ and $B$ will be constants and if the density is constant, the mass flow term will reduce to velocity. An example of voltage versus velocity for a wire operated with a CTA is presented in figure 15 for various values of total temperature. (Also see ref. 93-97).**

**Hot-wires have also been calibrated in the form of $u = f(E)$ rather than the more conventional form of $E = f(u)$. The constant $T_o$ and $r$ version of King's law for a CTA is $E^2 = A + B\sqrt{u}$ and when expressed as $u = f(E)$ gives:**

$$u = A_1 - A_2 E^2 + A_3 E^4 \qquad (18)$$

**In this equation George et. al.,[98] noted that $A_1 - A_3$ are functions of $T_o$. They proposed the following equation for the calibration of wires that is independent of $T_o$ for a limited range:**

$$Re_t = B_1 + B_2 Nu^{\frac{1}{2}} + B_3 Nu + B_4 Nu^{\frac{3}{2}} + B_5 Nu^2 \qquad (19)$$

**where $m$ is evaluated at $T_o$ and $k$ evaluated at $T_f$.**

**<u>Examples of Data</u>**

**A summary of heat transfer data from cylinders in terms of $Nu_t$ vs. $Re_t$ taken in the subsonic continuum flow regime was presented in reference 21. The results from these experiments are compared with the theoretical results of Boussinesq and King in figure 16. This figure shows that there is a relatively good agreement between the measured results and King's theory over a wide range of Reynolds numbers. There is a substantial difference between Boussinesq's theory**

and King's theory and the measured results for Reynolds numbers less than about 100.

A large amount of heat transfer data was also presented by McAdam[99] in terms $Nu_f$ vs. $Re_f$ and he recommended the following equation:

$$Nu_f = 0.32 + 0.43\left(Re_f\right)^{0.52} \quad (20)$$

In comparision, King's equation with $Pr = 0.70$ is:

$$Nu_t = 0.3183 + 0.6676\left(Re_t\right)^{0.50} \quad (21)$$

For Reynolds number equal to zero the two equations give essentially the same value for the Nusselt number. At higher values of Reynolds number King's equation is about 40 percent higher than the values of Nusselt number presented by McAdam. A film temperature is often used as the temperature at which $k$, $r$ and $m$ are evaluated when correlating $Nu$ versus $Re$. However, $r$ is sometimes evaluated at the free stream static temperatures. The use of the film temperature for evaluating fluid properties has been questioned in reference 100. However, in this reference the density in the Reynolds number was evaluated at $T_f$, where as, in reference 99 this apparently was not the case.

Bradshaw[27] notes that there is a difference of opinion throughout the hot-wire anemometry community about the usefulness of a universal correlation based on variables evaluated at a film temperature. These correlations provide a useful guide for plotting results and comparing mean flow results obtained by different investigators. However, if good accuracy is to be obtained for the fluctuations, individual calibration of probes is required.

Often attempts are made to measure mean velocities using hot-wire anemometry. It can be shown using equation (13) that the voltage across a wire is a $f\left(u, r, T_o, T_w\right)$. Therefore, to measure the mean velocity, the other variables must be held constant or a method must be used to correct the data for any variation in variables other than velocity[65,71,101]. Because of this, the hot-wire anemometer is not a very good mean flow measuring device, even if one utilizes some of the corrections that have been developed. However, for limited variations in the independent variables, corrected velocity measurements were reported in reference 101.

Very Low Velocities

At very low velocities the heated wire can cause a relatively significant vertical movement of a fluid due to buoyancy effects on the lower density fluid adjacent to the wire. This results in a change in the effective velocity around the wire. Efforts were made to calibrate and use hot-wire anemometry at very low velocities[102-107] where natural convection effects were present. The influences of natural convection are parameterized by the Grashof number. Experimental evidence[108] indicated that if $Gr < Re^3$ then free convection effects were negligible. An example of the effect of low velocities on the Nusselt number is presented in figure 17.

King also provided an equation suitable for low speed flows:

$$P = \frac{2p\,Lk_t\left(T_w - T_{adw}\right)}{\log\left(b/r_w\right)} \quad (22)$$

where $b = k_t e^{1-g}/c_p ru$ and $g$ = Euler's Constant = 0.57721. In terms of non-dimensional quantities, equation (22) becomes:

$$Nu_t = \frac{2}{\log\left[2e^{1-g}/\left(Pr\,Re_t\right)\right]} \quad (23)$$

Equation (22) is valid for $ud_w$ < 0.0187 where $u$ is in cm/sec and $d_w$ is in cm. Equation (13) is valid for $ud_w$ > 0.0187.

For velocities as low as 1.0 cm/sec, Haw and Foss[102] attempted to correlate their data using King's equation in the form:

$$E^2 = A + Bu^n \quad (24)$$

A deviation of their data from a fitted curve was observed at $u \approx 30$ cm/sec. The diameter of the wire used in their experiment[102] was not noted. However, if one assumes a value of 0.00015 inch or

0.00020 inch, the limits for the application of equations (13) and (22) indicate velocities of 49 cm/sec or 37 cm/sec, which are not too different from 30 cm/sec. The use of equation (22) would not improve the correlation presented in reference 102 since it can be shown that as $u \to 0$ in equation (22) $E_w \to 0$. The data of reference 102 indicates that at $u = 0$ the intercept of the curve is greater than the value indicated by the intercept in equation (24). Correlations obtained using the results of a theory based on Oseen[108] flow would not improve the correlation since this approach gives results that are similar to those obtained using equation (22). For a heated wire tested in horizontal wind tunnels, $u_{eff}$ cannot reach zero since the effective velocity is:

$$u_{eff}^2 = u^2 + u_B^2 \qquad (25)$$

and for a heated wire $u_B \neq 0$.

## SUBSONIC SLIP FLOW AND TRANSONIC FLOW

### Theoretical Considerations

These two flow regimes will be treated together since the experimental results are similar. Kovasznay[6] extended hot-wire anemometry results to compressible flows and showed that there was a significant difference between the heat transfer in compressible and incompressible flows. Several experimenters obtained heat transfer measurements at low speeds and found an apparent compressibility or Mach number effect[35,64,109] at Mach numbers as low as 0.1. Spangenberg[110] conducted extensive tests over a wide range of variables and determined that the apparent compressible flow effects at Mach number as low as 0.05 was really due to gas rarefaction (e.g., slip flow).

In this flow regime the heat transfer from the heated wire is generally given as:

$$Q = P = p\, Lk_t \left(T_w - hT_o\right) Nu_t \qquad (26)$$

In transonic flow and subsonic slip flows the Nusselt number is no longer only a function of Reynolds number and Kings' law is no longer applicable. The most common functional relationship for the Nusselt number in these flow regimes is[58]:

$$Nu_t = f\left(M, Re_t, q\right) \qquad (27)$$

since it was found that $Nu_t$ is also a function of a temperature parameter. Another functional relationship that was used to analyze gas rarefaction effects is[35]:

$$Nu_t = f\left(M, Kn, t_w\right) \qquad (28)$$

In subsonic compressible flows the recovery temperature of the wire can change and functional relationships for $h$ are:

$$h = f\left(M, Re_t\right) \quad \textbf{or} \quad h = f\left(M, Kn\right) \qquad (29)$$

| | Dependent Variable | Independent Variable | Reference |
|---|---|---|---|
| ① | $Nu_t$ | $Re_t$, $M_\infty$, $q$ | Morkovin[58] |
| ② | $Nu_t$ | $Kn$, $M_\infty$, $t_w$ | Baldwin[35] |
| ③ | $Nu_t$ | $Re_t$, $M_\infty$, $t_w$ | |
| ④ | $Nu_t$ | $Kn$, $M_\infty$, $q$ | |
| ⑤ | $h$ | $Re_t$, $M_\infty$ | Morkovin[58] |
| ⑥ | $h$ | $Kn$, $M_\infty$ | Vrebalovich[111] |

Table I. Functional Relationships for $Nu_t$ and $h$.

Morkovin chose $Nu_t = f\left(M_\infty, Re_t, q\right)$ and $h = f\left(M_\infty, Re_t\right)$ for the development of his equations. In order to emphasize the gas rarefaction effects, Baldwin chose $Nu_t = f\left(M_\infty, Kn, t_w\right)$ and $h = f\left(M_\infty, Kn\right)$. Independent variables that might be used to relate $Nu_t$ and $h$ to the dependent variables are presented in Table 1. Although Morkovin and Baldwin chose the variables of ① and ②, one could just as well have chosen the variables noted in ③ or ④. It will be shown later that the variables in ④ might be the most efficient group to use.

### Examples of Data

Baldwin[35] and Spangenberg[110] investigated the heat transfer from wires over a wide range of $Re_t$, $M$, and $T_w$ in the slip flow and transonic flow regimes. Their results, presented in figures 18a-b, shows that $Nu_t = f\left(Re_t, M\right)$ for Mach numbers ranging from 0.05 to 0.90 and Reynolds

numbers ranging from 1 to about 100. The effects of wire overheat on the values of $Nu_t$ were also determined by Baldwin and Spangenberg and examples of these effects are shown in figure 19. The values of $Nu_t$ can increase or decrease with increased overheat depending on the Mach number and Knudsen number.

Results from theoretical calculations made for the effects of slip flow on heat transfer from wires were reported in reference 31. An example of these results is presented in figure 20. The levels of the calculated Nusselt number do not agree with measured results, however, the trends of the theoretical results agree with the experimental trends shown in figure 18.

## SUPERSONIC CONTINUUM FLOW

General results for compressible flow shows that $Nu_t = f(M, Re_t, q)$. However, it was experimentally[21,112] determined that $Nu_t \neq f(M)$ for Mach numbers greater than about 1.4. Typical heat transfer data for supersonic flow is presented in figure 21 to illustrate the approximate invariance of $Nu_t$ with $M$. At higher Mach number and relatively low total pressures, there is a high probability that much of the data presented for supersonic and hypersonic flows are in the slip flow regime.

## FREE MOLECULAR FLOW

Standler, Goodwin and Creager[33] computed the heat transfer from wires for free molecular flow and an example of their results along with measurements are presented in figure 22. A combination of continuum flow, slip flow and free molecular flow results[10] are shown in figure 23. From this figure it can be seen that for continuum flow at large Reynolds number $Nu_t \approx Re_t^{1/2}$. For free molecular flow $Nu_t \approx Re_t$ and slip flow results smoothly connect the two regimes. Therefore, for slip flows, $Nu_t$ varies with exponent of Reynolds number which range from ½ to 1.

## RECOVERY TEMPERATURE RATIO

The recovery temperature ratio must be known to compute the heat transfer from heated wires. In general, the recovery temperature ratio is a function of Mach and Reynolds numbers or Mach and Knudsen numbers. However, for Mach number greater than about 1.4 the recovery temperature ratio is not a function of Mach number for continuum flow. A "*universal*" curve presented by Vrebalovich[111] (figure 24) correlated the temperature recovery ratio with Knudsen number for all Mach numbers. Using the results presented in figure 24, the temperature recovery ratio for continuum flow and free molecular flow, curves of $h$ vs. $M$ and $Kn$ can be calculated. An example of these calculations is presented in figure 25.

## FLUCTUATION MEASUREMENTS

## SUBSONIC INCOMPRESSIBLE FLOW

### Theoretical Considerations

#### a. Constant Temperature Anemometer

For a constant temperature anemometer, King's[3] equation can be expressed as:

$$\frac{E^2}{R_w} = L\left[k_t + \sqrt{2\pi k_t c_p ru d_w}\right]\left[T_w - hT_o\right] \qquad (30)$$

where $R_w$ and $T_w$ are constants.

If one assumes that the changes in $k_t$, $c_p$ and $h$ can be neglected, the change in $E$ will be a function of $ru$ and $T_o$ as given by the following equation for small perturbations:

$$\frac{e'}{E} = S_m \frac{m'}{m} + S_{T_o} \frac{T_o'}{T_o} \qquad (31)$$

where

$$S_m = \frac{1}{4} \frac{\sqrt{2p\, Re_t Pr}}{\left[1 + \sqrt{2p\, Re_t Pr}\right]} \quad \text{and} \quad S_{T_o} = -\frac{1}{2}\frac{h}{t_w} \qquad (32)$$

From the above equation it can be seen that $S_m \to 0$ as $Re_t \to 0$ and $S_m \to ¼$ as $Re_t \to \infty$. For the

**temperature sensitivity,** $S_{T_o} \to -\infty$ **as** $t_w \to 0$ **and** $S_{T_o} \to 0$ **as** $t_w \to \infty$**. Equation (31) shows that** $E = f(m, T_o)$ **where** $S_m = \partial \log E / \partial \log m$ **and** $S_{T_o} = \partial \log E / \partial \log T_o$**.**

**Since equation (31) shows that** $E = f(m, T_o)$**, the fluctuation of mass flow and total temperature can be measured using a CTA [113-115]. This can best be done by using two wires operated at different, but high overheats, digitizing the data, and solving two equations for** $m'$**,** $T_o'$ **and** $m'T_o'$ **as functions of time.**

**If the total temperature and the Mach number varies significantly, then** $k_t$ **and** $c_p$ **must be differentiated with respect to** $T_o$ **and** $h$ **differentiated with respect to Mach number. Under these conditions it would be more appropriate to use the equation obtained by Rose and McDaid[8] with the assumption that** $Nu_t \neq f(M)$**.**

**Instead of using King's equation, consider equation (15) for measuring mass flow and total temperature fluctuation. For a CTA equation (15) becomes:**

$$d\log E = \frac{nB'(T_o)m^n}{2\left[A'(T_o) + B'(T_o)m^n\right]} d\log m + \frac{1}{2}\left\{\frac{A'(T_o)\frac{\partial \log A'(T_o)}{\partial \log T_o}}{\left[A'(T_o) + B'(T_o)m^n\right]} + \frac{m^n B'(T_o)\frac{\partial \log B'(T_o)}{\partial \log T_o}}{\left[A'(T_o) + B'(T_o)m^n\right]} - \frac{h}{t_w}\right\} d\log T_o \qquad (33)$$

**b. <u>Constant Current Anemometer</u>**

**For the CCA anemometer, Kings' equation becomes:**

$$EI = L\left[k_t + \sqrt{2\pi k_t c_p r u d_w}\right]\left[T_w - hT_o\right] \qquad \textbf{(34)}$$

**Again assume that** $k_t$**,** $c_p$ **and** $h$ **are constant, the change in** $E$ **is given by the following equation:**

$$\frac{e'}{E} = S_m \frac{m'}{m} + S_{T_o}\frac{T_o'}{T_o} \qquad \textbf{(35)}$$

**where**

$$S_m = \frac{(1-e)}{4(e_f - e)}\frac{\sqrt{2\pi Re_t Pr}}{\left[1 + \sqrt{2\pi Re_t Pr}\right]} \quad \text{and} \quad S_{T_o} = -\frac{(1-e)}{2(e_f - e)}\frac{h}{(q-h)} \qquad (36)$$

**If** $d\log I = 0$ **then**

$$S_m = \frac{1}{4e_f}\frac{\sqrt{2\pi Re_t Pr}}{\left[1 + \sqrt{2\pi Re_t Pr}\right]} \textbf{ and } S_{T_o} = -\frac{1}{2e_f}\frac{h}{\left[q-h\right]} \qquad \textbf{(37)}$$

**Equation (36) and (37) shows that** $S_m = f(t_w)$**. If** $Re_t \to 0$ **then** $S_m \to 0$**, but if** $Re_t \to \infty$ **then** $S_m = \frac{k_t t_w}{2\left[k_t t_w - q\right]}$**. On the other hand, if** $t_w \to 0$ **then** $S_m \to 0$ **and if** $t_w \to \infty$ **then** $S_m \to \frac{1}{2}\frac{\sqrt{2\pi Re_t Pr}}{\left[1 + \sqrt{2\pi Re_t Pr}\right]}$**. If** $t_w \to 0$ **then** $S_{T_o} \to \frac{k_t h}{q}$ **and if** $t_w \to \infty$ **then** $S_{T_o} \to 0$**. Again, it is possible to measure both** $\tilde{m}$**,** $\tilde{T}_o$ **and** $R_{mT_o}$ **using a CCA [113] and the fluctuation diagram developed by Kovasznay[6]. An example of fluctuation diagrams for two discrete frequencies measured with a CCA is presented in figure 26. Again if the total temperature and the Mach number varies significantly, then it would be more appropriate to use Morkovin's equation with the assumption that** $Nu_t \neq f(M)$**.**

**Similarly, to measure mass flow and total temperature fluctuation,equation (15) for CCA becomes:**

$$d\log E = \frac{(1-e)}{2(e_f - e)}\left\{\frac{nB'(T_o)m^n}{\left[A'(T_o) + B'(T_o)m^n\right]}\right\} d\log m + \frac{(1-e)}{2(e_f - e)}\left\{\frac{A'(T_o)\frac{\partial \log A'(T_o)}{\partial \log T_o}}{\left[A'(T_o) + B'(T_o)m^n\right]} + \frac{m^n B'(T_o)\frac{\partial \log B'(T_o)}{\partial \log T_o}}{\left[A'(T_o) + B'(T_o)m^n\right]}\right\} d\log T_o \qquad (38)$$

**Mass flow fluctuations measured in subsonic flows can be very misleading where there is a significant amount of far-field sound. The mean square value of mass flow fluctuation is:**

$$\overline{\left(\frac{m'}{m}\right)^2} = \overline{\left(\frac{u'}{u}\right)^2} + 2R_{ur}\left(\frac{\tilde{u}}{u}\right)\left(\frac{\tilde{r}}{r}\right) + \overline{\left(\frac{r'}{r}\right)^2} \qquad \textbf{(39)}$$

**The magnitude of the mass flow fluctuation depends on** $\tilde{u}$**,** $\tilde{r}$**, and** $R_{ur}$ **where** $-1 \le R_{ur} \le 1$**. As an**

example, assume $R_{ur} = 1$, indicating downstream moving sound, and $\tilde{u}/u = \tilde{r}/r$. Under these assumption the mass flow fluctuation equals twice the velocity or density fluctuation. However, if $R_{ur} = -1$, indicating upstream moving sound, and $\tilde{u}/u = \tilde{r}/r$; the mass flow fluctuation are zero.

Examples of Data

Most of the measurements made using hot-wire anemometry were and still are being made in the subsonic, incompressible, continuum flow regime. An extensive amount of data was accumulated over the years in various flow fields[25]. Some of these data will be presented in the following section.

a. Freestream

Some of the first fluctuation measurements made using hot-wire anemometers were obtained in the freestream of wind tunnels to help evaluate the effects of turbulence on the transition of laminar boundary layers[116]. The purpose of this effort was an attempt to extend wind tunnel transition data to flight conditions in order that the on-set of transition might be predicted on full scale aircraft. Measurements in the freestream are also required to study the effect of freestream disturbances on laminar boundary layer receptivity. An example of measurements made in the freestream is presented in figure 27 for the Low Turbulence Pressure Tunnel located at the NASA Langley Research Center[37]. The filled symbols represent data taken in the facility during 1940[117] and the curves represent measurements made in 1980. The agreement between the two sets of data is very good when it is noted that the data taken in 1940 was obtained at $p_o = 4$ atmospheres and the low datum point at $Re_t = 5 \times 10^5$ is for $M \approx 0.02$.

Fluctuation measurements were also made in various location within wind tunnel circuits, predominantly in the settling chamber. Anemometry was used to evaluate the efficiency of contractions in reducing vorticity levels in the test section[118]. An example of the results obtained through a contraction is presented in figure 28. The absolute value of the velocity fluctuation in the direction of the flow was reduced through the contraction but the relative values were greatly reduced depending on the area ratio of the contraction. For example in figure 28 the velocity fluctuation downstream of the contraction are ratioed to the mean flow in the large section of the contraction where the local velocity is low. If these downstream velocity fluctuations were ratioed to the local mean velocity, these normalized fluctuations would be substantially smaller, i.e., $\tilde{u}/u_{sc} = 2.6$ vs. $\tilde{u}/u = 0.16$.

b. Grids

It was found that screens or grids can effectively reducevorticity fluctuations. Because of this attenuation, screens have been extensively investigated[25,38,119] using hot-wire anemometry to optimize their characteristics for use in wind tunnels to reduce the vorticity levels in the test section. An example of these measurements is presented in figure 29 where the turbulent reduction factor is given as a function of the $\Delta p/q_\infty$ across the screens[120]. Therefore, the use of screens in the settling chamber along with a contraction of adequate area ratio, can substantially reduce velocity fluctuations in the test section due tovoriticity[121]. (Also see ref. 122-130).

c. Boundary Layers

Hot-wire measurements were made in turbulent boundary layers[42] to measure the Reynolds stresses and other fluctuation quantities to furnish data for the development of turbulent boundary layer theories. An example of measurements made in the boundary layer on a flat plate[131] is presented in figure 30a-b. Figure 30a shows the significant variation of the velocity fluctuation across the boundary layer while figure 30b shows an example of the local streamwise velocity fluctuation ratioed to the local velocity. Forming the ratio in this latter manner indicates that the velocity fluctuations can exceed 40 percent, a value that is too large for an accurate assumption of small perturbation.

Extensive measurements were made of turbulent flows in pipes[40,41] to compare theoretical and measured results. From these measurements many statistical quantities were obtained including Reynolds stresses; triple and quadruple correlations; energy spectra; rates of turbulent energy production, dissipation, and diffusion; and turbulent energy balance. An

example of the streamwise velocity fluctuations across a pipe is presented in figure 31a-b.

Hot-wire anemometry has been extensively used to investigate the characteristic of various boundary layer flow manipulators such as Large Eddy Break-up devices (LEBUS) [132], Riblets[133] and roughness elements[134]. Laminar boundary layer transition due to T-S waves[135], cross flow[136] and Gortler vortices[137] was extensively studied using the hot-wire techniques. Also the effects of heat addition[138], sound[139] and vorticity[140] on boundary layer characteristics have been investigated.

The hot-wire anemometer with a single wire cannot determine the direction of flow. However, a technique using a multi-wire, "*ladder probe*" was developed[141] to study the separated boundary layer where a significant amount of reverse flow occurred. This technique was used to determine the location of the zero average velocity in a subsonic turbulent boundary layer. (Also see ref. 142-144).

d. Laminar Boundary Layer Receptivity

One of the major impediments to a through understanding of laminar boundary layer transition is the ability to predict the process by which freestream disturbances are assimilated into the boundary layer. These free stream disturbances can be either vorticity, entropy, sound or a combination of these fluctuations.

The effect offreestream fluctuations on the stability of the laminar boundary can be investigated by making measurements in the freestream and in the boundary layer to evaluate the receptivity of the boundary layer to fluctuations[145] in the freestream. An example of fluctuations measured in a subsonic boundary layer on a flat plate for various frequency bands is presented in figure 32. Kendall[145] presented three types of measurements made in a laminar boundary layer due to velocity fluctuations from the free stream. The first type is illustrated by thex's and consisted of broadband velocity fluctuation where the peak level occurs towards the inner part of the boundary layer. This type of measurement is noted as the Klebanoff's mode and is represented by the solid line. The results obtained when the data were filtered at the Tollmein-Schlichting (T-S) frequency are represented by circles. Although the frequencies were identical to those of T-S waves they were not T-S waves since the convection velocity was equal to the free stream value. The maximum level of these fluctuations occurred at the outer part of the boundary layer. The third type of fluctuation is represented by the dotted line. These were true T-S waves which occurred in packets and had a convective velocity of 0.35 to 0.4 of the free stream velocity. These peak fluctuation levels occurred near the wall. (Also see ref. 146-156).

e. Jets

Hot-wire measurements were obtained in jets[45-47] to measure the Reynolds stresses associated with free shear layers and to help evaluate the RMS levels and frequencies associated with jet noise. An example of the velocity and temperature fluctuations measured[157] across a heated jet is presented in figure 33. The two types of fluctuations were normalized by the maximum and the local mean values, respectively. (Also see ref. 158-160).

f. Wakes

Various statistical quantities were measured downstream of a heated cylinder by Townsend[43] to obtain experimental results to help improve turbulent theories applicable to this type of flow. Some of the quantities obtained included turbulent intensities, sheer stress, velocity-temperature correlation, triple velocity correlation, diffusion rate and energy dissipation. Measurements were made from 500 to 950 diameter downstream of the cylinder where dynamical similarity was assumed to exist. An example of the mean curve fitted to the u-component of the velocity fluctuation is presented in figure 34 and shows good similarity. Uberoi and Freymuth[44] made extensive spectral measurements downstream of a cylinder and their data indicated that only the spectra of large-scale turbulence were dynamically similar.

## SUBSONIC SLIP FLOW AND TRANSONIC FLOW

### Theoretical Considerations

In compressible flows the heat transfer from a wire is usually described by the following equation:

$$Q = p\,Lk_t\left(T_w - hT_o\right)Nu_t \qquad (40)$$

Differentiating the above equation for the case where $Q = P$ gives:

$$d\log P - \frac{q}{t_w}d\log t_w = d\log Nu_t - \frac{h}{t_w}d\log h - \frac{h}{t_w}d\log T_o + d\log k_t \qquad (41)$$

The terms on the right hand side of the above equation depend only on the functional forms assumed for $Nu_t$ and $h$ (Table I) and the chosen independent variables (Table II). Ultimately these terms depend on the variation of $Nu_t$ and $h$ with the flow variables along with the aerodynamic and thermodynamic properties of the flow. The final form for the left hand side of the equation depends on the type of anemometer used.

It was shown in reference 161 that, for a wire mounted normal to the flow, $E = f\left(u, r, T_o, T_w\right)$. Morkovin[58] and Baldwin[35] related $Nu_t$ and $h$ to the non-dimensional variables noted in Table I. However, recent results presented by Barre et.al.,[162] suggested advantages from using the following variables: $E = f\left(m, M_\infty, T_o, T_w\right)$ and $E = f\left(p, m, T_o, T_w\right)$. In order to obtain the equation for the CCA, they transformed Morkovin's equations into their variables. This transformation is not necessary, since once the variables are chosen, the equations can be derived directly using a method similar to the one described by Anders[161].

The equations obtained using the variables of ❷ from table II gives the same results as those of ❶, Morkovin[58], namely $E = f\left(m, T_o\right)$ under the condition where $Nu_t \neq f\left(M_\infty\right)$ and $S_u = S_r$. Using the variables in ❸, Barre et.al.,[162] applied the resultant equations to measurements made in a turbulent boundary layer under the assumption that $\tilde{p} = 0$ without assuming that $S_u = S_r$. They also extended the equation to the case of supersonic flow in the test section of wind tunnels by assuming that all the fluctuations were sound, again not assuming $S_u = S_r$.

Once the independent variables are chosen, it is not necessary to derive the equations using $Nu_t$ and $h$. The "*primitive*" variables, $u$, $r$, $T_o$ etc., greatly simplifies the manipulation of the calibration data and can be used to correlate $E$ as a function of $u$, $r$, $T_o$ etc., without evaluating $Nu_t$ and $h$. This technique might have advantages in the calibration of wires and the ease of operation of calibration facilities.

The possible sets of variables based on the above discussion is presented in Table II.

| | Dependent Variable | Independent Variable | Reference |
|---|---|---|---|
| ❶ | $E$, $Nu_t$, $h$ | $u$, $r$, $T_o$ | Baldwin[35], Morkovin[58] |
| ❷ | $E$, $Nu_t$, $h$ | $m$, $M_\infty$, $T_o$ | Barr, Quine and Dussauge[162] |
| ❸ | $E$, $Nu_t$, $h$ | $p_\infty$, $m$, $T_o$ | Barr, Quine and Dussauge[162] |
| ❹ | $E$ | $u$, $r$, $T_o$ | Rose and McDaid[8] Stainback and Johnson[85] |
| ❺ | $E$ | $m$, $M_\infty$, $T_o$ | |
| ❻ | $E$ | $p_\infty$, $m$, $T_o$ | |

**Table II. Various Independent Variables to Derive the Hot-Wire Anemometry Equations**

Therefore, there are many forms for the hot-wire equations depending on the variables chosen and the anemometer used. One should choose the variables that are most convenient for the flow situation under investigation.

#### a. Constant Current Anemometer

Using the heat transfer equation (40) and the functional relationship from equation (27) and (29), the change in voltage across a wire can be related to the changes in $u$, $r$, and $T_o$. An example of a set of equations obtained for a constant current anemometer was given by Morkovin[58] as:

$$\frac{e'}{E} = -S_u \frac{u'}{u} - S_r \frac{r'}{r} + S_{T_o} \frac{T_o'}{T_o} \qquad (42)$$

**where**

$$S_u = \frac{\P \log E}{\P \log u} = \frac{E'A_w'}{t_{wr}} \left[ t_{wr} \left( \frac{\P \log Nu_t}{\P \log Re_t} + \frac{1}{a} \frac{\P \log Nu_t}{\P \log M} \right) - \left( \frac{1}{a} \frac{\P \log h}{\P \log M} + \frac{\P \log h}{\P \log Re_t} \right) \right] \qquad (43)$$

$$S_r = \frac{\P \log E}{\P \log r} = \frac{E'A_w'}{t_{wr}} \left[ t_{wr} \frac{\P \log Nu_t}{\P \log Re_t} - \frac{\P \log h}{\P \log Re_t} \right] \qquad (44)$$

$$S_{T_o} = \frac{\P \log E}{\P \log T_o} = \frac{E'A_w'}{t_{wr}} \left[ \begin{array}{c} k_t t_{wr} (1 + A_w') + A_w' t_{wr} \left( -1 - n_t + m_t \frac{\P \log Nu_t}{\P \log Re_t} + \frac{1}{2a} \frac{\P \log Nu_t}{\P \log M} \right) \\ - A_w' \left( \frac{1}{2a} \frac{\P \log h}{\P \log M} + m_t \frac{\P \log h}{\P \log Re_t} \right) \end{array} \right] \qquad (45)$$

**For a large range of Reynolds numbers and Mach numbers, $S_u$ and $S_r$ in equation (42) are unequal[35]. Following Kovasznay's technique for supersonic flow, dividing equation (42) by $S_{T_o}$, squaring and forming the mean gives:**

$$\overline{f'^2} = q^2 \overline{\left( \frac{u'}{u} \right)^2} + s^2 \overline{\left( \frac{r'}{r} \right)^2} + \overline{\left( \frac{T_o'}{T_o} \right)^2} + 2qsR_{ur} \frac{\tilde{u}\tilde{r}}{ur} - 2qR_{uT_o} \frac{\tilde{u}\tilde{T}_o}{uT_o} - 2sR_{rT_o} \frac{\tilde{r}\tilde{T}_o}{rT_o} \qquad (46)$$

**This is a general equation for a wire mounted normal to the flow in compressible flows where $S_u \neq S_r$. This is a single equation with six unknowns. In principal, this equation can be solved by operating a single wire at six overheats and solving six equations to obtain the three fluctuating quantities and their correlations. In the past, it was generally stated that the calibration of the wire cannot be made sufficiently accurate or the velocity and density sensitivities cannot be made sufficiently different to obtain a suitable solution using this technique. Demetriades[163] noted that the coefficient in equation (46) must occur to at least the fifth degree. This constraint, however, appears to be too restrictive. For example, assume that $s$ is a function of $q$ as follows:**

$$s = a_1 + a_2 q^{b_1} + a_3 q^{b_2} + a_4 q^{b_3} \qquad (47)$$

**It can be shown that $b_1$, $b_2$ and $b_3$ can have any value provided that the substitution of the relationship for $s$ into equation (46) results in an equation having at least six terms. An analysis of data obtained at transonic Mach number by Spangenberg indicates that $s$ can be non-linearly related to $q$ and suggest that a solution to equation (46) is possible. A more detailed discussion of this can be found in ref. 164.**

**If solutions for equation (46) are possible, what is the form of the fluctuation diagram? In equation (46), $f$ is a function of $q$ and $s$, therefore, the fluctuation diagram exists on a three-dimensional surface, a hyperboloid, rather than a plane as for the case when $S_u = S_r$. However, the important information, fluctuation quantities, exists in the $f-q$ and $f-s$ planes. For example when $s = 0$, equation (46) reduces to an equation for a hyperbola in the $f-q$ plane, where the asymptote gives the velocity fluctuations. If $q = 0$, equation (46) reduces to an equation for a hyperbola in the $f-s$ plane and the asymptote represents the density fluctuations. When $q$ and $s$ both are zero, the intercept on the $f$ axis gives the total temperature fluctuation. In planes parallel to the $q-s$ plane, the locus of points of the fluctuation diagram is governed by the velocity and density fluctuations and their correlation. The cross product term, $qs$, requires a rotation of the axis before the characteristics of the locus can be identified. The locus of points on the surface of the hyperboloid will depend on the relative changes in $q$ and $s$ as the overheat of the wire is changed.**

**Although the fluctuation diagram exists on the surface of a hyperboloid, the fluctuations can be determined from the intersection of thehyperboloid with the $f-q$ and $f-s$ planes. Because of this, the fluctuation and mode diagrams were defined as the traces of these intersections in the noted planes[165,166]. A general schematic representation of the fluctuation diagram for equation (46) is presented in figure 35.**

**Even though there is much evidence that $S_u \neq S_r$ over a large range of $Re_t$ and $M_\infty$ in subsonic compressible flow, some experimenters have conducted tests[167-169] under the condition where $S_u = S_r$. When $S_u = S_r$ for subsonic compressible flow, the fluctuation and mode diagram technique developed by Kovasznay can be used to obtain the**

mass flow and total temperature fluctuations. The general fluctuation diagram is identical to the one for supersonic flow, namely, a hyperbola. Also, the mode diagrams for entropy and vorticity modes are identical. The sound mode is, however, different. For supersonic flow the angle that plane sound waves makes with respect to the axis of a probe can have only two values. If the sound source is fixed then $\cos q_1 = -1/M$. If the sound source has a finite velocity then $\cos q_1 = -1\Big/\left(\frac{u}{a} - \frac{u_s}{a}\right)$. However, for subsonic flows the values of $q_1$ can range from 0° to 360°. An example of fluctuation diagrams measured in subsonic compressible flows under the condition where $S_u = S_r$ is presented in figure 36a-b.

b. <u>Constant Temperature Anemometer</u>

The hot-wire equation for a CTA that corresponds to equation (42) for a CCA is:

$$\frac{e'}{E} = S_u \frac{u'}{u} + S_r \frac{r'}{r} + S_{T_o} \frac{T_o'}{T_o} \qquad (48)$$

and for $S_u \neq S_r$ is a single equation with three unknowns. Hinze indicated that a CTA cannot be used to obtain fluctuations using the mode diagram technique since the frequency response of the anemometer approaches the frequency response of the wire at low overheats. Because of these problems, it was suggested that a three wire probe be used and the voltage from the anemometer digitized at a suitable rate[85]. Then three equations are obtained that can be solved for $u'$, $r'$, $T_o'$ as a function of time. Statistical techniques can then be used to obtain statistical quantities of interest.

To insure that the solution to the three equations are sufficiently accurate, the three wires are operated at different and high overheats to make $S_u$ and $S_r$ as different as possible. This will insure that the condition number for the solution matrix is reasonably low. A complete description of this technique is given in references 85 and 86.

Some experimenters have conducted tests[8,170] where $S_u = S_r$ in transonic flows. For these tests a set of equations similar to those given by Morkovin for a CCA were derived for a CTA.

The functional relationship for the voltage across a wire for subsonic slip flows is identical to the functional relationship for transonic flow. Therefore, the three wire probe technique under development for transonic flows should be applicable for both regimes. Since slip flows are identified by the Knudsen number, the possibility of obtaining useful measurements using a three wire probe might be improved by using different diameter wires in addition to using different overheats.

<u>Hot-Wire Calibration</u>

Evaluating the required partial derivatives requires care when carrying out the mean flow calibration. For example, consider Morkovin's equations (42-45). The evaluation of $(\partial \log Nu_t / \partial \log Re_t)_{M,q}$ must be obtained by varying $p_o$ only and the Mach number, $q$, and the total temperature must be held constant. On the other hand, the evaluation of $(\partial \log Nu_t / \partial \log M)_{Re_t,q}$ requires that the total pressure be changed when the Mach number is varied in order to maintain $Re_t$ constant. Similar constraints also must be observed when $(\partial \log h / \partial \log Re_t)_M$ and $(\partial \log h / \partial \log M)_{Re_t}$ are evaluated. Similar care must also be taken in evaluating the partial derivatives when using other dependent and independent variables. Some of these variations and their constraints makes the operation of wind tunnels very time consuming if an accurate mean flow calibration is to be obtained.

If $Nu_t$ is assumed to be a $f(M_\infty, Re_t, q)$, the above described constraints applied, and the operational envelope of the facility considered, there is a skewing of the $Nu_t$ vs. $Re_t$ curves for constant Mach numbers because $Re_t = f(u, r)$ (figure 18b)[171]. Because of this, the region over which the partial derivation can be evaluated is reduced due to this skewing. If $Nu_t$ is assumed to be a $f(M_\infty, Kn, t_w)$, plots of $Nu_t$ vs. $Kn$ for constant Mach number is not as skewed and a more complete set of derivatives can be evaluated from a given number of data points (figure 37). This efficient use of data can also be obtained for $E = f(u, r, T_o)$ with the wire voltage correlated in term of these primitive variables. The use of $t_w$ as an independent variable can cause

extra complications in the calibration of wires when $h$ varies with $M$ or $Re_t$. Under these conditions the wire temperature must be changed when $h$ varies to hold $t_w$ constant[110].

Based on past experience[85,172-175], the following method appears to provide a reasonable technique for correlating data to obtain the required sensitivities. Consider the correlation of Nusselt number for the situation where $Nu_t = f(M, Kn, t_w)$. First the measured variation of $Nu_t$ with one independent variable must be obtained with the other independent variables held constant. The variation of $Nu_t$ with the remaining independent variables must be obtained under the same constraints. After these data are obtained, $Nu_t$ must be curve fit to one of the independent variables, say $Kn$, for all constant values of $M$ and $t_w$. The curve fitting process will, in general, result in $\P \log Nu_t / \P \log Kn = f(M, Kn, t_w)$. This method must be used to obtain other partials ie., $\P \log Nu_t / \P \log M = f(M, Kn, t_w)$ and $\P \log Nu_t / \P \log t_w = f(M, Kn, t_w)$. A similar technique should be used to obtain $\P \log h / \P \log Kn$ and $\P \log h / \P \log M$. After the partial derivatives are obtained, the sensitivities, i.e., $S_u$, $S_r$ and $S_{T_o}$ can be determined. Each of these sensitivities will, in general, be functions of all the independent variables. Spangenberg published the only data known to the authors which were obtained under the above constraints. He presented the Nusselt number as a function of $M$, $r$, and $t$ but for a given diameter wire $r$ and $Kn$ are reciprocals of each others. An example of the sensitivities obtained for one set of Spangenberg data is presented in figures 38a-c. These figures shows that each sensitivity, is in general, a function of the three independent variables.

## Examples of Data

### a. Freestream

Mean flow measurements were made in the transonic and slip flow regime in the 1950's[35,110]. It was only during the 1970's and 1980's that attempts were made to measure[8,49,85,86,170] fluctuations in these regimes because of the complexity of the response of the heated wire to velocity, density and total temperature.

In order to evaluate the effect of free stream fluctuations on boundary layer transition, hot-wire measurements were made in the Langley Research Center 8' Transonic Pressure Tunnel during the Laminar Flow Control experiments[86]. For these flow conditions $S_u \neq S_r$ with $S_u < S_\rho$. Because of this situation a three wire probe was used to measure $\tilde{u}/u$, $\tilde{r}/r$, $\tilde{T}_o/T_o$ and $\tilde{m}/m$ and examples of these measurements are presented in figure 39a-d. (Also see ref. 176-178).

### b. Boundary Layer

Horstman and Rose[170] made measurements at transonic speeds where, for their flow condition, it was found that $S_u \approx S_r$. For this condition the transonic hot-wire problem degenerated to the supersonic flow problem where only $\tilde{m}/m$, $\tilde{T}_o/T_o$ and $R_{mT_o}$ could be measured. From their measurement of $\tilde{m}/m$, the velocity and density fluctuations were computed by assuming that $\tilde{T}_o/T_o$ and $\tilde{p}/p$ were zero. An example of these results is presented in figure 40. In this figure Horstman and Rose's hot-wire results, represented by the circles, are compared with the thin film results obtained by Mikulla[170].

### c. Flight in Atmosphere

Any attempts to extrapolate the effect of wind tunnel disturbances on laminar boundary layer transition to flight conditions requires some knowledge of the disturbance levels in the atmosphere. Much of the fluctuation data obtained in the atmosphere was measured using sonic anemometers on towers[179]. There was a limited amount of data obtained in the atmosphere using hot-wire anemometry on flight vehicles[49,180]. Otten et. al.,[49] expanded the methods devised by Rose and McDaid by using a two wire probe. One wire was operated by a CCA at a low over heat to measure $\tilde{T}_o$. The other wire was operated with a CTA that was sensitive to $\tilde{m}$ and $\tilde{T}_o$. The results from these two wires were used to measure $\tilde{m}$ and $\tilde{T}_o$ in the atmosphere. An example of spectral data obtained in the atmosphere is presented in figure 41 and reveals the expected $-5/3$ slope, for $\tilde{m}$ and $\tilde{T}_o$.

**d. Subsonic Slip Flow**

**For this regime** $Nu_t = f(M_\infty, Re_t, t_w)$ **and** $S_u \neq S_r$**. These results are identical to those in the transonic flow regime and attempts have been made to apply the three wire technique developed for transonic flows to subsonic slip flows. For tests in subsonic slip flows the three wires were of different diameters in addition to being operated at different overheats. Some very preliminary data obtained using this technique in the Langley LTPT tunnel is presented in figure 42a-b where comparison with results obtained using King's equation are made.**

## HIGH SUPERSONIC AND HYPERSONIC FLOW

### Theoretical Consideration

**a. Constant Current Anemometer**

**In the 1950's and 1960's hot-wire anemometry was extended into the high supersonic and hypersonic flow regime[6,7,181,182]. For high supersonic flows it was found experimentally that** $S_u = S_r$ **and equation (42) becomes:**

$$\frac{e'}{E} = -S_m \frac{m'}{m} + S_{T_o} \frac{T_o'}{T_o} \qquad (49)$$

**Dividing equation (49) by the total temperature sensitivity, squaring, and then taking the mean results in the following equation:**

$$\overline{f'^2} = r^2 \overline{\left(\frac{m'}{m}\right)^2} - 2rR_{mT_o}\left(\frac{\tilde{m}}{m}\right)\left(\frac{\tilde{T}_o}{T_o}\right) + \overline{\left(\frac{T_o'}{T_o}\right)^2} \qquad (50)$$

**This equation was derived by Kovasznay[6] and used to generate fluctuation diagrams for supersonic flows. This equation was also used in references 167 and 168 for subsonic compressible flows. The general form of equation (50) is a hyperbola where the intercept on the** $f$ **-axis represents the total temperature fluctuation and the asymptotes represent the mass flow fluctuation[7].**

**Kovasznay demonstrated that the basic linear perturbation in compressible flows consists of vorticity, entropy and sound. He termed these basic fluctuations as "***modes***". If the fluctuation diagram is assumed to consist of a single mode the diagrams were termed "***mode diagrams***". An example of a general fluctuation diagram and the various mode diagrams for supersonic flow are presented in figures 43 and 44.**

**b. Constant Temperature Anemometer**

**For this case equation (42) becomes:**

$$\frac{e'}{E} = S_m \frac{m'}{m} + S_{T_o} \frac{T_o'}{T_o} \qquad (51)$$

**This is a single equation in two unknowns and a two wire probe can be used to obtain** $m'$**,** $T_o'$ **and** $m'T_o'$ **similar to the compressible subsonic flow case[61,183,184].**

### Examples of Data

**a. Freestream**

**In order to evaluate the relative "***goodness***" of supersonic wind tunnels and to relate the levels of disturbances in the test section to laminar boundary layer transition on models, a large amount of hot-wire measurements were made in the test sections of supersonic and hypersonic wind tunnels. In 1961 Laufer[185] presented measurements made in the test section of the Jet Propulsion Laboratory 18 x 20 inch supersonic wind tunnel over a Mach number range from 1.6 to 5.0 using CCA. An example of the fluctuation diagrams obtained by Laufer is presented in figure 45. From these diagrams the mass flow and total temperature fluctuations were obtained. Examples of the mass flow fluctuations are presented in figure 46a. There was a significant increase of** $\tilde{m}/m$ **with Mach number ranging from 0.07% at** $M = 1.6$ **to about 1.0 to 1.35% at** $M = 5.0$**, depending on Reynolds number. All of the fluctuation diagrams were straight lines and Laufer demonstrated that these results indicated that the fluctuations were predominantly pressure fluctuations due to sound. Examples of the calculated pressure fluctuations are presented in figure 46b. Laufer concluded that the pressure fluctuations originated at the turbulent boundary on the wall of the tunnel and because of the finite value of the temperature fluctuations the sound source had a finite velocity. An example of the sound source velocities is presented in figure 47.**

**A large amount of hot-wire data was taken in the freestream of various facilities to measure**

disturbance levels in efforts to develop quiet supersonic wind tunnels. A review of this effort was reported in reference 186.

Measurements in the freestream of the Langley Research Center Mach 20 High Reynolds number Helium Tunnel were performed by Wagner and Weinstein[181]. All of their fluctuation diagrams were straight lines similar to the results obtained in supersonic flows. Examples of their measured mass flow and total temperature fluctuations are presented in figure 48. The mass flow fluctuations were substantially higher than the values measured by Laufer at $M = 5.0$. Pressure fluctuation measurements presented in figure 49 indicate that at low total pressures the boundary layer on the nozzle wall was probably transitional at the acoustic origin of the sound source. Relative sound source velocities are presented in figure 50. The source velocities for the Mach 20 tunnel at the higher pressures are significantly higher than those measured by Laufer at Mach numbers up to 5. (Also see ref. 187).

b. Boundary Layer

Measurements were made in supersonic and hypersonic turbulent boundary layers to extend the range of Reynolds stress measurements needed in the development of turbulent boundary layer theories. Barre et. al.,[162] conducted hot-wire tests in a supersonic boundary layer where transonic effects were accounted for by using a transformation of equation (42-45) from $u$, $r$, $T_o$ to $p$, $m$, and $T_o$. Using the assumption that $E = f(p, m, T_o)$ and $\tilde{p}/p \approx 0$, reduced their equation to $E = f(m, T_o)$. Under these condition the fluctuation diagram developed by Kovasznay was used to obtain $\tilde{m}/m$, $\tilde{T}_o/T_o$ and $R_{mT_o}$ without the assumption that $S_u = S_r$.

Examples of their results are presented in figures 51 and 52. Figure 51 shows that the quantity $\sqrt{ru'^2/t_w}$ is greatly underestimated if the assumption is made that $S_u = S_r$ when the velocity in the boundary is transonic and $S_u \neq S_r$. Figure 52 show the variation of $R_{uT_o}$ with the local Mach number through the boundary layer. The expected value for $R_{uT_o}$ is -0.85 and the data obtained for $S_u \neq S_r$ agrees well with this value. However, data evaluated where $S_u$ was assumed to be equal to $S_r$ were substantially higher at the lower transonic Mach numbers.

Fluctuations in a hypersonic boundary layer were made by Laderman and Demitrades[182] and reported in reference 188. An example of the mass flow and total temperature fluctuations measured across the boundary layer is presented in figure 53. The velocity, density, static temperature, and pressure fluctuations were calculated using the mass flow and total temperature fluctuations and various assumptions. An example of these measurements is presented in figures 54 and 55.

Additional measurements were made in hypersonic boundary layers by Laderman[189] and on an ogive cylinder by Owen and Horstman[59] at $M \approx 7.0$. The measurements made by Owen and Horstman included not only data for $\tilde{m}$, $\tilde{T}_o$ and $R_{mT_o}$ but integral scales and microscales, probability density distributions, skewness, kurtosis and intermittancy distribution across the boundary layer. A summary paper by Owen[190] presents additional data which included space-time correlation, convective velocities, disturbance inclination angle, and turbulence life time distributions. (Also see ref. 87, 191-196).

c. Wake

An example of fluctuation diagrams measured in the wake behind a 15° half angle wedge at $M = 15.5$ is presented in figure 56. From these results Wagner and Weinstein concluded that the predominant fluctuation in this wake was entropy since the fluctuation diagrams were straight lines that intersected the $r$-axis at approximately $-a$.

d. Downstream of Shock

In supersonic and hypersonic flows the disturbances measured in the freestream of the test section are not necessarily the disturbances that can affect the transition of the laminar boundary layer on a body. The passage of sound waves through shocks will result in a combination of vorticity, entropy, and sound downstream of the shock[197]. Because of this the fluctuation diagram will no longer be a straight line but a general

hyperbola[48]. An example of this result is presented in figure 57. (Also see ref. 198-201).

## CONFIRMATION OF THEORETICAL RESULTS

Hot-wire anemometry was used extensively to validate or confirm theoretical results. Some examples of these efforts are presented below.

Theoretical studies of the stability of laminar boundary layers to small disturbances were initially performed by Tollmein[202,203] and Schlichting[204]. These calculations indicated that disturbances of a given frequency could decrease, remain constant or be amplified depending on the frequency chosen and the Reynolds number. The first experimental verification of the theory was made by Schubauer and Skramstad[135]. An example of recent experimental and theoretical results for the determination of the neutral stability boundary[205] in a laminar boundary layer is presented in figure 58.

Hot-wire measurements were made downstream of "*grids*" to evaluate the theory for the decay of turbulence. Tests conducted by Kistler and Vrebalovich[206] to evaluate the "*linear*" decay law is presented in figure 59 and confirm this law for large values of the Reynolds number. At lower Reynolds number[25] the exponent can be closer to 1.20 - 1.25. Measurements of spectra for velocity fluctuations downstream of grids was also made and compared with theory. Two examples of these spectra are presented[206,207] in figure 60a-b. The spectra in figure 60a had an insignificant amount of energy in the expected inertial sub-range indicated by a slope of $-5/3$. This result was attributed to the low Reynolds number of the flow. The spectra presented in figure 60b was measured in a high Reynolds number flow and revealed a significant amount of energy in the inertial sub-range. Theoretical calculations were made for the temperature spectra in a heated jet and downstream of a heated grid. An example of the theory and measurements[207] is presented in figure 61. Attempts have been made to predict the influence of measured freestream fluctuations on laminar boundary transition. An example of this efforts[208] is presented in figures 62.

A considerable amount of data was obtained by Stetson et. al.,[209] in hypersonic flow to study the stability of laminar boundary layer. An example of these results are presented in figure 63 and indicates the existence of first and second mode instabilities in the laminar boundary layer. These results were in agreement with those obtained by Kendall[155] and Demetriades[210] and was in qualitative agreement with the theoretical results obtained by Mack[156].

## OTHER APPLICATIONS

Hot-wire anemometry was used in shock tubes in an attempt to check the frequency response of probes and to trigger other events[52,211].

Theoretical results indicated that there would be "*temperature fronts or steps*" in cryogenic wind tunnels due to the injection of liquid nitrogen into the circuit. Measurements were made using a hot-wire anemometer to determine the possible occurrences of these thermal steps[53].

A pulsed hot-wire was used to measure the velocities and flow angle in low speed flows[212]. A wire, which was operated by an anemometer, was place in the wake of a second wire which could be alternately heated. The time lag between heating the forward wire, this pulse being detected by the second wire and the distance between the wires was used to compute the velocity of the flow. In reference 213 a somewhat different technique was described that used two CCA's and a CTA to measure the velocity and flow angle.

Hot-wire anemometry was used to obtain the location of transition in a laminar boundary in addition to obtaining some information on the fluctuations in the laminar, transitional and turbulent boundary layers[214,215]. In some flows where the fluctuation levels are high, such as a jet, a moving hot-wire probe was found to improve the accuracy of the results[216]. This technique is usually noted as flying hot-wire anemometry. (Also see ref. 217-221).

Hot-wire anemometry was used[222] to measure the focal points of the laser beams for

Laser Transit anemometry (LTA) . Using a traversing mechanism and a CTA, the distance between the two beams was determined by measuring the difference between the two maximum voltage outputs from the anemometer. It was noted that additional information could be obtained such as the mean value of the beam intensity intersected by the wire, laser beam power, beam separation, beam diameter, beam divergence, cross-sectional beam-intensity distribution and relative beam intensity.

## CONDITIONAL SAMPLING

Organized motion or structures in a turbulent boundary layer has been extensively studied[20,223-225] using the concept of conditional sampling. The flow of a turbulent boundary layer over a concave surface was studied in reference 226 to search for organized motion in the boundary layer. The possible existence of organized motion is illustrated in figure 64 from measurements made with two hot-wire probes located $0.1d$ apart. The conditional sampling technique was used to determine the characteristic shape of the mass flow signal during the passage of an organized motion. An example of these results are presented in figure 64. Figure 65 shows that the measured event at an upstream and a downstream station had the same general characteristic shape.

## COMPARISON OF HOT-WIRE MEASUREMENTS WITH OTHER TECHNIQUES

In the past the hot-wire anemometer, with all its limitations, was the only instrument available that was capable of measuring fluctuations with adequate fidelity[12]. To some extent, this is no longer the case as other techniques such as LV, LIF, CARS, and Raman scattering are now available for measuring various mean flow and fluctuating quantities. In inviscid flow where the fluctuations can be low, the anemometer is presently the only reliable instrument available. Compared to other techniques the anemometer is still relatively simple to operate and relatively inexpensive. Because of its long history, the results obtained using anemometry is still often used as a standard for evaluating measurements obtained using other techniques. The extent to which the anemometer can maintain these advantages depends on the continued development of the other techniques.

Tests were conducted in turbulent boundary layers to compare hot-wire results with other techniques to validate hot-wire/laser velocimeter (LV)[227,228] and hot-wire/laser-induced fluorescence (LIF)[229] techniques. An example of velocity fluctuations obtained using hot-wire anemometer and a LV system is presented in figure 66 for streamwise velocity fluctuations. The agreement between the two sets of data is very good. Measured density and static temperature fluctuations measured with a hot-wire and a LIF system in a turbulent supersonic boundary layer is presented in figure 67. Again, except for two values for the density fluctuation obtained with the LIF system, the agreement between the two sets of data is very good. Various experiments were made using LIF and LIF/RAMAN techniques to measure $\tilde{T}_o / T_o$ and $\tilde{r}/r$ where results were compared with hot-wire measurements[228]. An example[230] of these results is presented in figure 68. The only disagreement between the hot-wire and the other results was attributed to a shock that apparently did not cross the hot-wire probe.

## CONCLUDING REMARKS

A review was made to illustrate the versatility of hot-wire anemometry in addition to noting some of its limitations. The review included examples of results obtained in the various flow regimes and various types of flow fields. Examples of data were presented for the subsonic incompressible flow regime that were used to evaluate the flow quality in the test section of wind tunnels, to obtain measurements in turbulent boundary layer, and to substantiate or validate various theories of turbulence.

Recently attempts to extend hot-wire anemometry into the transonic and subsonic slip flow regimes were presented for cases where $S_u = S_r$ and $S_u \neq S_r$. Examples of data obtained at high supersonic and hypersonic Mach numbers were presented. These results revealed that the fluctuation diagrams measured in the test section

**were a straight line, indicating that the disturbances in the test sections were due to sound mode.**

**Examples were also presented to illustrate measurements made to substantiate turbulent theories, to compare with other techniques, and to illustrate the concept of conditional sampling.**


## ACKNOWLEDGMENT

**The authors acknowledge the support of this research by the National Aeronautics and Space Administration under contracts NAS1-19320 and NAS1-19672 respectively.**


## REFERENCES


1. **Comte-Bellot, G., 1977,** "*Hot-Wire and Hot-Film Anemometers*," **Measurement of Unsteady Fluid Dynamic Phenomena, Hemisphere Publishing Co., pp. 123-162.**

2. **Boussinesq, J., 1905,** "*An Equation for the Phenomena of Heat Convection and an Estimate of the Cooling Power of Fluids*," **Journal de Mathematiques, Vol. 1, pp. 285-332, also ComptesRendus, Vol. 133, pp. 257.**

3. **King, L.V., 1914,** "*On the Convection of Heat from Small Cylinders in a Stream of Fluid*," **Phil. Trans. of Roy. Soc. (London), Ser. A. Vol. 214, No. 14, pp. 373-432.**

4. **Dryden, H.L., and Kuethe, A.M., 1929,** "*The Measurement of Fluctuations of Air Speed by the Hot-Wire Anemometer*," **NACA-TR-320.**

5. **Ziegler, M., 1934,** "*The Construction of a Hot-Wire Anemometer with Linear Scale and Negligible Lag*," **Proc. K. Ned. Akad. Wet. 15, No. 1.**

6. **Kovasznay, L.S.G., 1950,** "*The Hot-Wire Anemometer in Supersonic Flows*," **Journal of the Aeronautical Sciences, Vol. 17, No. 9, pp. 565-584.**

7. **Kovasznay, L.S.G., 1953,** "*Turbulence in Supersonic Flow*," **Journal of the Aeronautical Sciences, Vol. 20, No. 10, pp. 657-674.**

8. **Rose, W.C., and McDaid, E.P., 1976,** "*Turbulence Measurement in Transonic Flow*," **Proceedings of the AIAA 9th Aerodynamic Testing Conference, Arlington, Texas.**

9. **Sandborn, V.A., 1974,** "*A Review of Turbulence Measurements in Compressible Flow*," **NASA-TMX-62337.**

10. **Baldwin, L.V., Sandborn, V.A., and Laurence, J.C., 1960,** "*Heat Transfer from Transverse and Yawed Cylinders in Continuum, Slip, and Free Molecule Air Flows*," **Journal of Heat Transfer, Transaction of ASME, C82, pp. 77-86.**

11. **Vagt, J.D., 1979,** "**H***ot-Wire Probes in Low Speed Flow*," **Progress in Aerospace Sciences, Vol. 18, pp. 271-323.**

12. **Kovasznay, L.S.G., 1959,** "*Turbulence Measurements*," **Applied Mechanics Reviews, Vol. 12, No. 6, pp. 375-380.**

13. **Owen, F.K., and Foire, A.W., 1986,** "*Principles and Practices of Hot-Wire Anemometers*," **Complere Inc., Palo Alto, CA.**

14. **Laufer, J., 1975,** "*New Trends in Experimental Turbulent Research*," **Annual Review of Fluid Mechanics, Vol. 7, pp. 307-326.**

15. **Olivari, D., 1980,** "*Hot Wire Techniques: Conditional Sampling and Intermittency*," **Von Karman Institute for Fluid Dynamics, Lecture Series - 3, Measurements and Predictions of Complex Turbulent Flows.**

16. **Ardonceau, P., 1980,** "*Turbulence Measurements in Supersonic Flows*," **Von Karman Institute for Fluid Dynamics, Lecture Series - 3, Measurements and Predictions of Complex Turbulent Flows.**

17. **Proceedings of the Dynamic Flow Conference on Dynamic Measurements in Unsteady Flow, 1978, Editors: Kovasznay, L.S.G., Favre, A., Buchhave, P., Fulachier, L., and Hansen,**

**B.W.H., IMST, Marseille, France, John Hopkins University Baltimore, MD, Sept. 11-14, 1978.**

18. **The Heuristics of Thermal Anemometry, 1990, ASME-FED Vol. 97, Editors: Stock, D.E., Sherif, S.A., and Smits, A.J., The 1990 Spring Meeting of the Fluids Engineering Division, University of Toronto, Toronto, Ontario, Canada, June 4-7.**

19. **Symposium on Thermal Anemometry, 1987, Editor: Stock, D.E., 1987, ASME-FED Vol. 53, The 1987 ASME Applied Mechanics, Bioengineering, and Fluids Engineering Conference, Cincinnati, Ohio, June 14-17.**

20. **Comte-Bellot, G., Charnay, G., and Sabot, J., 1981,** "*Hot-Wire and Hot-Film Anemometry and Conditional Measurements: A Report on Euromech 132*," **Journal of Fluid Mechanics, Vol. 110, pp. 115-128.**

21. **Sandborn, V.A., 1972,** "*Resistance Temperature Transducers*," **Metrology Press, Fort Collins, Colorado.**

22. **Perry, A.E., 1982,** "*Hot-Wire Anemometry*," **Oxford:Clarendon Press.**

23. **Lomas, C.G., 1986,** "*Fundamentals of Hot-Wire Anemometry*," **Cambridge University Press.**

24. **Goldstein, R.J., 1983,** "*Fluid Mechanics Measurements*," **Hemisphere Publishing Corporation.**

25. **Hinze, J.O., 1975,** "*Turbulence*," **McGraw-Hill Book Co., New York.**

26. **Smol'yakov, A.V., and Tkachenko, V.M., 1983,** "*The Measurement of Turbulent Fluctuations : An Introduction of Hot-Wire Anemometry and Related Transducers*," **Springer-Verlag, New York.**

27. **Bradshaw, P., 1971,** "*An Introduction to Turbulence and Its Measurement*," **Pergamon Press, New York.**

28. **Blackwelder, R.F., 1981,** "*Hot-Wire and Hot-Film Anemometers*," **Methods of Experimental Physics: Fluid Dynamics, Editor: Emrich, R.J., Vol. 18, Part A, Academic Press Inc., New York.**

29. **Corrsin, S., 1963,** "*Turbulence: Experimental Methods*," **Handbook of Physics, 8/2, pp. 523-590.**

30. **Kovasznay, L.S.G., 1954,** "*Methods to Distinguish Between Laminar and Turbulent Flow*," **Article F-1, Volume IX, Physical Measurements in Gas Dynamics and Combustion, Princeton University Press, pp. 213-285.**

31. **Sauer, F.M., and Drake, Jr., R.M., 1953,** "*Forced Convection Heat Transfer from Horizontal Cylinders in a Rarefied Gas*," **Journal of the Aeronautical Sciences, Vol. 20, pp. 175-180, 209.**

32. **Weltmann, R.N., and Kuhns, P.W., 1960,** "*Heat Transfer to Cylinders in Crossflow in Hypersonic Rarefied Gas Streams*," **NASA-TND-267.**

33. **Standler, J.R., Goodwin, G., and Creager, M.O., 1951,** "*A Comparison of Theory and Experiment for High-Speed Free-Molecule Flow*," **NACA Rep. 1032 (Supersedes NACA-TN-2244).**

34. **Kennard, E.H., 1938,** "*Kinetic Theory of Gases*," **McGraw-Hill Book Co., Inc.**

35. **Baldwin, L.V., 1958,** "*Slip-Flow Heat Transfer From Cylinders in Subsonic Airstreams*," **NACA-TN-4369.**

36. **Dryden, H.L., and Kuethe, A.M., 1930,** "*Effect of Turbulence in Wind Tunnel Measurements*," **NACA-TR-342.**

37. **Stainback, P.C., and Owen, F.K., 1984,** "*Dynamic Flow Quality Measurements in the Langley Low Turbulence Pressure Tunnel*," **AIAA-84-0621.**

38. **Schubauer, G.B., Spangenberg, W.G., and Klebanoff, P.S., 1950,** "*Aerodynamic Characteristics of Damping Screens*," **NACA-TN-2001.**

39. **Klebanoff, P.S., Tidstrom, K.D., and Sargent, 1962,** "*The Three-Dimensional Nature of Boundary-Layer Instability*," **Journal of Fluid Mechanics, Vol. 12, pp. 1-37.**

40. **Laufer, J., 1954,** "*The Structure of Turbulence in Fully Developed Pipe Flow*," **NACA Report 1174.**

41. **Sandborn, V.A., 1955,** "*Experimental Evaluation of Momentum Terms in Turbulent Pipe Flow*," **NACA-TN-3266.**

42. **Sandborn, V.A., and Slogar, R.J., 1955,** "*Longitudinal Turbulent Spectrum Survey of Boundary Layers in Adverse Pressure Gradients*," **NACA-TN-3453.**

43. **Townsend, A.A., 1949,** "*The Fully Developed Turbulent Wake of a Circular Cylinder*," **Australian Journal of Scientific Research, Series A, Physical Sciences, Vol. 2, pp. 451-468.**

44. **Uberoi, M.S., and Freymuth, P., 1969,** "*Spectra of Turbulence in Wakes Behind Circular Cylinders*," **The Physics of Fluids, Vol. 12, No. 7, pp. 1359-1363.**

45. **Miksad, R.W., Jones, F.L., Powers, E.J., Kim, Y.C., and Khadra, L., 1982,** "*Experiments on the Role of Amplitude and Phase Modulations During Transition to Turbulence*," **Journal of Fluid Mechanics, Vol. 123, pp. 1-29.**

46. **Wygnanski, I., and Fiedler, H., 1969,** "*Some Measurements in the Self-Preserving Jet*," **Journal of Fluid Mechanics, Vol. 38, Part 3, pp. 577-612.**

47. **Corrsin, S., 1943,** "*Investigation of Flow in an Axially Symmetrical Heated Jet of Air*," **NACA-WR-W-94, (Issued as: NACA-ACR-3L23).**

48. **Weinstein, L.M., 1972,** "*Oblique Shock-Sound Interaction at $M_\infty \cong 20$ in Helium*," **AIAA Journal, Vol. 10, No. 12, pp. 1718-1720.**

49. **Otten, L.J., Pavel, A.L., Finley, W.E., and Rose, W.C., 1981,** "*A Survey of Recent Atmospheric Turbulence Measurements from a Subsonic Aircraft*," **AIAA-81-0298.**

50. **Okiishi, T.H., and Schmidt, D.P., 1978,** "*Measurement of the Periodic Variation of Turbomachine Flow Fields*," **Proceedings of the Dynamic Flow Conference, pp. 249-269.**

51. **Wilkinson, S.P., and Malik, M.R., 1985,** "*Stability Experiments in the Flow over a Rotating Disk*," **AIAA Journal, Vol. 23, No. 4, pp. 588-595.**

52. **Darshan, S.D., 1953,** "*Use of a Hot-Wire Anemometer as a Triggering and Timing Device for Wave Phenomena in a Shock Tube*," **Ph.D., Thesis, Part I and II, JohHopkins University.**

53. **Johnson, C.B., and Stainback, P.C., 1984,** "*A Study of Dynamic Measurements Made in the Settling Chamber of the Langley 0.3-Meter Transonic Cryogenic Tunnel*," **AIAA-84-0596.**

54. **Kovasznay, L.S.G., 1978,** "*Measurement in Intermittent and Periodic Flow*," **Proceedings of the Dynamic Flow Conference, pp. 133-159.**

55. **Blackwelder, R.F., 1978,** "*Pattern Recognition of Coherent Eddies*," **Proceedings of the Dynamic Flow Conference, pp. 173-190.**

56. **Wagner, T.C., and Kent, J.C., 1987,** "*Measurement of Intake Valve/Cylinder Boundary Flows Using a Multiple Orientation Hot-Wire Technique*," **Symposium on Thermal Anemometry, ASME-FED Vol. 53, pp. 79-85.**

57. **Mangalam, S.M., Sarma, G.R., Kuppa, S., and Kubendran, L.R., 1992,** "*A New Approach to High-Speed Flow Measurements Using Constant Voltage Anemometry*," **AIAA-92-3957.**

58. **Morkovin, M.V., 1956,** "*Fluctuations and Hot-Wire Anemometry in Compressible Flows*," **AGARDograph 24.**

59. **Owen, F.K., and Horstman, C.C., 1974,** "*Turbulence Measurements in an Equilibrium Hypersonic Boundary Layer*," **AIAA-74-0093.**

60. **Bonnet, J.P., and Alziary de Roquefort, T., 1980,** "*Determination and Optimization of Frequency Response of Constant Temperature Hot-Wire Anemometers in Supersonic Flows*," **Rev. Sci. Instrum. Vol. 51, No. 2, pp. 234-239.**

61. **Walker, D.A., Ng, W.F., and Walker, M.D., 1989,** "*Experimental Comparison of Two Hot-Wire Techniques in Supersonic Flow*," **AIAA Journal, Vol. 27, No. 8, pp. 1074-1080.**

62. **Weinberg, B.C., and Laderman, S., 1969,** "*Constant Current Anemometer Diagnostics of Flow Fields*," **Contract No. Nonr-839(38), Report of Aerospace Engineering and Applied Mechanics, Polytechnic Institute of Brooklyn.**

63. **Kidron, I., 1967,** "*The Signal-to-Noise Ratio of Constant-Current and Constant-Temperature Hot-Wire Anemometers*," **IEEE Transaction on Instrumentation and Measurement, Vol 1M-16, No. 1, pp. 68-73.**

64. **Lowell, H.H., 1950,** "*Design and Application of Hot-Wire Anemometers for Steady-State Measurements at Transonic and Supersonic Airspeeds*," **NACA-TN-2117.**

65. **Ram, V.V., 1992,** "*On the Effects of Fluid Temperature on Hot-Wire Characteristics. Part 2: Foundations of a Rational Theory*," **Experiments in Fluids, Vol. 13, pp. 267-278.**

66. **Frenkiel, F.N., 1954,** "*Effect of Wire Length in Turbulence Investigation with Hot-Wire Anemometer*," **The Aeronautical Quarterly, Vol. V, pp. 1-24.**

67. **Dreksen, R.W., and Azad, R.S., 1983,** "*An Examination of Hot-Wire Length Corrections*," **The Physics of Fluids, Vol. 26, No. 7, pp. 1751-1754.**

68. **Larsen, S., and Hojstrop, J., 1982,** "*Spatial and Temporal Resolution of a Thin-Wire Resistance Thermometer*," **Journal of Physics, Series E - Scientific Instruments, Vol. 15, pp. 471-477.**

69. **Westpal, R.V., 1990,** "*Near-Wall Measurement Errors For Hot-Wire Probes with Finite Spatial Resolution*," **The Heuristics of Thermal Anemometry, ASME-FED Vol. 97, pp. 1-8.**

70. **Hebbar, K.S., 1980,** "*Wall Proximity Correction for Hot-Wire Readings in Turbulent Flows*," **DISA Information No. 25, pp. 15-16.**

71. **Kanevce, G., and Oka, S., 1973,** "*Correcting Hot-Wire Readings for Influence of Fluid Temperature Variation*," **DISA Information No. 15, pp. 21-24.**

72. **Martinez-Val, R., Jimenez, J., and Rebollo, M., 1982,** "*Sensor Contamination Effects in Hot-Wire Anemometry in Air*," **DISA Information No. 27, pp. 12-14.**

73. **Paranthoen, P., Lecordier, J.C., and Petit, C., 1982,** "*Influence of Dust Contamination on Frequency Response of Wire Resistance Thermometers*," **DISA Information No. 27, pp. 36-37.**

74. **Drubka, R.E., Tan-Atichat, J., and Nagib, H.M., 1977,** "*Analysis of Temperature Compensating Circuits for Hot-Wires and Hot-Films*," **DISA Information No. 22, pp. 5-14.**

75. **Oka, S., and Kostic, Z., 1972,** "*Influence of Wall Proximity on Hot-Wire Velocity Measurements*," **DISA Information No. 13, pp. 29-33.**

76. **Klatt, F., 1973,** "*A Study of Systematic Errors in Measurements with the Constant-Temperature Anemometer in High-Turbulence Flow With and Without Hot-Wire Signal Linearization*," **DISA Information No. 14.**

77. **Hardin, J.C., 1986,** "*Introduction to Time Series Analysis*," **NASA-RP-1145.**

78. **Bendat, J.S., and Piersol, A.G., 1985,** "*Random Data*," **A Wiley Interscience Publication.**

**79. Bruun, H.H., 1978,** "*Multi-Probes and Higher Moments*," **Proceedings of the Dynamic Flow Conference, pp. 943-961.**

**80. Frenkiel, F.N., and Klebanoff, P.S., 1967,** "*Higher-Order Correlation in a Turbulent Fluid*," **The Physics of Fluids, Vol. 10, No. 3, pp. 507-520.**

**81. Van Atta, C.W., 1978,** "*Multi Channel Measurements and High-Order Statistics*," **Proceedings of the Dynamic Flow Conference, pp. 919-941.**

**82. Frenkiel, F.N., and Klebanoff, P.S., 1967,** "*Correlation Measurements in a Turbulent Flow Using High-Speed Computing Methods*," **The Physics of Fluids, Vol. 10, No. 8, pp. 507-520.**

**83. George, W.K, 1978,** "*Processing of Random Signals* **(with appendices by Beuther, P.D., and Lumley, J.L.,),**" **Proceedings of the Dynamic Flow Conference, pp. 757-800.**

**84. Bendat, J.S., and Piersol, A.G., 1980,** "*Engineering Applications of Correlation and Spectral Analysis*," **A Wiley Interscience Publication.**

**85. Stainback, P.C., and Johnson, C.B., 1983,** "*Preliminary Measurements of Velocity, Density and Total Temperature Fluctuations in Compressible Subsonic Flow*," **AIAA-83-0384.**

**86. Jones, G.S., Stainback, P.C., Harris, C.D., Brooks, C.W., and Clukey, S.J., 1989,** "*Flow Quality Measurements for the Langley 8-Foot Transonic Pressure Tunnel LFC Experiment*," **AIAA-89-0150.**

**87. Owen, F.K., and Horstman, C.C., 1972,** "*Hypersonic transitional Boundary Layers*," **AIAA Journal, Vol. 10, No. 6, pp. 769-775.**

**88. Sato, H., 1951,** "*Experimental Study of the Spectrum of Isotropic Turbulence, I*," **Journal of Phys. Soc. Japan, Vol. 6, pp. 387-392. (Also, 1952,** "*Experimental Study of the Spectrum of Isotropic Turbulence, II*," **Journal of Phys. Soc. Japan, Vol. 7, pp. 392-396).**

**89. Champagne, F.H., 1978,** "*The Fine-Scale Structure of the Turbulent Velocity Field*," **Journal of Fluid Mechanics, Vol. 86, Part 1, pp. 67-108.**

**90. Uberoi, M.S., and Kovasznay, L.S.G., 1952,** "*On Mapping and Measurement of Random Fields*," **Vol. X, No. 4, pp. 375-393.**

**91. Gagne, Y., Hopfinger, E.J., and Marechal, J., 1978,** "*Measurements of Internal Intermittency and Dissipation Correlations in Fully Developed Turbulence*," **Proceedings of the Dynamics Flow Conference, pp. 271-277.**

**92. Schumann, U., and Patterson, G.S., 1978,** "*Numerical Study of Pressure and Velocity Fluctuations in Nearly Isotropic Turbulence*," **Journal of Fluid Mechanics, Vol. 88, part 4, pp. 685-709.**

**93. Artt, D.W., and Brown, A., 1971,** "*The Simultaneous Measurement of Velocity and Temperature*," **Journal of Physics E: Scientific Instruments, Vol. 4, pp. 72-74.**

**94. Davis, M.R., and Davies, P.O.A.L., 1972,** "*Factors Influencing the Heat Transfer from Cylindrical Anemometer Probes*," **Journal of Heat and Mass Transfer, Vol. 15, pp. 1659-1677.**

**95. Cimbala, J.M., and Park, W.J., 1990,** "*A Direct Hot-Wire Calibration Technique to Account for Ambient Temperature Drift in Incompressible Flow*," **Experiments in Fluids, Vol. 8, pp. 299-300.**

**96. Boman, U.R., 1992,** "*Hot-Wire Calibration Over a Large Temperature Range*," **Experiments in Fluids, Vol. 12, pp. 427-428.**

**97. Fulachier, L., 1978,** "*Hot-Wire Measurements in Low Speed Heated Flow*," **Proceedings of the Dynamic Flow Conference.**

**98. George, W.K., Beuther, P.D., and Shabbir, D., 1987,** "*Polynomial Calibrations for Hot-Wires in Thermally-Varying Flows*," **Symposium on Thermal Anemometry, ASME-FED Vol. 53, pp. 1-6.**

99. **McAdam, W.H., 1954,** "*Heat Transmission*," **McGraw-Hill Book Company Inc.**

100. **Kostka, M., and Ram, V.V., 1992,** "*On the Effects of Fluid Temperature on Hot Wire Characteristics. Part 1: Results of Experiments*," **Experiments in Fluids, Vol. 13, pp. 115-162.**

101. **Crimbala, J.M., and Pork, W.J., 1990,** "*A Direct Hot-Wire Calibration Technique to Account for Ambient Temperature Drift in Incompressible Flow*," **Experiments in Fluids, Vol. 8, pp. 299-300.**

102. **Haw, R.C., and Foss, J.F., 1990,** "*A Facility for Low Speed Calibration*," **The Heuristics of Thermal Anemometry, ASME-FED-Vol. 97, pp. 29-33.**

103. **Haw, R.C., Ali, S.K., and Foss, J.F., 1987,** "*Gravitationally Defined Velocities for a Low Speed Hot-Wire Calibration*," **Symposium on Thermal Anemometry, ASME-FED Vol. 53, pp. 7-14.**

104. **Collin, D.C., and Williams, M.J., 1959,** "*Two Dimensional Convection From Heated Wires at Low Reynolds Numbers*," **Journal of Fluid Mechanics, Vol. 6, pp. 357-384.**

105. **Andrews, G.E., Bradley, D., and Hardy, G.F., 1972,** "*Hot-Wire Anemometer Calibration for Measurements of Small Gas Velocities*," **Int. Journal of Heat and Mass Transfer, Vol. 15, pp. 1765-1786.**

106. **Bruun, H.H., 1971,** "*Interpretation of a Hot-Wire Signal using a Universal Calibration Law*," **Journal of Physics, E, Vol. 4, pp. 225-231.**

107. **Zabat, M., Browand, F.K., and Plocher, D.,** "*In-Situ Swinging Arm Calibration for Hot-Film Anemometers*," **Experiments in Fluids, Vol. 12, pp. 223-228.**

108. **Cole, J.D., and Roshko, A., 1954,** "*Heat Transfer from Wires at Reynolds Numbers in the Oseen Range*," **Proceedings Heat Transfer and Fluid Mechanics Institute, Stanford, California, pp. 13-24.**

109. **Laurence, J.C., and Landes, L.G., 1952,** "*Auxiliary Equipment and Techniques for Adapting the Constant-Temperature Hot-Wire Anemometer to Specific Problems in Air-Flow Measurements*," **NACA-TN-2843.**

110. **Spangenberg, W.G., 1955,** "*Heat Loss Characteristics of Hot-Wire Anemometers at Various Densities in Transonic and Supersonic Flows*," **NACA-TN-3381.**

111. **Vrebalovich, T., 1962,** "*Heat Loss From Hot-Wires in Transonic Flow*," **Research Summary No. 36-14, Jet Propulsion Lab., Pasadena, California.**

112. **Laufer, J., and McClellan, R., 1956,** "*Measurement of Heat Transfer from Fine Wires in Supersonic Flow*," **Journal of Fluid Mechanics, Vol. 1, pp. 276-289.**

113. **Corrsin, S., 1949,** "*Extended Applications of the Hot-Wire Anemometer*," **NACA-TN-1864.**

114. **Fiedler, H., 1978,** "*On Data Acquisition in Heated Turbulent Flows*," **Proceedings of the Dynamic Flow Conference, pp. 81-100.**

115. **Champagne, F.H., 1978,** "*The Temperature Sensitivity of Hot-Wires*," **Proceedings of the Dynamic Flow Conference, pp. 101-114.**

116. **Millikan, C.B., and Klein, A.L., 1933,** "*The Effect of Turbulence - An Investigation of Maximum Lift Coefficient and Turbulence in Wind Tunnels and in Flight*," **Aircraft Engineering, Vol. V, pp. 169-174.**

117. **von Doenhoff, A.E., and Abbott, F.T., 1947,** "*The Langley Two-Dimensional Low-Turbulence Pressure Tunnel*," **NACA-TN-1283.**

118. **Uberoi, M.S., 1956,** "*Effect of Wind-Tunnel Contraction on Free-Stream Turbulence*," **Journal of the Aeronautical Sciences, Vol. 23, No. 8, pp. 754-764.**

119. **Wigeland, R.A., Tan-atichat, J., and Nagib, H.M., 1981,** "*Evaluation of a New Concept for Reducing Freestream Turbulence in Wind*

*Tunnels*," **Journal of Aircraft, Vol. 18, No. 7, pp. 528-536, (also AIAA-80-0432R).**

120. **Scheiman, J., and Brooks, J.D., 1980,** "*A Comparison of Experimental and Theoretical Turbulence Reduction from Screens, Honeycomb and Honeycomb-Screen Combinations*," **AIAA-80-0433.**

121. **Dryden, H.L., and Abbott, I.H., 1949,** "*The Design of Low-Turbulence Wind Tunnels*," **NACA-R940.**

122. **Budwig, R., Tavoularic, S., and Corrsin, S., 1985,** "*Temperature Fluctuations and Heat Flux in Grid-Generated Isotropic Turbulence with Streamwise and Transverse Mean-Temperature Gradients*," **Journal of Fluid Mechanics, Vol. 153, pp. 414-460.**

123. **Warhaft, Z., and Lumley, J.L., 1978,** "*An Experimental Study of the Decay of Temperature Fluctuation in Grid-Generated Turbulence*," **Journal of Fluid Mechanics, Vol. 88, part 4, pp. 659-684.**

124. **Warhaft, Z., 1980,** "*On Experimental Study of the Effect of Uniform Strain on Thermal Fluctuations in Grid-Generated Turbulence*," **Journal of Fluid Mechanics, Vol. 99, part 3, pp. 545-573.**

125. **Tucker, M., 1953,** "*Combined Effect of Damping Screens and Stream Convergence on Turbulence*," **NACA-TN-2878.**

126. **Taylor, G.I., and Batchelor, G.K., 1949,** "*The Effect of Wire Gauze on Sound Disturbances in a Uniform Stream*," **Quarterly Journal of Mech. and Applied Math, Vol. II, part I, pp. 1-29.**

127. **Tucker, H.J., and Ali, S.F., 1973,** "*Decay of Anisotropic Turbulence*," **AIAA Journal, Vol. 11, No. 4, pp. 546-548.**

128. **Frenkiel, F.N., Klebanoff, P.S., and Huag, T.T., 1979,** "*Grid Turbulence in Air and Water*," **The Physics of Fluids, Vol. 22, No. 9, pp. 1606-1617.**

129. **Tucker, H.J., and Reynolds, A.J., 1968,** "*The Distortion of Turbulence by Irrotational Plane Strain*," **Journal of Fluid Mechanics, Vol. 32, part 4, pp. 657-673.**

130. **Durbin, P.A., 1982,** "*Analysis of the Decay of Temperature Fluctuations in Isotropic Turbulence*," **Physics of Fluids, Vol. 25, No. 8, pp. 1328-1332.**

131. **Klebanoff, P.S., 1954,** "*Characteristics of Turbulence in a Boundary Layer with Zero Pressure Gradient*," **NACA Report 1247 (Supersedes NACA-TN-3178).**

132. **Bardakhnov, S.P., Kozlov, V.V., and Larichkin, V.V., 1989,** "*Influence of an Acoustic Field on the Flow Structure Behind a LEBU in a Turbulent Boundary Layer*," **Second IUTAM Symposium on Structure of Turbulence and Drag Reduction, Zurich, Switzerland, pp. 503-506.**

133. **Coustols, E., Gleyzes, C., Schmitt, V., and Berrue, P., 1988,** "*Etude Experimentale de la Reduction du Frottement Turbulent au Moyen de Parois Rainurees*," **L'Aeronautique et L'Astronautique, No. 34, No. 129, pp. 34-46.**

134. **Azad. R.S., and Doell, B., 1989,** "*Behaviour of Separation Bubble with Different Roughness Elements at the Leading Edge of a Flat Plate*," **Second IUTAM Symposium on Structure of Turbulence and Drag Reduction, Zurich, Switzerland, pp. 85-92.**

135. **Schubauer, G.B., and Skramstad, H.K., 1948,** "*Laminar-Boundary-Layer Oscillations and Transition on a Flat Plate*," **NACA-TR-909.**

136. **Kohama, Y., Ohta, F., and Segawa, K., 1989,** "*Development and Interaction of Instabilities in the Cross Flow Field*," **Laminar-turbulent transition; Proceedings of the IUTAM Symposium, Toulouse, France, pp. 431-440.**

137. **Ito, A., 1985,** "*O-Kyoku Men ni Tomonau Tate Uzu Hokai no Kozo*," **Nihon Koku Uchu Gakkai-shi, Vol. 33, No. 374, pp. 58-65. (Journal of Japan Society for Aeronautical and Space Sciences).**

138. **Dovgal', A.V., Levchenko, V.Ya., and Timofeyev, V.A., 1989,** "*LaminarizatsiyPogranichnovo Sloya Putem Loklizovannovo Nagrevaniya Poverkhnosti*," **Izvestiya Sibirskovo Otdeleniya Akademii Nauk SSSR, Seriya Tekhnicheskoy Nauk, ISS. 3, pp. 60-65.**

139. **Mechel, F., and Schilz, W., 1986,** "*Studies of Acoustic Effects on a Flow Boundary Layer in Air*," **NASA-TM-77981.**

140. **Kendall, J.M., 1985,** "*Experimental Study of Disturbances Produced in a Pre-Transitional Laminar Boundary Layer by Weak Freestream Turbulence*," **AIAA-85-1695.**

141. **Sokolov, M., and Giant, Z., 1992,** "*The Ladder Probe: Reverse Flow Measurements with a Hot-Wire Rake*," **Experiments in Fluids, Vol. 12, pp. 307-318.**

142. **Rose, W.C., and Otten, L.J, 1983,** "*High Reynolds-Number Shear-Stress Measurements*," **AIAA-83-0053.**

143. **Wyngaard, J.C., 1968,** "*Measurement of Small-Scale Turbulence Structure with Hot-Wires*," **Journal of Scientific Instruments, (Journal of Physics E), Series 2, Vol. 1, pp. 1105-1108.**

144. **Davies, P.O.A.L., and Yule, A.J., 1974,** "*Structure of Turbulence*," **I.S.V.R.**

145. **Kendall, J.M., 1990,** "*Boundary Layer Receptivity to Freestream Turbulence*," **AIAA-90-1504.**

146. **Goldstein, M.E., 1983,** "*The Evolution of Tollmien-Schlitching Waves Near a Leading Edge*," **Journal of Fluid Mechanics, Vol. 127, pp. 59-81.**

147. **Kerschen, E.J., 1989,** "*Boundary Layer Receptivity*," **AIAA-89-1109.**

148. **Klebanoff, P.S., 1971,** "*Effect of Freestream Turbulence on the Laminar Boundary Layer (Abstract)*," **Bulletin of American Physical Society, Vol. 10, No. 11, pp. 1323.**

149. **Arnal, D., and Juillen, J., 1978,** "*Contribution Experimentale a l'Etude de la Receptivite d'une Couche Limite Laminaire, a la Turbulence de l'Ecoulement General*," **ONERA Technical Report No. 1/5018-AYD.**

150. **Kosyrigin, V., Levchenko, Y., and Polyakov, N., 1988,** "*The Laminar Boundary Layer in the Presence of a Moderately Turbulent Freestream*," **Preprint No. 16-88, USSR Academy of Sciences, Institute for Theoretical and Applied Mechanics, Novosibirsk.**

151. **Suder, K., O'Brien, J., and Reshotko, E., 1988,** "*Experimental Study of Bypass Transition in a Boundary Layer*," **NASA-TM-100913.**

152. **Kendall, J.M., 1982,** "*Study of the Effect of Freestream Turbulence Upon Disturbances in the Laminar Boundary Layer*," **Report AFWAL-TR-82-3002.**

153. **Kendall, J.M., 1984,** "*Experiments on the Generation of Tollmien-Schlichting Waves in a Flat Plate Boundary Layer by Weak Freestream Turbulence*," **AIAA-84-0011.**

154. **Kendall, J.M.,** "*Hot-Wire and Shadowgraph Studies Relating to Boundary Layer Transition on a Slender Cone at Mach 4.5*," **(Private Communications).**

155. **Kendall, J.M., 1975,** "*Wind Tunnel Experiments Relating to Supersonic and Hypersonic Boundary Layer Transition*," **AIAA Journal, Vol. 13, No. 3, pp. 290-299.**

156. **Mack, L.M., 1975,** "*Linear Stability Theory and Problem of Supersonic Boundary Layer Transition*," **AIAA Journal, Vol. 13, No. 3, pp. 278-289.**

157. **Corrsin, S., and Uberoi, M.S., 1949,** "*Further Experiments on the Flow and Heat Transfer in a Heated Turbulent Air Jet*," **NACA-TN-1865 (Issued as NACA Report 998, 1950).**

158. **Manjunath, A., Gowda, B.H.L., and Natarajan, R., 1992,** "*Studies on the Mixing of Two Non-Axial Jets in a Confined Passage-Turbulence*

*Characteristics*," **Experiments in Fluids, Vol. 13, pp. 147-154.**

159. **Laurence, J.C., 1955,** "*Intensity, Scale, and Spectra of Turbulence in Mixing Region of Free Subsonic Jet*," **NACA-TN-3561.**

160. **Miksad, R.W., Jones, F.L., and Powers, E.J., 1983,** "*Measurements of Nonlinear Interactions During Natural Transition of a Symmetric Wake*," **The Physics of Fluids, Vol. 26, No. 6, pp. 1402-1409.**

161. **Anders, J.B., Jr., 1974,** "*Turbulence Measurements in Hypersonic Helium Flow*," **Report 1157, Gas Dynamics Laboratory, Princeton University, Princeton, New Jersey.**

162. **Barre, S., Quine, C., and Dussauge, J.P., 1992,** "*Compressibility Effects on the Structure of Supersonic Mixing Layers: Experimental Results*," **Institut de Mécanique de Marseilles, Institut de Mécanique Statistique de la Turbulence, U.M. CNRS- Université Aix-Marseille II n° 380033, 12 avenue du Général Lecleerc, 13003, MARSEILLES, FRANCE.**

163. **Demetriades, A., 1978,** "*Probes for Multivariant Flow Characteristics*," **Proceedings of the Dynamic Flow Conference on Dynamic Measurements in Unsteady Flows, IMST, Marseille, France, pp. 13-44.**

164. **Stainback, P.C., and Nagabushana, K.A.,** "*Reinvestigation of Hot-Wire Anemometry Applicable to Subsonic Compressible Flows Using Fluctuation Diagrams*," **(submitted to Journal of Fluids Engineering, Transactions of the ASME, Log No. 3538-DPT).**

165. **Stainback, P.C., Nagabushana, K.A., and Bushnell, D.M., 1992,** "*Mode Diagrams for Hot Wire Anemometry in Subsonic Flows*," **International Conference on Methods of Aerophysical Research, organized by Institute of Theoretical and Applied Mechanics (ITAM) of the Siberian Division of the Russian Academy of Sciences, Novosibirsk, RUSSIA.**

166. **Stainback, P.C., and Nagabushana, K.A., 1991,** "*Fluctuation Diagrams for Hot Wire Anemometry in Subsonic Compressible Flows*," **NASA-CR-189580.**

167. **Zinov'ev, V.N., and Lebiga, V.A., 1988,** "*Measurements of Fluctuations For High Subsonic Velocities Using a Hot-Wire Anemometer*," **Plenum Publishing Corp. Novosibirsk, Translated from Zhurnal Prikladoni Mekhanikii Teckhnicheskoi Fiziki, No. 3, pp. 80-84.**

168. **Lebiga, V.A., and Zinoviev, V.N., 1989,** "*Hot-Wire Measurements in Compressible Flow*," **ICIASF'89 Record, IEEE-89CH2762-3., The 13th International Congress on Instrumentation in Aerospace Simulation Facilities, DFVLR Research Center, Göttingen.**

169. **Lebiga, V.A., and Zinovyev, V.N., 1991,** "*Acoustic Measurements with a Hot-Wire Anemometer at High Subsonic Velocities*," **Dantec Information No. 10, 14-16.**

170. **Horstman, C.C., and Rose, W.C., 1977,** "*Hot-Wire Anemometry in Transonic Flow*," **AIAA Journal, Vol. 15, No. 3, pp. 395-401.**

171. **Davies, P.O.A.L., and Fisher, M.J., 1964,** "*Heat Transfer from Electrically Heated Cylinders*," **Proceedings of the Royal Society, Series A, Mathematical and Physical Sciences, Vol. 280, No. 1383, pp. 486-527.**

172. **Jones, G.S., Stainback, P.C., and Nagabushana, K.A., 1992,** "*A Comparison of Calibration Techniques for Hot-Wires Operated in Transonic Slip Flows*," **AIAA-92-4007.**

173. **Stainback, P.C., Nagabushana, K.A., and Jones, G.S., 1993,** "*A Status Report for Hot-Wire Anemometry Development at the Langley Research Center for Transonic and Subsonic Slip Flow Regimes*," **Third International Symposium on Thermal Anemometry - ASME Fluids Engineering Division Summer Meeting, Washington,D.C.**

174. **Stainback, P.C., Nagabushana, K.A., Clukey, S.J., and Jones, G.S., 1991,** "*Heat Transfer From Heater Cylinders in Subsonic Flows*,"

**First Joint ASME-JSME Fluids Engineering Conference, Portland, Oregon.**

175. **Stainback, P.C., and Nagabushana, K.A., 1992,** "*Re-investigation of Hot-WIre Anemometry Applicable to Subsonic Compressible Flows Using Fluctuation Diagrams*," **to appear in JNASA-CR-4429.**

176. **Rong, B.S., Tan, D.K.M., and Smits, A.J., 1985,** "*Calibration of the Constant Temperature Normal Hot-Wire Anemometer in Transonic Flow*," **Report MAE-1696.**

177. **Barre, S., Dupont, P., and Dussauge, J.P., 1992,** "*Hot-Wire Measurements in Turbulent Transonic Flows*," **European Journal Mechanics B, Vol. 11, No. 4, pp. 439-454.**

178. **Winovich, W., and Stein, H.A., 1957,** "*Measurements of the Nonlinear Variation with Temperature of Heat-Transfer Rate from Hot-Wires in Transonic and Supersonic Flow*," **NACA-TN-3965.**

179. **Kaimal, J.C., Wyngaard, J.C., Izumi, Y., and Cote, O.R., 1972,** "*Spectral Characteristics of Surface-Layer Turbulence*," **Quarterly Journal of the Royal Meteorological Society, Vol. 98, No. 417, pp. 563-589.**

180. **MacCready, P.B., 1953,** "*Atmospheric Turbulence Measurements*," **Journal of Meteor, Vol. 10, No. 5, pp. 325-337.**

181. **Wagner, R.D., and Weinstein, L.M., 1974,** "*Hot-Wire Anemometry in Hypersonic Helium Flow*," **NASA-TN-D-7465.**

182. **Laderman, A.J., and Demetriades, A., 1973,** "*Hot-Wire Measurements of Hypersonic Boundary-Layer Turbulence*," **The Physics of Fluids, Vol. 16, pp. 179-181.**

183. **Smits, A.J., 1990,** "*An Introduction to Constant-Temperature Hot-Wire Anemometry in Supersonic Flows*," **The Heuristics of Thermal Anemometry, ASME-FED Vol. 97, pp. 35-40.**

184. **Smith, D.R., and Smits, A.J., 1993,** "*The Simultaneous Measurement of Velocity and Temperature Fluctuations in the Boundary Layer of a Supersonic Flow*," **Experimental Thermal and Fluid Science, Vol. 6.**

185. **Laufer, J., 1961,** "*Aerodynamic Noise in Supersonic Wind Tunnels*," **Journal of the Aerospace Sciences, Vol. 28, No. 9, pp. 685-692.**

186. **Wilkinson, S.P., Anders, S.G., Chen, F.-J., and Beckwith, I.E., 1992,** "*Supersonic and Hypersonic Quiet Tunnel Technology at NASA Langley*," **AIAA-92-3908.**

187. **Vrebalovich, T., 1962,** "*Application of Hot-Wire Techniques in Unsteady Compressible Flows*," **The ASME Hydraulic Division Conference, Symposium on Measurement in Unsteady Flow, pp. 61-70.**

188. **Laderman, A.J., and Demetriades, A., 1974,** "*Mean and Fluctuating Flow Measurements in the Hypersonic Boundary Layer Over a Cooled Wall*," **Journal of Fluid Mechanics, Vol. 63, pp. 121-144.**

189. **Laderman, A.J., 1974,** "*Hypersonic Viscous Flow over a Slender Cone, Part II: Turbulent Structures of the Boundary Layer*," **AIAA-74-0534.**

190. **Owen, F.K., 1988,** "*Measurements of Hypersonic Flow Fields*," **AGARD-FDP-VKI Special Course, Aerothermodynamics of Hypersonic Velocities.**

191. **Owen, F.K., and Calarence, W., 1987,** "*Turbulent Measurement in Hypersonic Flow*," **Paper No. 5, AGARD-CP-428, Fluid Dynamic Panal Symposium on Aerodynamic of Hypersonic Lifting Vehicles, Bristol, UK.**

192. **Smits, A.J., 1991,** "*Turbulent Boundary-Layer in Supersonic Flow*," **Phil. Trans. R. Soc., Lond. A, Vol. 336, pp. 81-93.**

193. **Smits, A.J., Hayakawa, K., and Muck, K.C., 1983,** "*Constant Temperature Hot-Wire Anemometer Practice in Supersonic Flows; Part 1: The Normal Wire*," **Experiments in Fluids, Vol. 1, pp. 83-92.**

194. **Dupont, P., and Debieve, J.F., 1992,** "*A Hot-Wire Method for Measuring Turbulence in Transonic or Supersonic Heated Flows*," **Experiments in Fluids, Vol. 13, pp. 84-90. (Also Twelfth Symposium on Turbulence, Department of Chemical Engineering, Continuing Education, University of Missouri-Rolla), 1990.**

195. **Rose, W.C., 1973,** "*The Behavior of a Compressible Turbulent Boundary Layer in a Shock-Wave-Induced Adverse Pressure Gradient*," **NASA TN D-7092, (Also Ph.D., Thesis, University of Washington 1972, CAT-7306-S).**

196. **Fisher, M.C., Maddalon, D.V., Weinstein, L.M., and Wagner, Jr., R.D., 1971,** "*Boundary Layer Pitot and Hot-Wire Surveys at* $M_\infty = 20$," **AIAA Journal, Vol. 9, No. 5, pp. 826-834.**

197. **Moore, F.K., 1953,** "*Unsteady Oblique Interaction of a Shock Wave with a Plane Disturbance*," **NACA-TN-2879, also NACA Rept. 1165.**

198. **D'iakov, S.P., 1958,** "*The Interaction of Shock Waves with Small Perturbations. I*," **Soviet Physics Jetp, Vol. 6(33), No. 4, pp. 729-739.**

199. **D'iakov, S.P., 1958,** "*The Interaction of Shock Waves with Small Perturbations. II*," **Soviet Physics JETP, Vol. 6(33), No. 4, pp. 740-747.**

200. **Dewey, Jr., C.F., 1961,** "*Hot-Wire Measurements in Low Reynolds Number Hypersonic Flows*," **ARS Journal, The American Rocket Society, Vol. 31, No. 12, pp. 1709-1718.**

201. **Stetson, K.F., and Kimmel, R.L., 1992,** "*On Hypersonic Boundary Layer Stability*," **AIAA-92-0737.**

202. **Tollmien, W., 1929,** "*Über die Entstehung der Turbulenz*," **1. Mitteilung, Nachr. Wiss. Göttingen, Math. Phys. Klasse, pp. 21-44, (also English translation** "*The production of turbulence*," **NACA-TM-609, 1931).**

203. **Tollmien, W., 1936,** "*General Instability Criterion of Laminar Velocity Distribution*," **NACA-TM-792.**

204. **Schlichting, H., 1987,** "*Boundary Layer Theory*," **McGraw-Hill Book Company, Co.**

205. **Saric, W.S., and Nayfeh, A.H., 1977,** "*Nonparallel Stability of Boundary Layer with Pressure Gradient and Suction*," **AGARD-CP-224.**

206. **Kistler, A.L., and Vrebalovich, T., 1966,** "*Grid Turbulence at Large Reynolds Numbers*," **Journal of Fluid Mechanics, Vol. 26, No. 37, pp. 37-47.**

207. **Pao., Y.H., 1965,** "*Structure of Turbulent Velocity and Scale Fields at Large Wave Number*," **The Physics of Fluids, Vol. 8, No. 6, pp. 1063-1075.**

208. **Mack, L.M., 1977,** "*Transition Prediction and Linear Stability Theory*," **AGARD-CP-224.**

209. **Stetson, K.F., Thompson, E.R., Donaldson, J.C., and Sibr, L.G., 1983,** "*Laminar Boundary Layer Stability Experiments on a Cone at Mach 8. Part 1: Sharp Cone*," **AIAA-83-1761.**

210. **Demetriades, A., 1971,** "*Laminar Boundary Layer Stability Measurements at Mach 7 Including Wall Temperature Effects*," **AFOSR-TR-77-1311.**

211. **Billington, I.J., 1955,** "*The Hot-Wire Anemometer and its use in Non-Steady Flow*," **University of Toronto, Ins. Aero. Phys., Tech. Note No. 5.**

212. **Toy, N., and Thoma, S.H., 1987,** "*The Twin Pulsed Wire Anemometer - A New Instrument for Measurements in Complex Flows*," **Symposium on Thermal Anemometry, ASME-FED Vol. 53, pp. 65-72.**

213. **Blackwelder, R.F., and McLean, 1987,** "*A Hot-Wire Probe for Velocity Measurement in Reverse Flows*," **Symposium on Thermal Anemometry, ASME-FED Vol. 53, pp. 73-78.**

**214. LaGraff, J.E., 1972,** "*Observation of Hypersonic Boundary Layer Transition Using Hot-Wire Anemometry*," **AIAA Journal, Vol. 10, No. 6, pp. 762-769.**

**215. Sandborn, V.A., and Wisniewski, R.J., 1960,** "*Hot-Wire Exploration of Transition on Cone in Supersonic Flow*," **Proceedings of Heat Transfer and Fluid Mechanics Institute Meeting, Stanford, Ohio, pp. 120-134.**

**216. Hussein, H.J., 1990,** "*Measurements of Turbulent Flows with Flying Hot-Wire Anemometry*," **The Heuristics of Thermal Anemometry, ASME-FED Vol. 97, pp. 77-80.**

**217. Spangler, J.G., and Wells, Jr., C.S., 1968,** "*Effects of Freestream Disturbances on Boundary Layer Transition*," **AIAA Journal, Vol. 6, No. 3, pp. 543-554.**

**218. Obremski, H.J., and Fejer, A.A., 1967,** "*Transition in Oscillating Boundary Layer Flows*," **Journal of Fluid Mechanics, Vol. 29, part 1, pp. 93-111.**

**219. Mack, L.M., 1975,** "*A Numerical Method for the Prediction of High-Speed Boundary-Layer Transition Using Linear Theory*," **NASA-SP-347, Part 1, pp. 101-123.**

**220. Reshotko, E., 1976,** "*Boundary-Layer Stability and Transition*," **Annual Review of Fluid Mechanics, Vol. 8, pp. 311-349.**

**221. Laufer, J., and Vrebalovich, T., 1960,** "*Stability and Transition of a Supersonic Laminar Boundary Layer on an Insulated Flat Plate*," **Journal of Fluid Mechanics, Vol. 9, part 2, pp. 257-299.**

**222. Takagi, S., 1992,** "*Simple Method for Determining the Laser-Velocimeter Focal Point with the Aid of the Hot-Wire Anemometer*," **AIAA Journal, Vol. 30, No. 6, pp. 1664-1665.**

**223. Blackwelder, R.F., and Kaplan, R.E., 1976,** "*On the Wall Structure of the Turbulent Boundary Layer*," **Journal of Fluid Mechanics, Vol. 26, pp. 89-112.**

**224. Moin, P., and Kim, J., 1985,** "*The Structure of the Vorticity Field in Turbulent Channel Flow, Part I, Analysis of Instantaneous Fields and Statistical Correlations*," **Journal of Fluid Mechanics, Vol. 155, pp. 441-464 .**

**225. Perry, A.E., and Cheng, M.S., 1982,** "*On the Mechanism of Wall Turbulence*," **Journal of Fluid Mechanics, Vol. 119, pp. 173-217.**

**226. Donovan, J.F., and Smits, A.J., 1987,** "*A Preliminary Investigation of Large Scale Organized Motion in a Supersonic Turbulent Boundary Layer on a Curved Surface*," **AIAA-87-1285.**

**227. Rose, W.C., and Johnson, D.A., 1974,** "*Study of Shock-Wave Turbulent Boundary Layer Interaction Using Laser Velocimeter and Hot-Wire Anemometer Techniques*," **AIAA-74-0095.**

**228. Polyakov, A.F., and Shindin, S.A., 1983,** "*Some Aspects of Measuring the Structure of Non-Isothermal Turbulence by Simultaneous Application of DISA's LDA and Hot-Wire Anemometer*," **DISA Information No. 28, pp. 10-14.**

**229. Logan, P., McKenzie, R.L., and Bershader, D., 1988,** "*Hot-Wire Accuracy in Supersonic Turbulence from Comparisons with Laser-Induced Fluorescence*," **AIAA Journal, Vol. 26, No. 3, pp. 316-322.**

**230. McKenzie, R.L., and Fletcher, D.G., 1992,** "*Laser-Spectroscopic Measurement Techniques for Hypersonic, Turbulent Wind Tunnel Flows*," **NASA-TM-103928.**

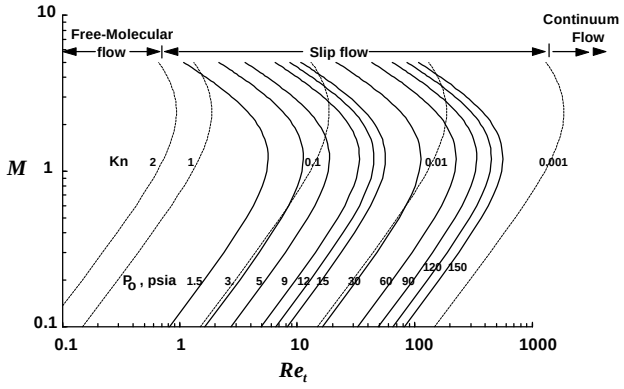


**Figure 1. Mach number vs. Reynolds number for lines of Constant Total Pressure and Constant Knudsen Number; $d_w = 0.00015\ inch$; $T_o = 560°F$.**

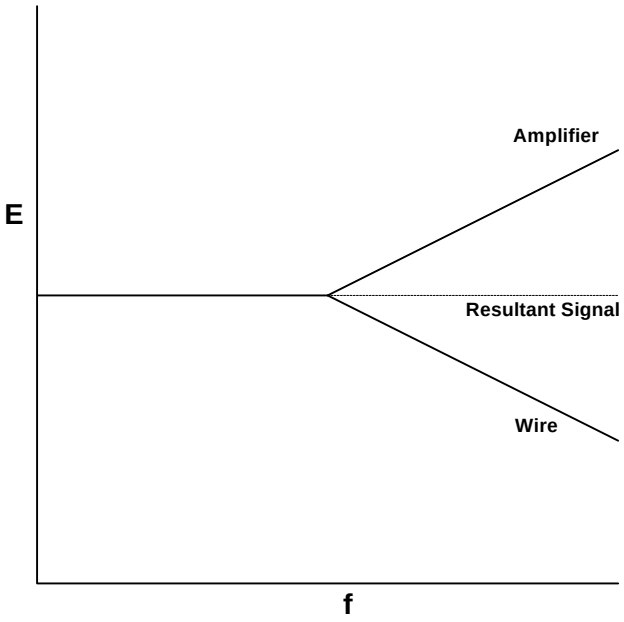


**Figure 2. Frequency Compensation for CCA.**

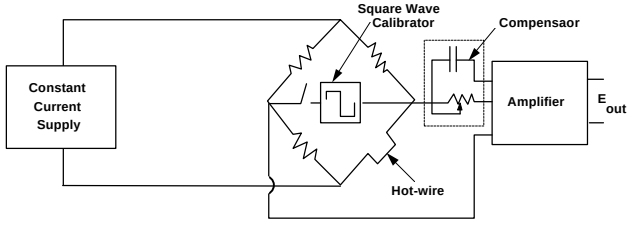


**Figure 3. Schematic Representation of Constant Current Hot-Wire System; (ref. 62).**

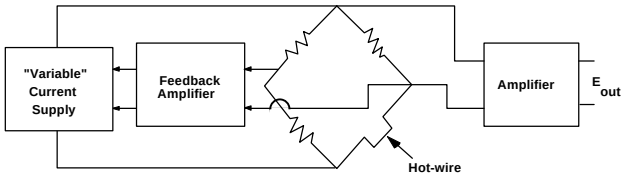


**Figure 4. Schematic Representation of Constant Temperature Hot-Wire System; (ref. 62).**

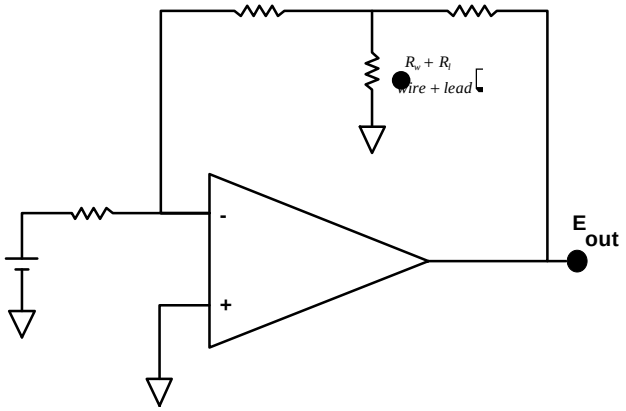


**Figure 5. Schematic Representation of Constant Voltage Hot-Wire System; (ref. 57).**

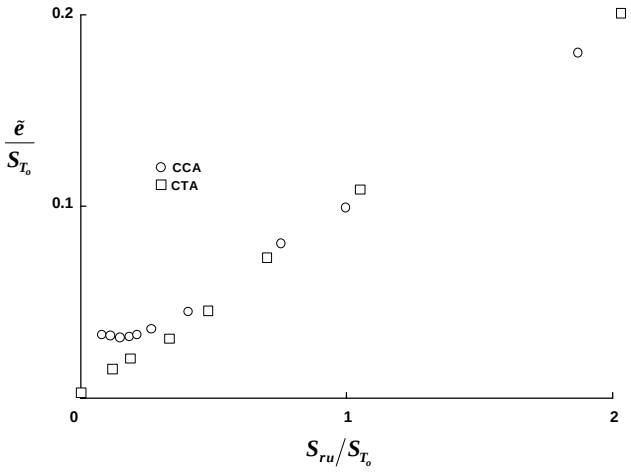


**Figure 6. Modal Analysis that Compares the CTA and CCA Systems; $y/d = 0.23$; (ref. 59).**

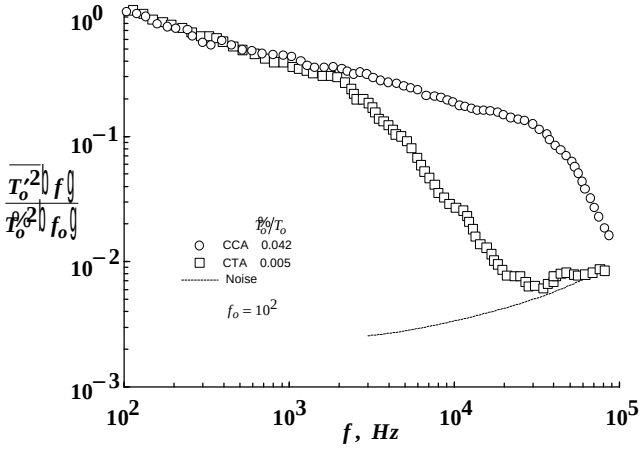


**(a) Low Overheat; Total Temperature Fluctuations**

**Figure 7. Normalized Power Spectra that Compare the Constant Temperature Anemometer (CTA) and Constant Current Anemometer (CCA) Systems; $y/d = 0.23$; (ref. 59).**

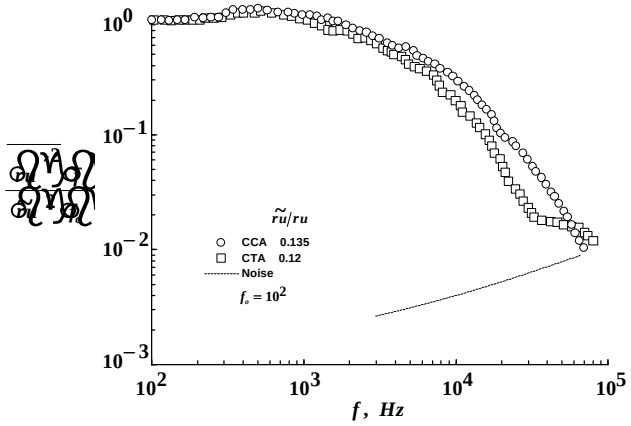


**(b) High Overheat; Mass-Flow Fluctuations**

**Figure 7. Concluded.**

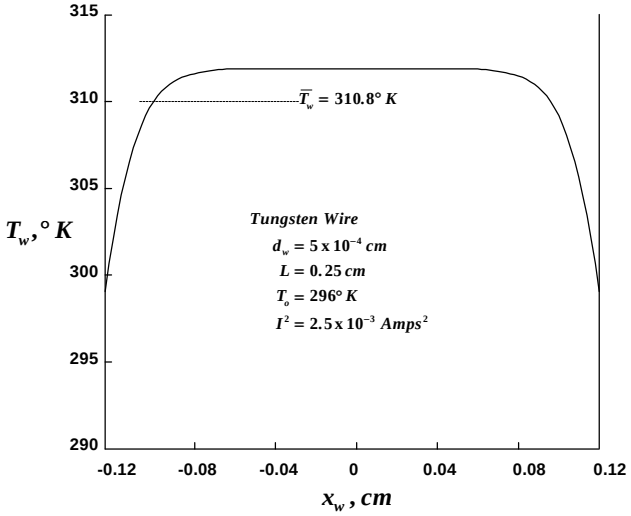


**Figure 8. Typical Temperature Distribution Along a Convection Controlled Hot-Wire; (ref. 21).**

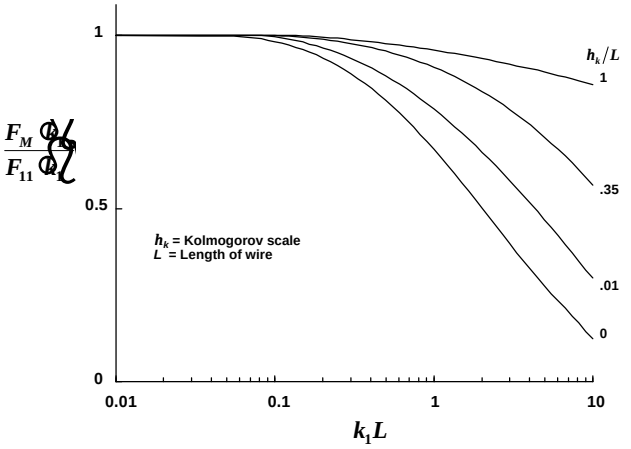


**Figure 9. Hot-Wire Spectral Transfer Function; (ref. 143).**

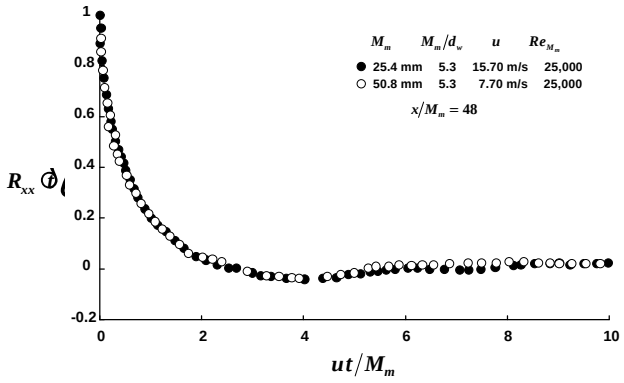


**Figure 10. Auto-Correlation Coefficient $R_{xx}(t)$; (ref. 25).**

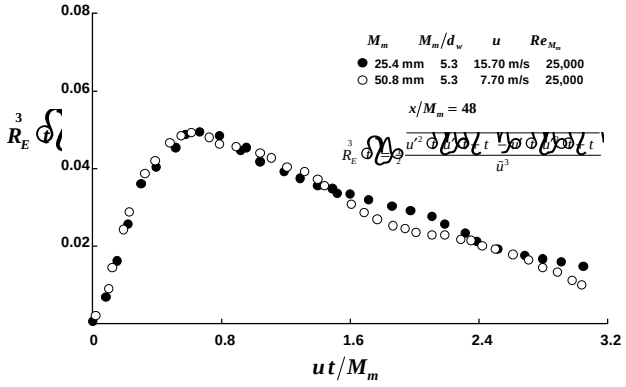


**Figure 12. Composite Third-Order Auto-Correlation Coefficient $R_E^3(t)$; (ref. 25).**

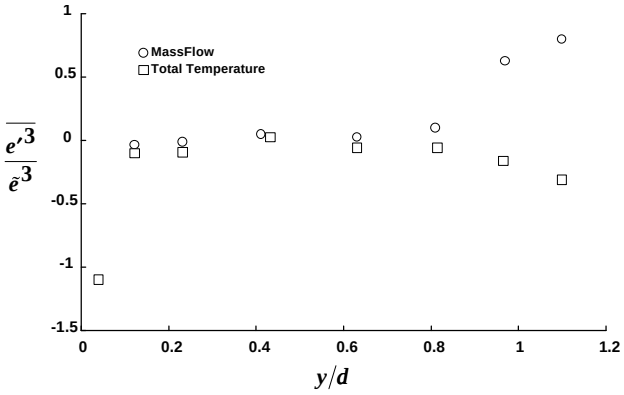


**(a) Third Moment, Skewness**

**Figure 11. Distribution of the Mass-Flow and Total Temperature Fluctuations Across the Boundary Layer; (ref. 59).**

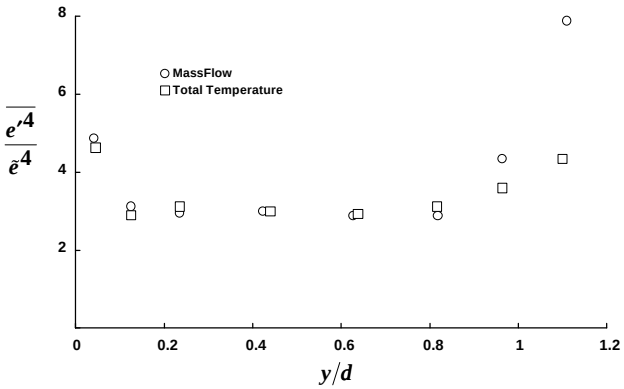


**(b) Fourth Moment; Flatness**

**Figure 11. Concluded.**

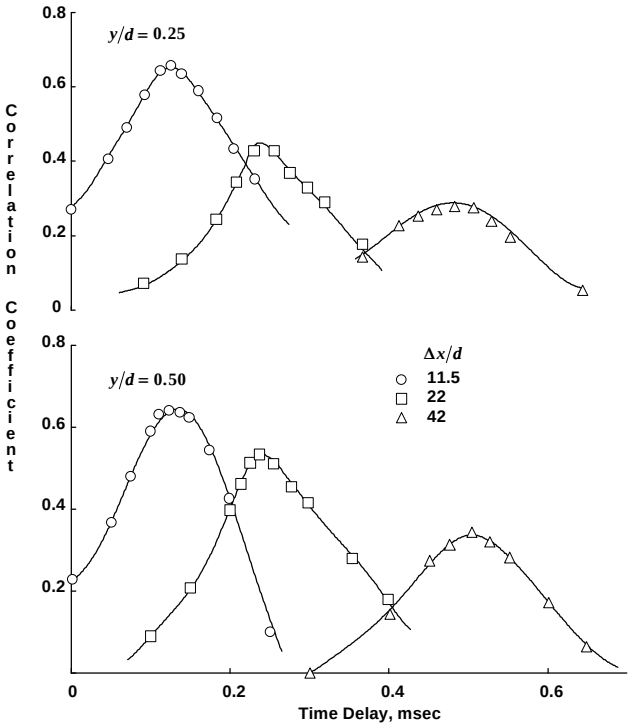


**Figure 13. Examples of Filtered Space-Time Correlation Coefficient - 4 kHz; (ref. 87).**

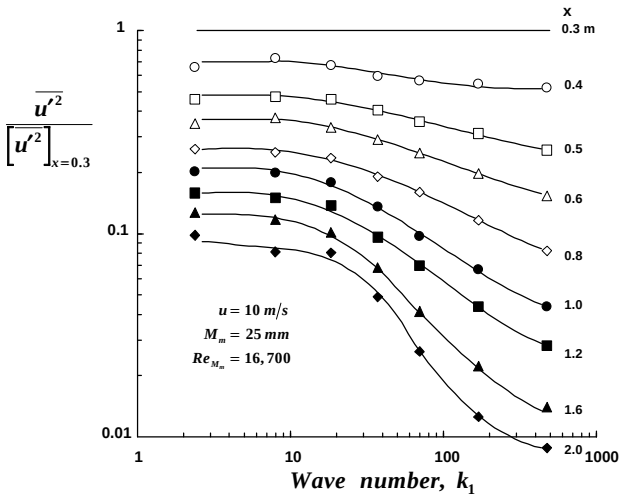


**Figure 14. Decay of Energy of the Spectral Components; (ref. 88).**

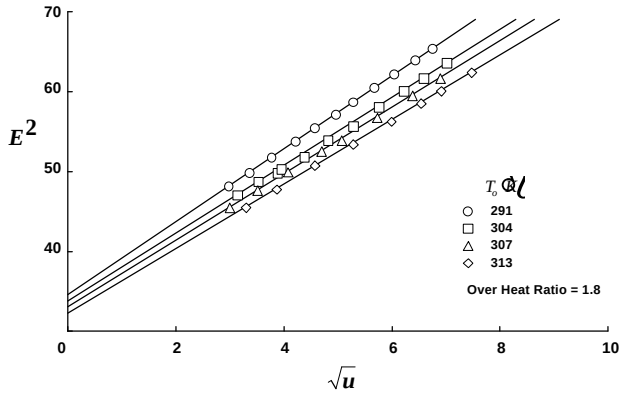


**Figure 15. Voltage vs. Velocity for a Wire Operated with CTA; (ref. 93).**

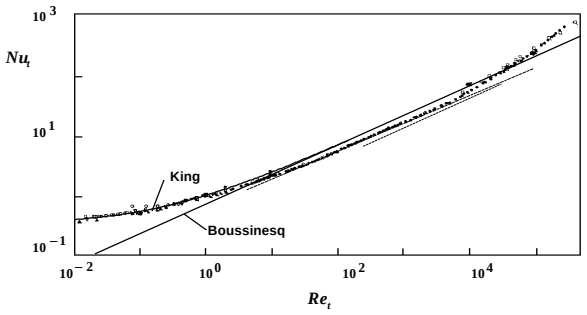


**Figure 16. Summary of Heat Loss from Circular Cylinders Over a Wide Range of Reynolds Number in Continuum Flow; (ref. 21).**

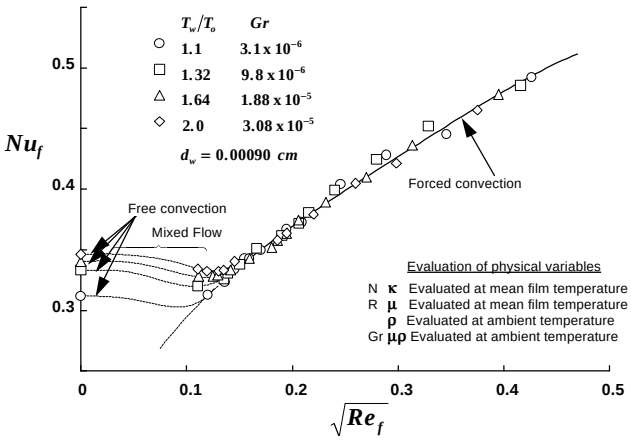


**Figure 17. Interaction of Free and Forced Convection; (ref. 104).**

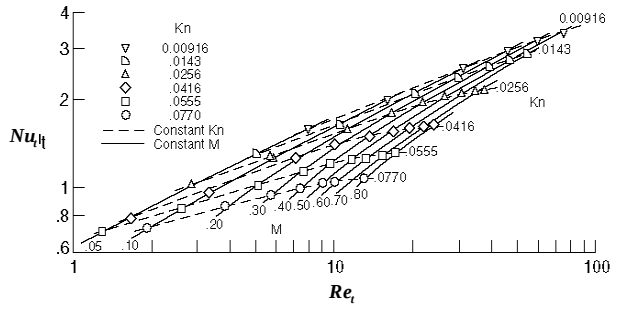


**Figure 18a. Nusselt Number Correlation for Cylinders in Subsonic Slip Flow; $T_o = 80°F$; $T_w = 584°F$; (ref. 35).**

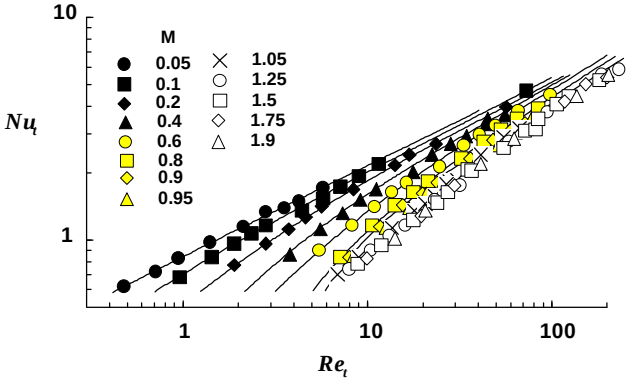


**Figure 18b. Spangenberg's Reported Heat Loss Measurements from Electrically Heated Wires in Air; (ref. 171).**

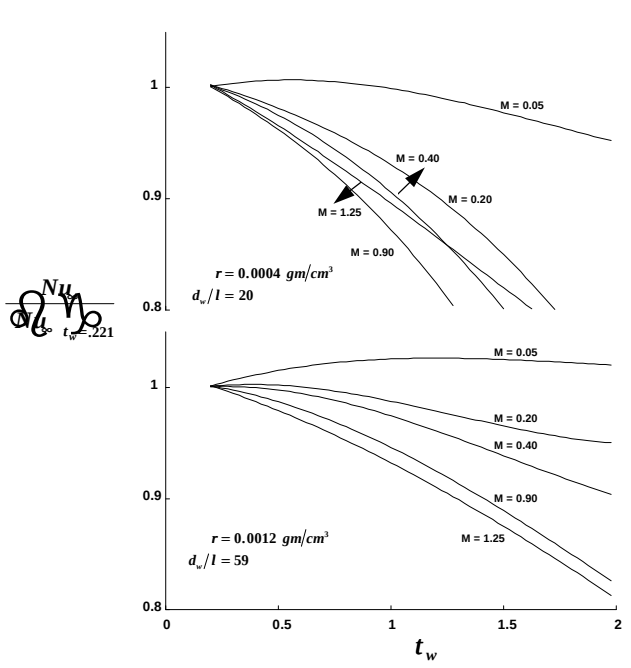


**Figure 19. Normalized Nusselt Number Variation with Overheat for 0.00015 inch Diameter Platinum Wire Containing 10% Rhodium; (ref. 110).**

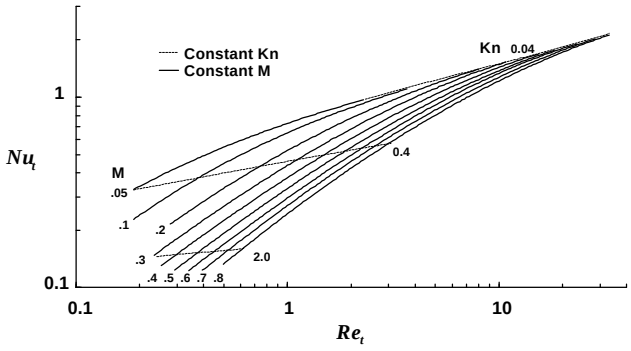


**Figure 20. Predicted Nusselt Number Correlation from Approximate Slip-Flow Theory; (ref. 35).**

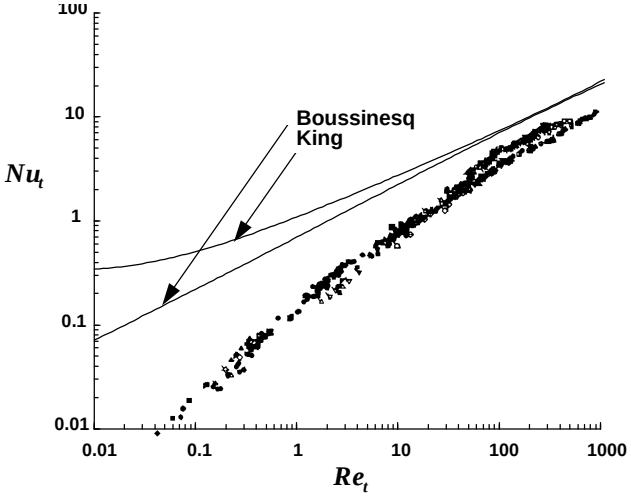


**Figure 21. Summary of Supersonic Heat Transfer from Transverse Cylinders in Rarefied Air Flow; (ref. 21).**

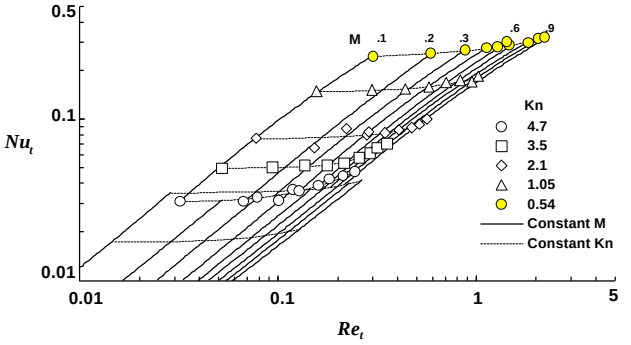


**Figure 22. Comparison of Heat-Transfer Data with Free-Molecule-Flow Theory Using $a = 0.57$; (ref. 33).**

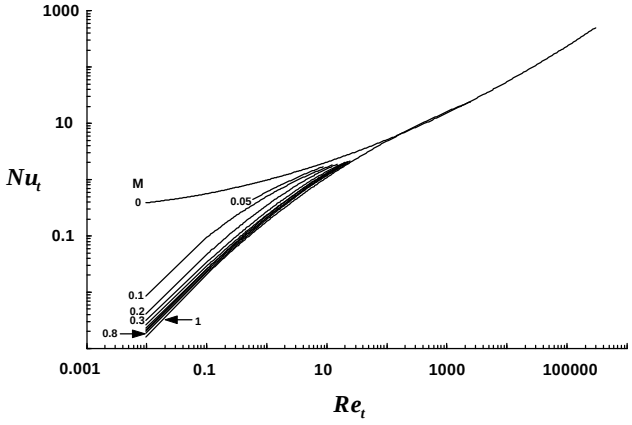


**Figure 23. Correlation of Convective Heat Transfer from Transverse Cylinders; (ref. 10).**

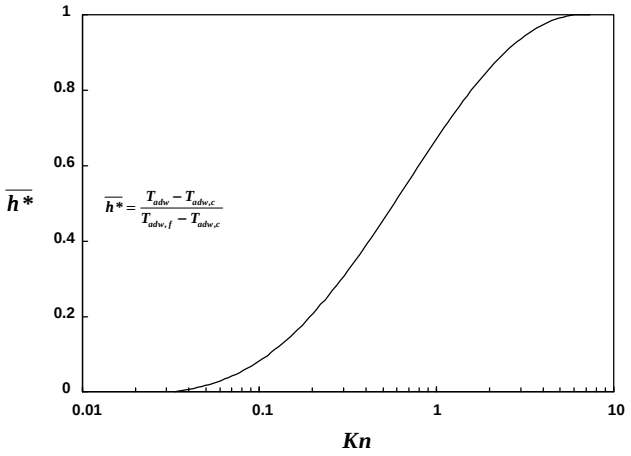


**Figure 24. Normalized Recovery Temperature Ratio vs. Free StreamKnudsen Number; (ref. 21).**

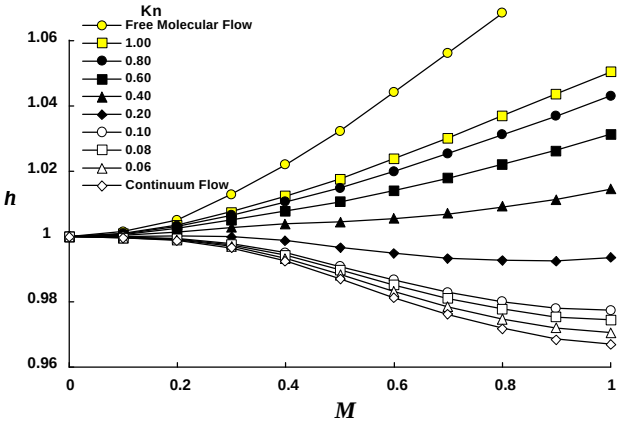


**Figure 25. Recovery Temperature Ratio vs. Mach Number for Constant Values of Knudsen Number.**

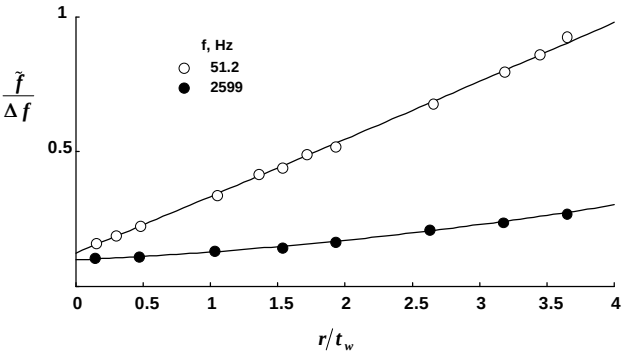


**Figure 26. Fluctuation-Diagram of the Filtered Signals (Single-Wire); (ref. 97).**

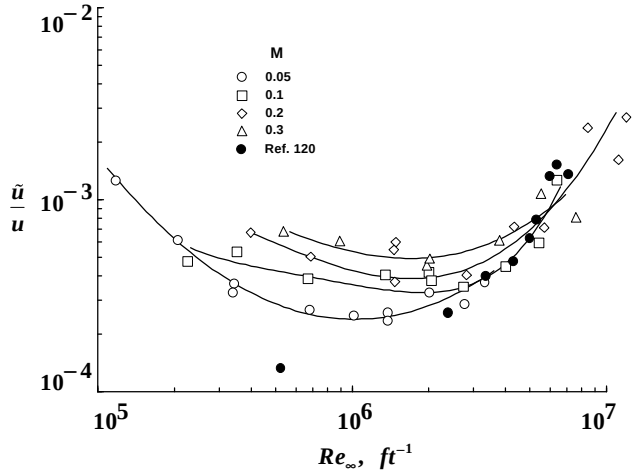


**Figure 27. Velocity Fluctuations Measured in the Test Section of LaRC Low Turbulence Pressure Tunnel; (ref. 37).**

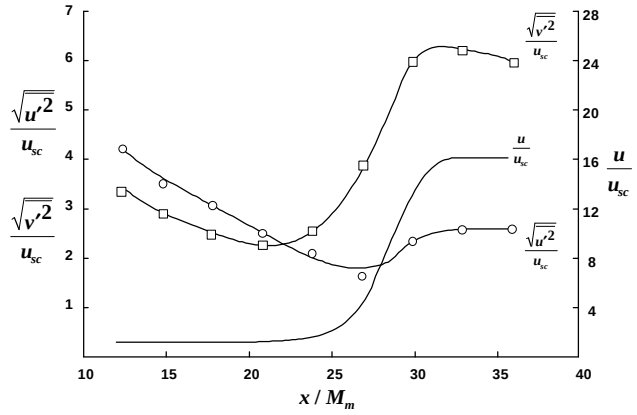


**Figure 28. Effect of 16:1 Contraction on Turbulence Generated by 2-inch Square Mesh Grid; $R_{M_m} = 3710$; (ref. 118).**

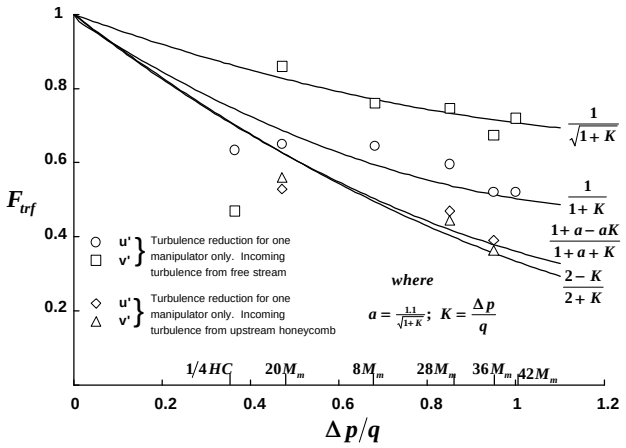


**Figure 29. Measured Turbulence Reduction Factor for Various Screens and Combinations of Screens with Honeycomb Compared With Different Theories; (ref. 120).**

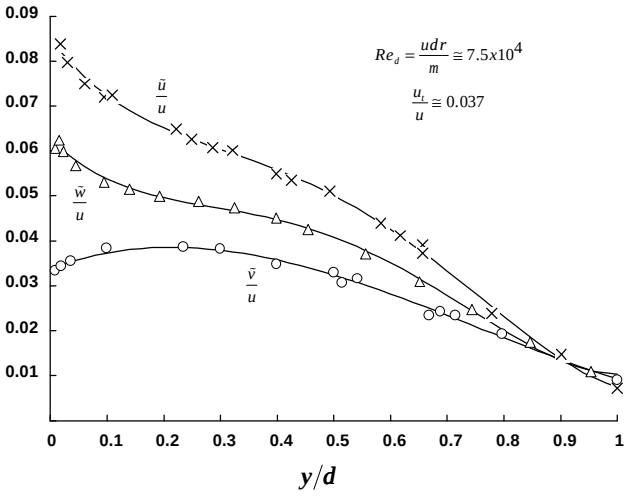


**(a) Zero Pressure Gradient**

**Figure 30. Relative Turbulence Intensities in a Boundary Layer Along a Smooth Wall; (ref. 131).**

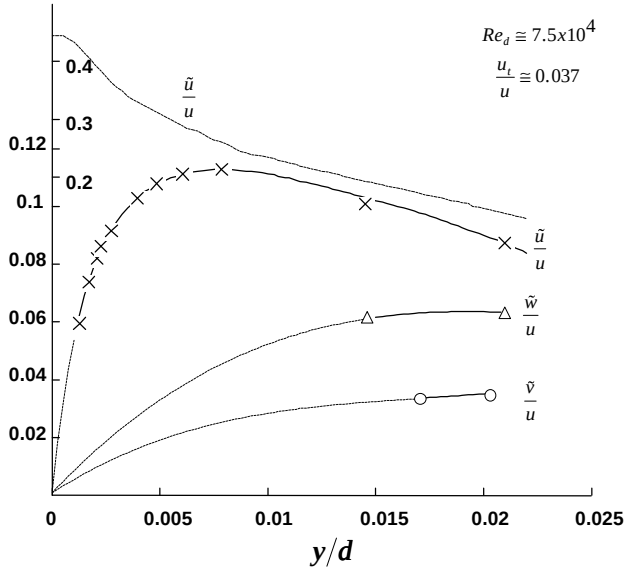


**(b) Constant-Stress Layer**

**Figure 30. Concluded.**

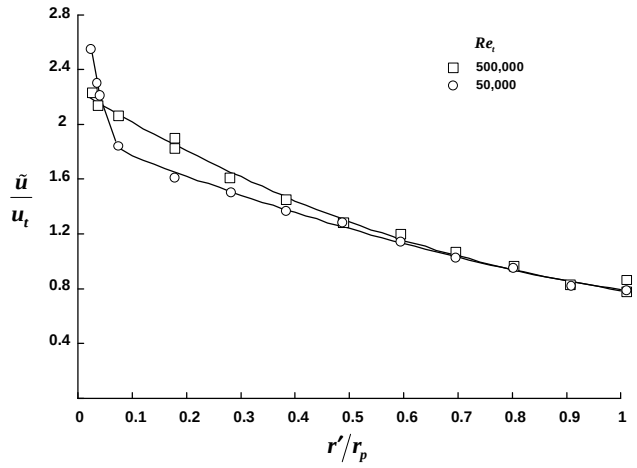


**(a) Across the pipe**

**Figure 31. Distribution of velocity fluctuation in a pipe; (ref. 40).**

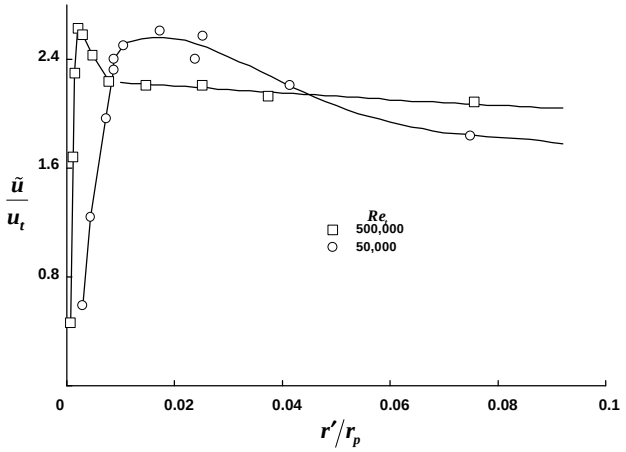


**(b) Near the wall**

**Figure 31. Concluded.**

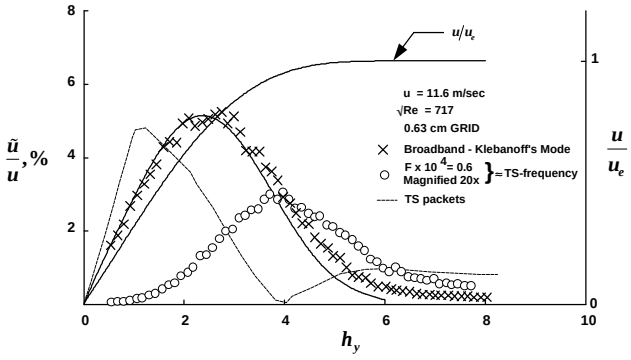


**Figure 32. Types of Fluctuation Simultaneously Present in Boundary Layer; (ref. 145).**

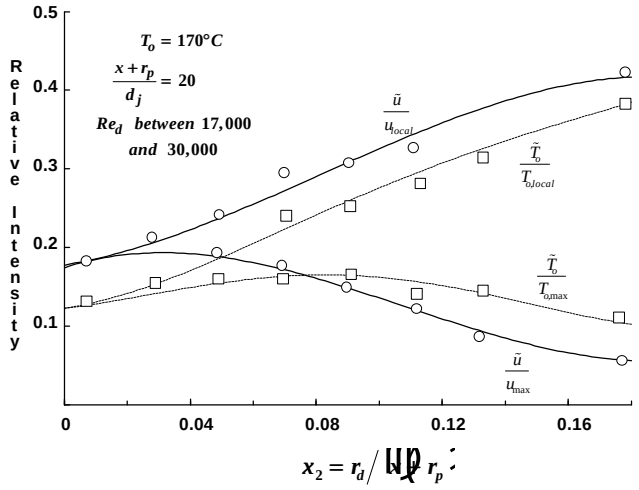


**Figure 33. Distribution of Relative Intensity of Turbulent Velocity and Temperature Fluctuations in a Hot Round Free Jet; (ref. 157).**

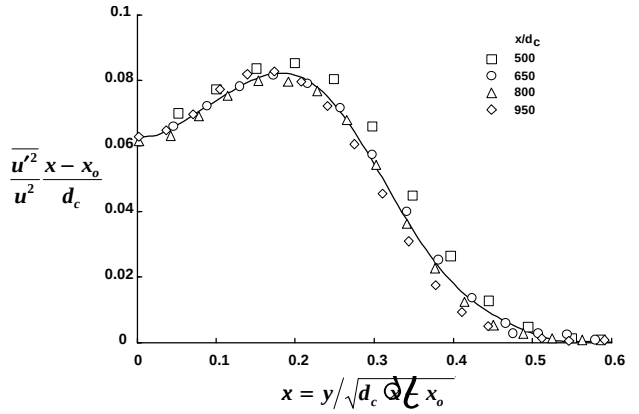


**Figure 34. Relative Turbulence Intensity ($u$-component) in the Wake of a Circular Cylinder; $Re_{d_w} = 1360$; (ref. 43).**

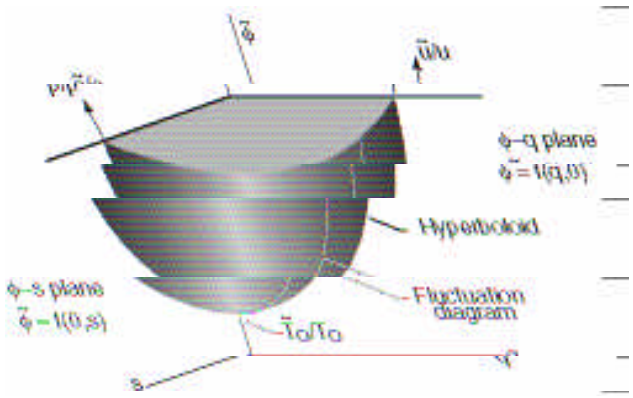


**Figure 35. General Fluctuation diagram for Subsonic Compressible Flow; (ref. 168).**

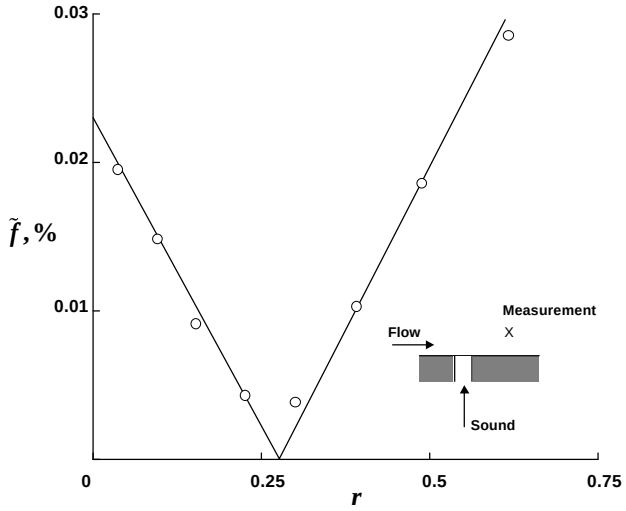


**(a) Disturbances from Single Sound Source**

**Figure 36. Fluctuation Diagram; $M = 0.76$; (ref. 167).**

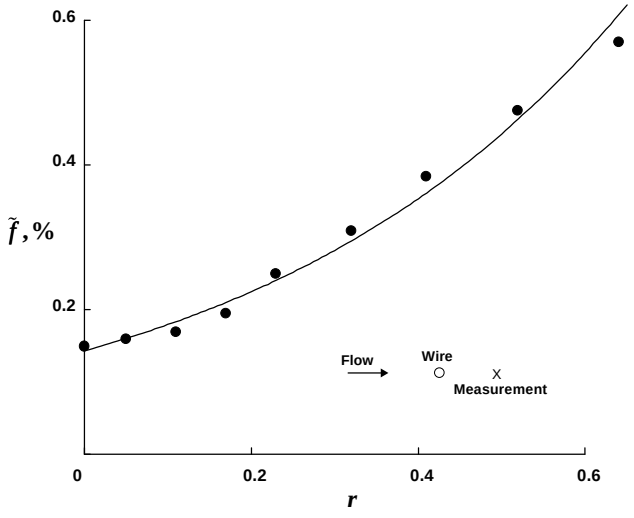


**(b) Combination of Vorticity and Entropy Modes Downstream of a Cylinder**

**Figure 36. Concluded.**

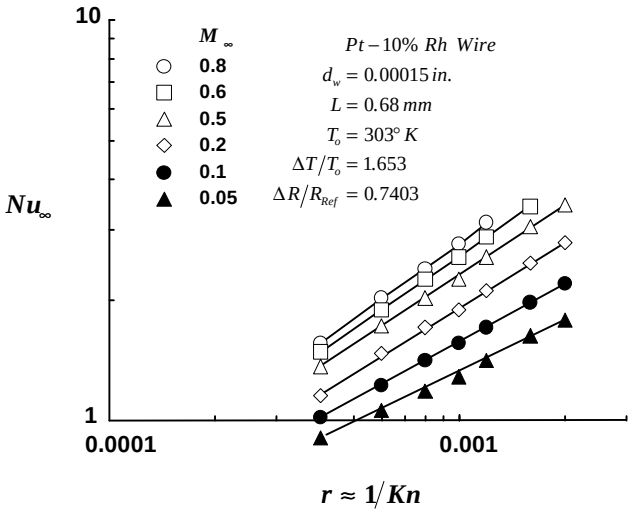


**Figure 37. Nusselt Number as a Function of ; (ref. 110).**

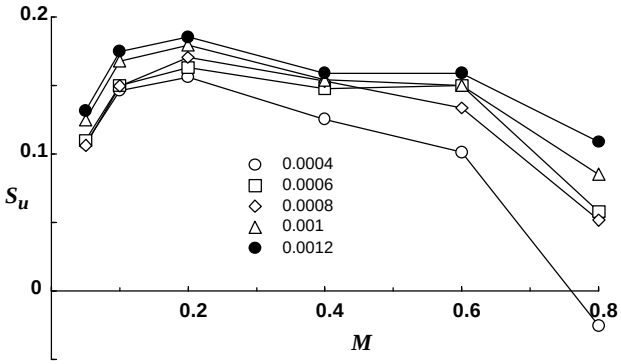


**(a) Velocity Fluctuations;** $T_o = 303° K$**;** $t_w = 0.672$**.**

**Figure 38. Spangenberg Data; (ref. 163).**

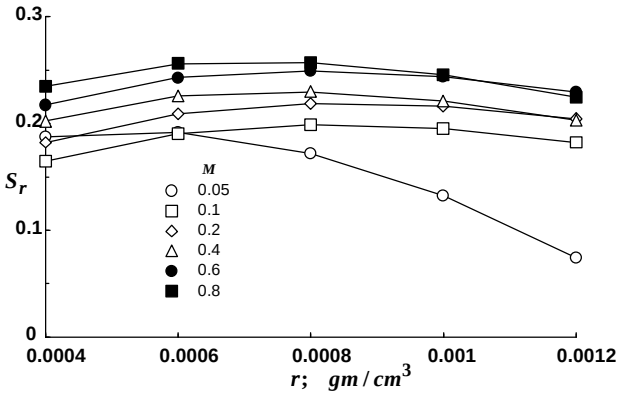


**(b) Density Fluctuations;** $T_o = 303° K$**;** $t_w = 0.672$**.**

**Figure 38. Continued.**

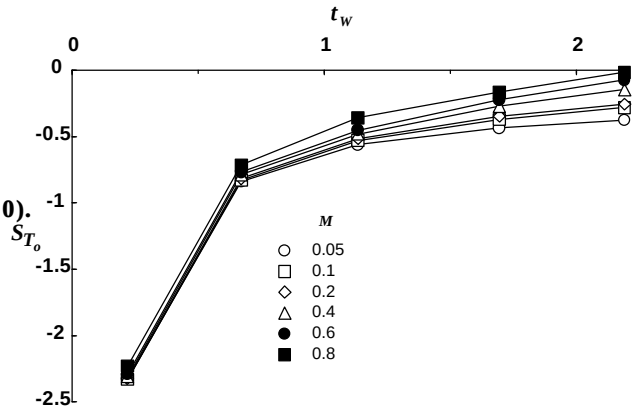


**(c) Total Temperature Fluctuations** $T_o = 303° K$**;** $r = 0.0008\ gm/cm^3$**.**

**Figure 38. Concluded.**

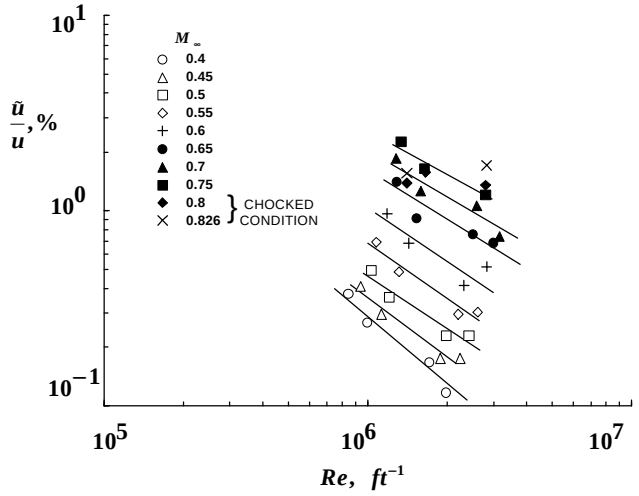


**(a) Velocity Fluctuations**

**Figure 39. Disturbances Measured in the LaRC 8' Transonic Pressure Tunnel using a Three Element Hot-Wire Probe; (ref. 86).**

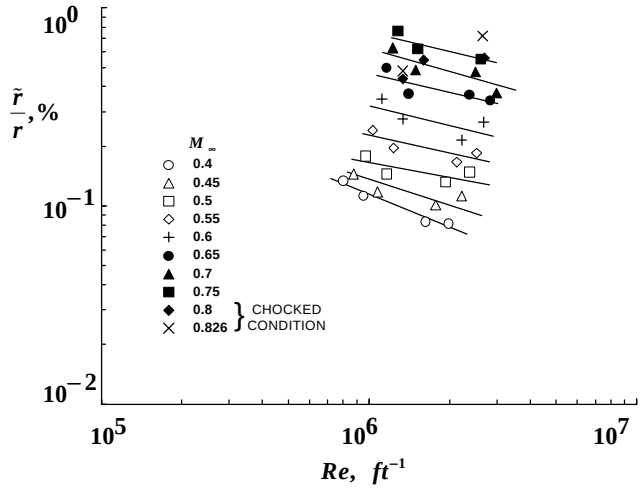


**(b) Density Fluctuations**

**Figure 39. Continued.**

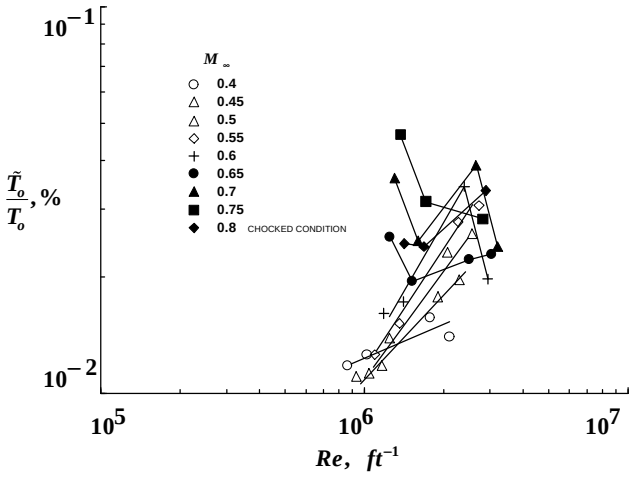


**(c) Total Temperature Fluctuations**

**Figure 39. Continued.**

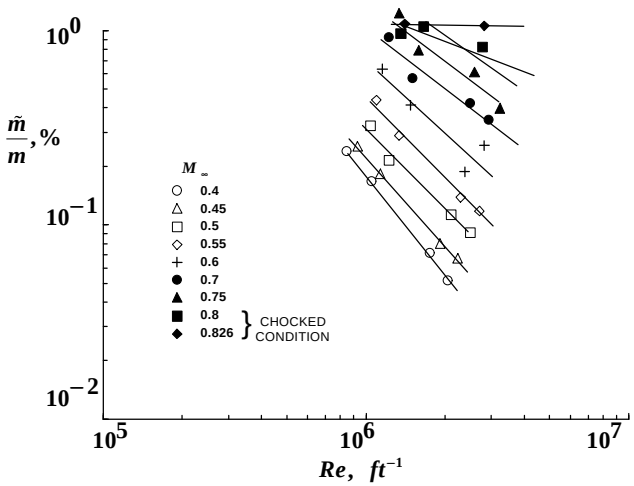


**(d) Mass Flow Fluctuations**

**Figure 39. Concluded.**

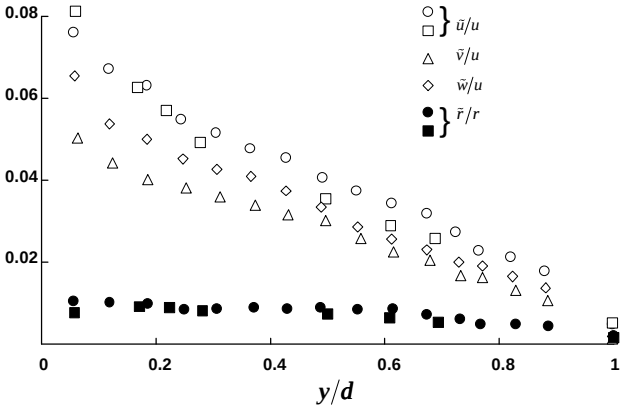


**Figure 40. Normalized RMS Velocity and Density Fluctuation Distribution Across the Boundary Layer; (ref. 170).**

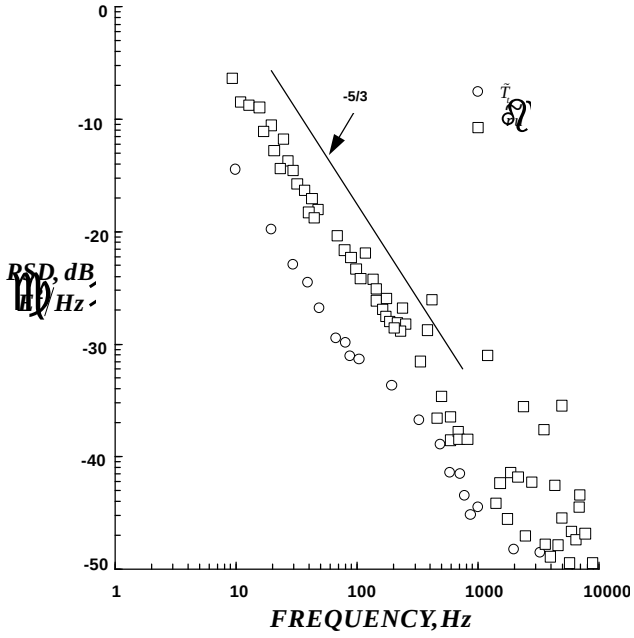


**Figure 41. Spectra of Mass Flux and Total Temperature Fluctuations; 3.6 km; $M = 0.57$; Feb. 79; (ref. 49).**

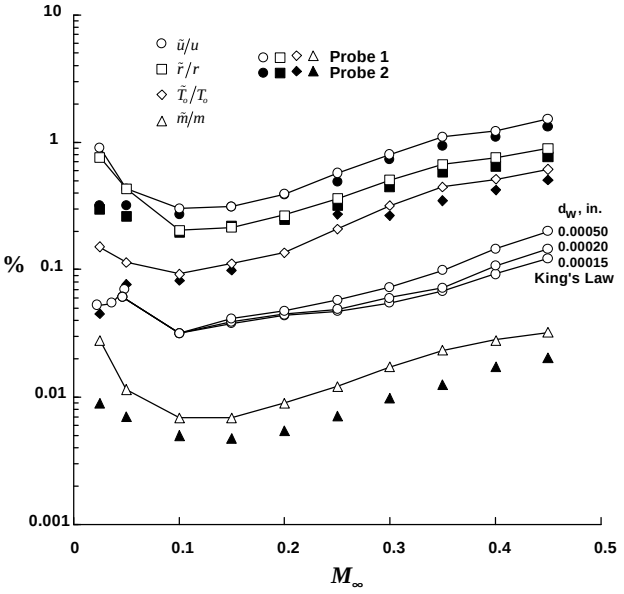


**(a) Measured Fluctuations**

**Figure 42. Fluctuations Measured in the LaRC Low Turbulence Pressure Tunnel; $p_o = 15$ *psia*; (ref. 172).**

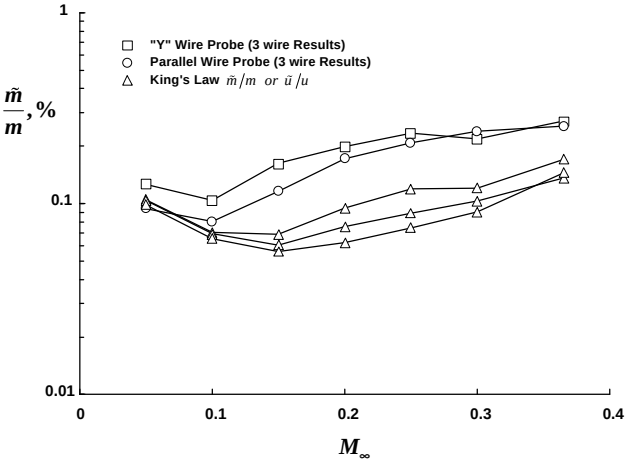


**(b) Mass Flow Fluctuations**

**Figure 42. Concluded.**

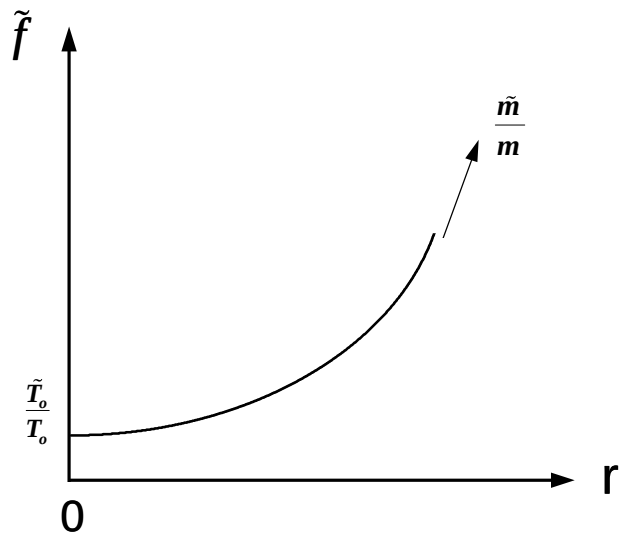


**Figure 43. Generalized Fluctuation Diagram for Supersonic Flow.**

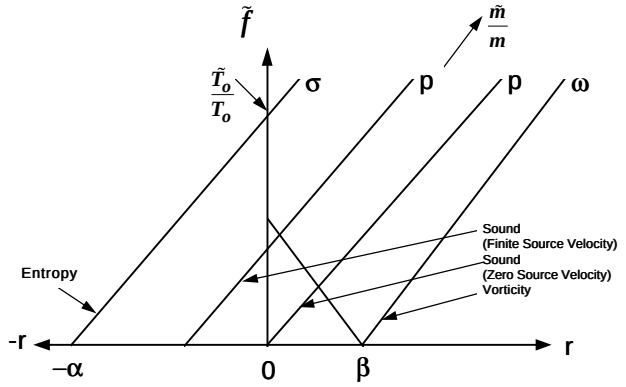


**Figure 44. Generalized Mode Diagram for Supersonic Flow.**

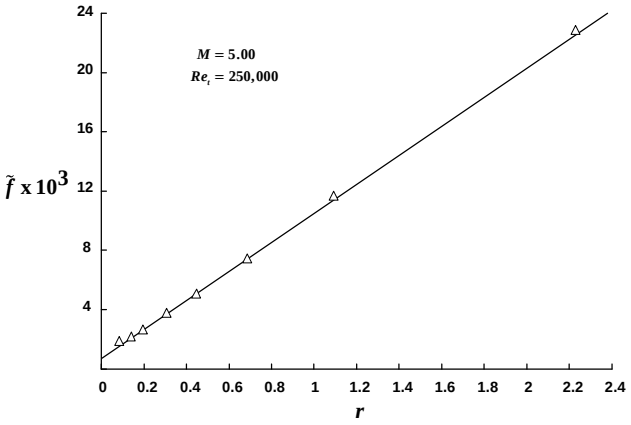


**Figure 45. Mode Diagram Measured in Test Section for $M = 5.0$; (ref. 185).**

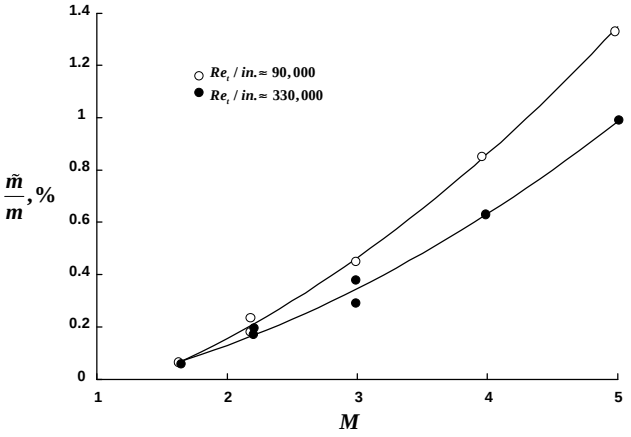


**(a) Mass Flow Fluctuations**

**Figure 46. Variation with Tunnel Mach Number; (ref. 185).**

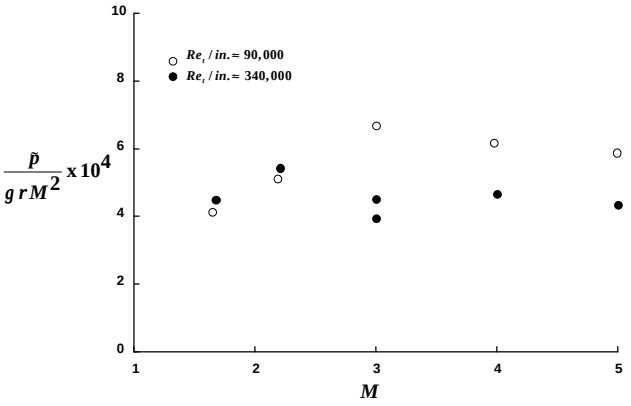


**(b) Pressure Fluctuation**

**Figure 46. Concluded.**

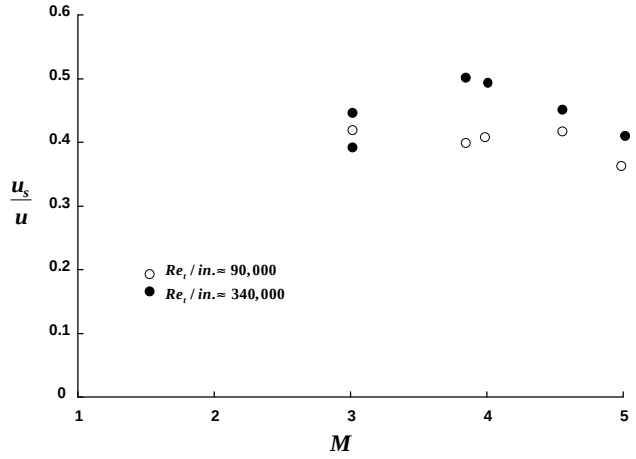


**Figure 47. Variation of Source Velocity with Tunnel Mach Number; (ref. 185).**

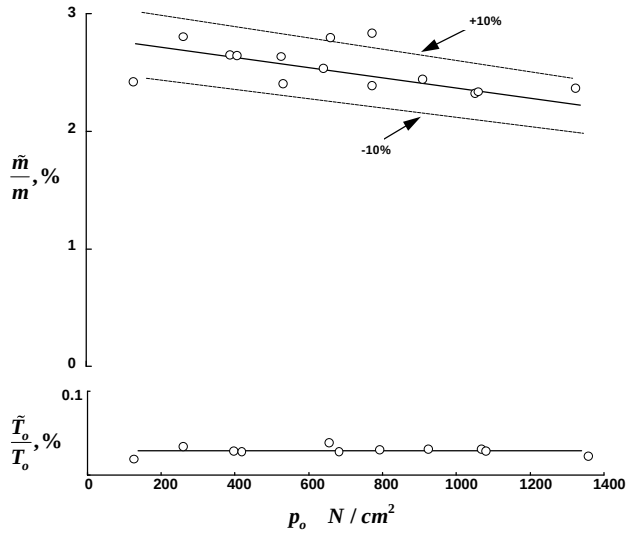


**Figure 48. Root-Mean-Square Mass-Flow and Total-Temperature Fluctuations in the LaRC 22" Hypersonic Helium Tunnel; (ref. 181).**

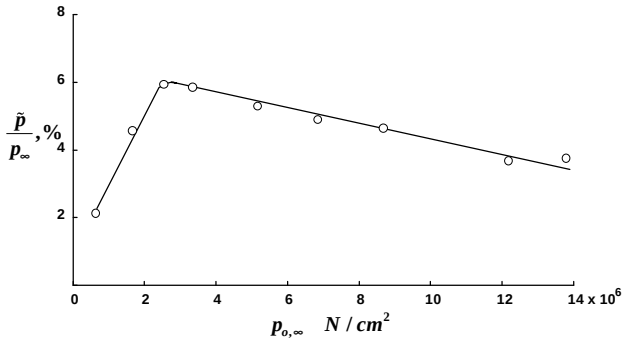


**Figure 49. Pressure Fluctuation in the LaRC 22" Hypersonic Helium Tunnel; (ref. 181).**

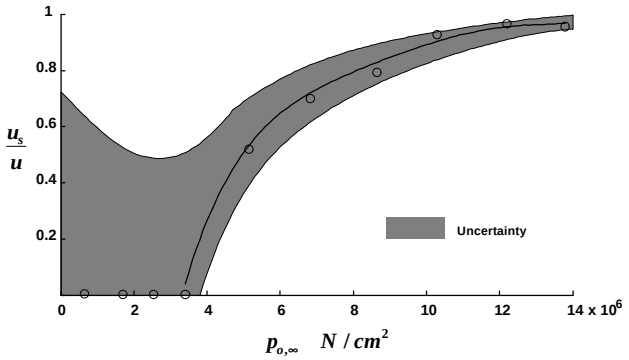


**Figure 50. Relative Source Velocities in the LaRC 22" Hypersonic Helium Tunnel; (ref. 181).**

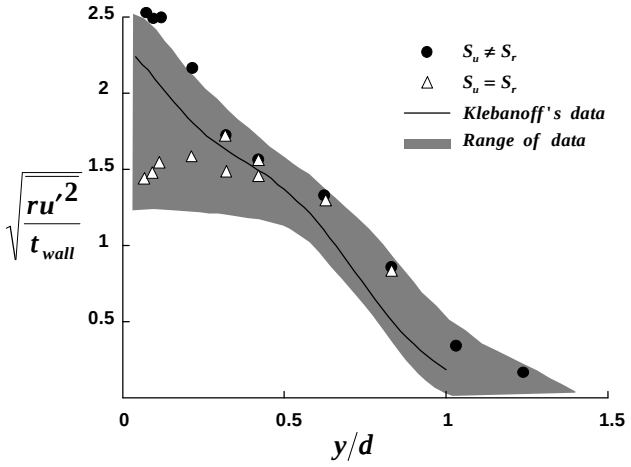


**Figure 51. Velocity Fluctuation Measurements in Boundary Layer; Influence of the Sensitivity Coefficient to Mach Number; Shaded Zone - Range of the Available Velocity Fluctuation Data in Supersonic Boundary Layers, Including Hot-Wire and Laser-Doppler Measurements; (ref. 162).**

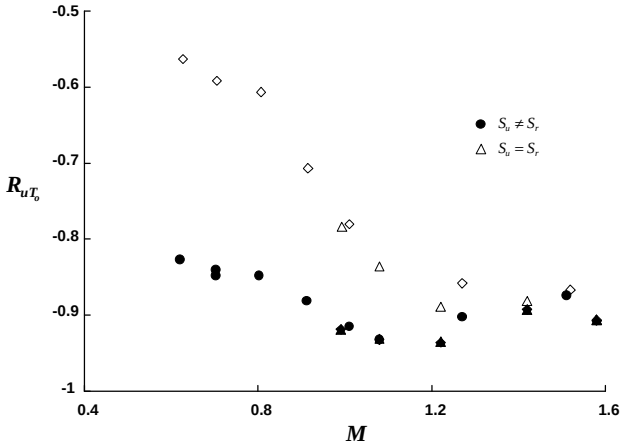


**Figure 52. Variation of $R_{uT_o}$ with Mach Number Through Boundary Layer; (ref. 177).**

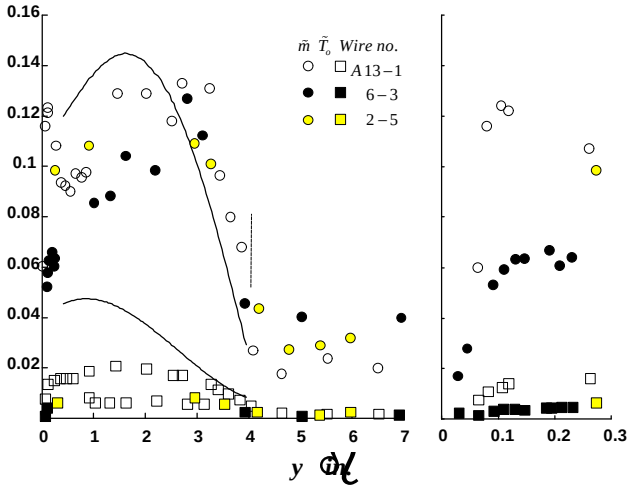


**Figure 53. Variation of Wide-Band RMS Mass-Flux and Total-Temperature Fluctuations Across the Boundary Layer. Kistler's Results at $M = 4.76$ (Solid Line) are Included for Comparison; (ref. 188).**

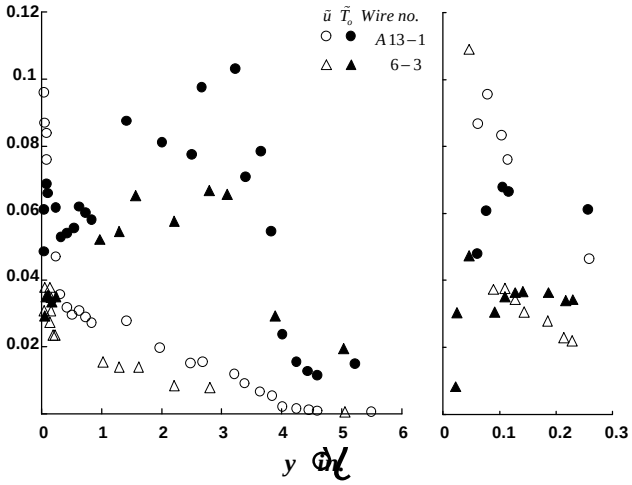


**Figure 54. Variation of Wide-Band RMS Velocity and Static Temperature Fluctuations Across the Boundary Layer; $p' \neq 0$; (ref. 188).**

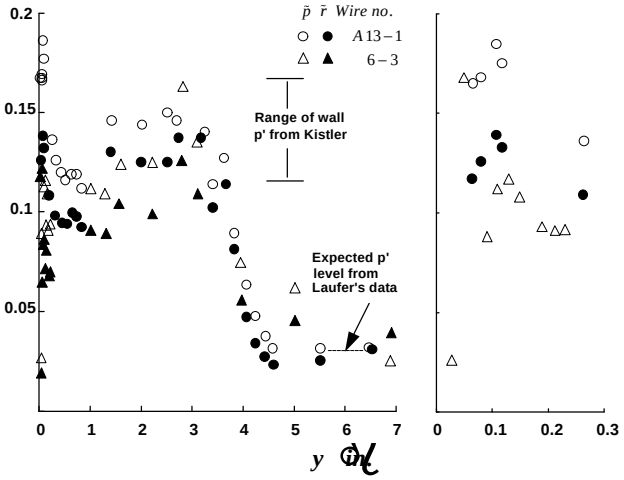


**Figure 55. Variation of Wide-Band RMS Pressure and Density Fluctuations Across the Boundary Layer; $p' \neq 0$; (ref. 188).**

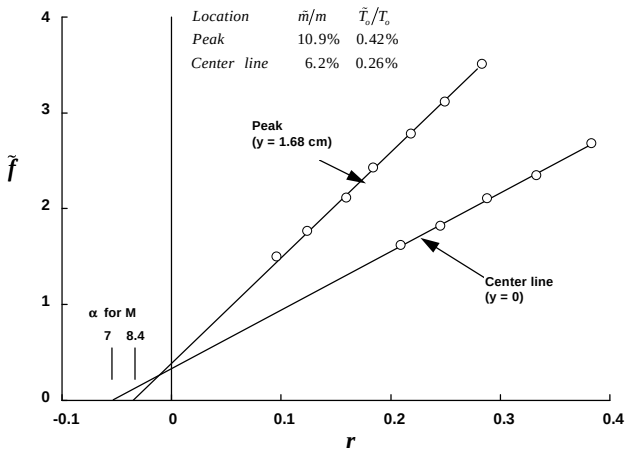


**Figure 56. Mode Diagrams in Wake of 15° Half-Angle Wedge; (ref. 181).**

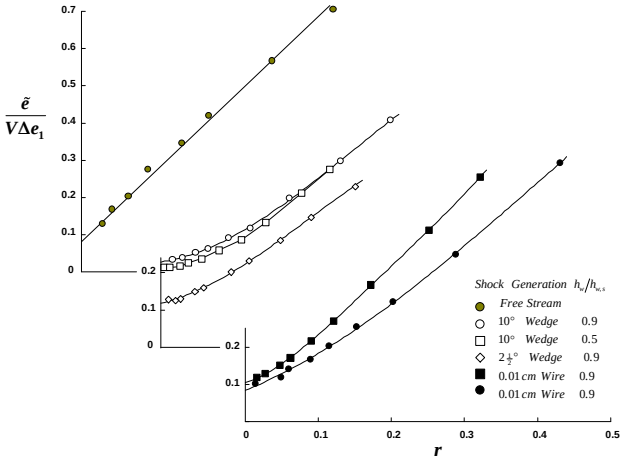


**Figure 57. Fluctuation Mode Plots; $M \approx 21$; $p_o = 12.41 \times 10^6 \quad N/m^2$; (ref. 48).**

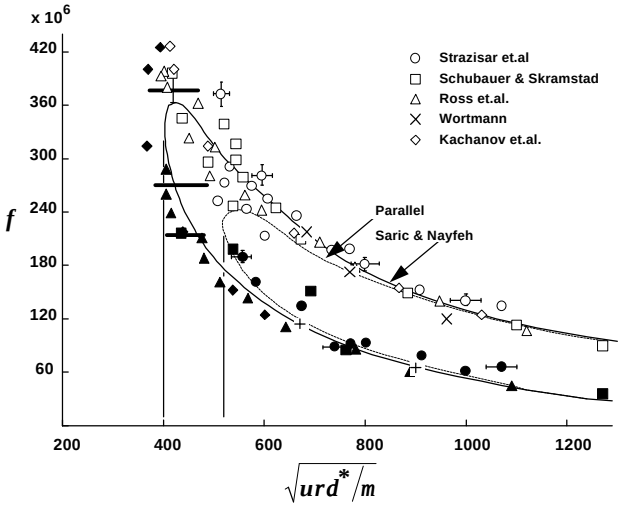


**Figure 58. Neutral Disturbance in Studies of Laminar Boundary Layer Stability; (ref. 205).**

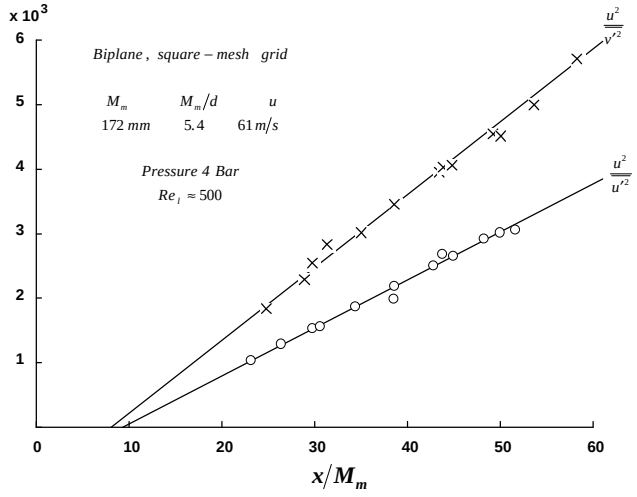


**Figure 59. Decay of $\frac{u^2}{u'^2}$ and $\frac{u^2}{v'^2}$ Downstream of a Grid; (ref. 206).**

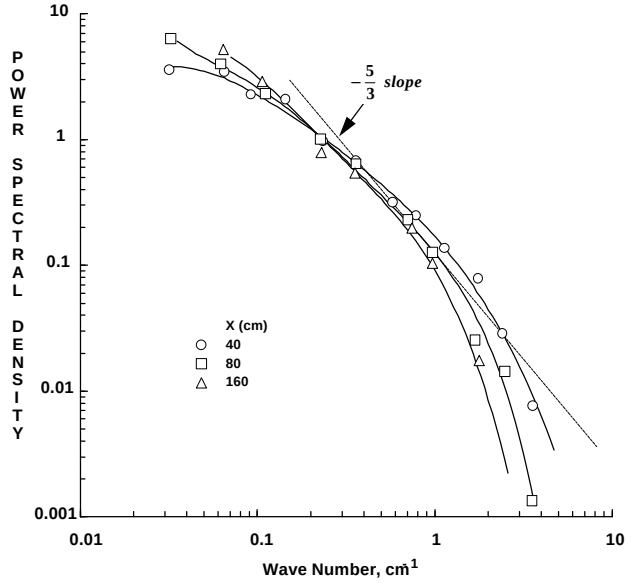


**(a) Poser Spectral Density of $u^2$; $u = 10\ m/s$; (ref. 88)**

**Figure 60. One-Dimensional Spectrum.**

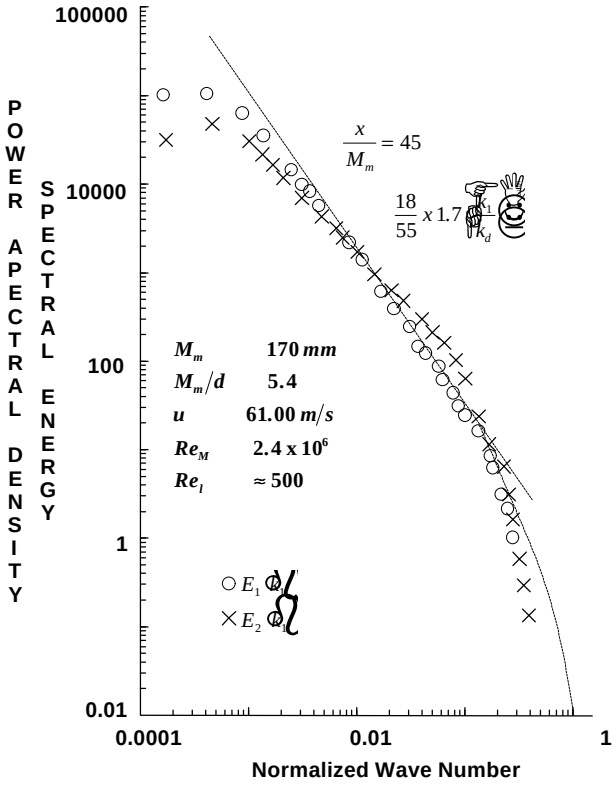


**(b) Spectral Energy; (ref. 206)**

**Figure 60. Concluded.**

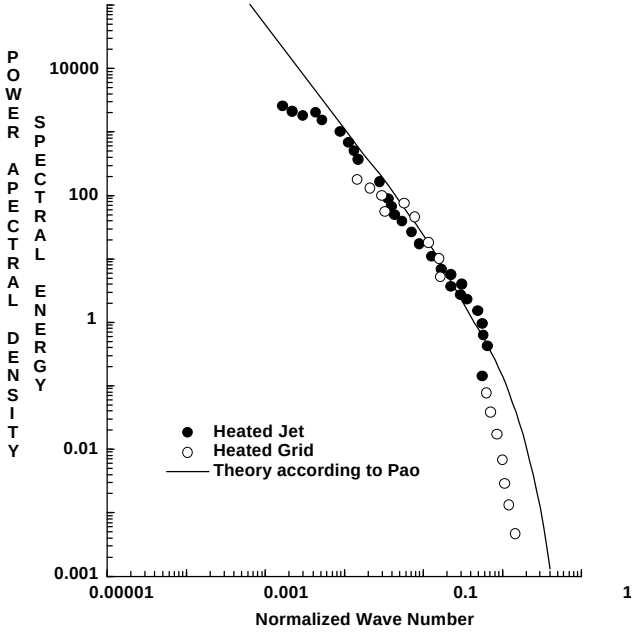


**Figure 61. One-Dimensional Temperature Spectrum; (ref. 207).**

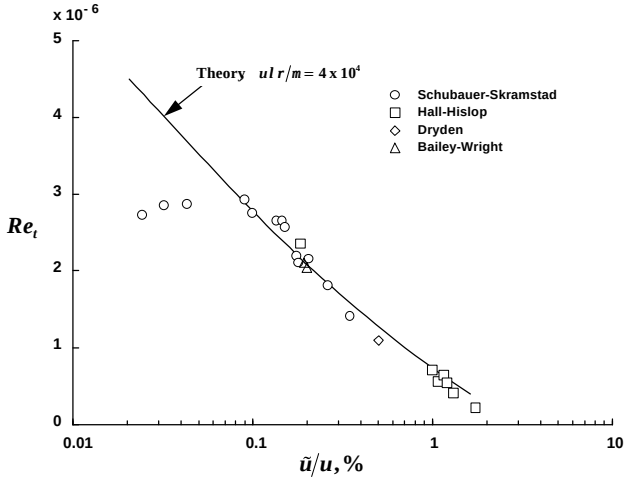


**Figure 62. Effect of Free-Stream Turbulence on Boundary Layer Transition; (ref. 208).**

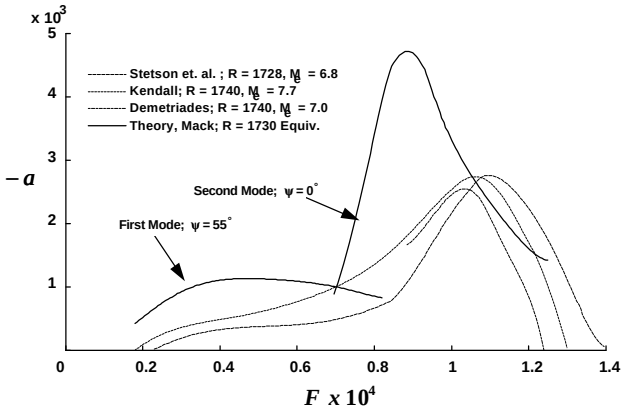


**Figure 63. Amplification Rate vs. Frequency, Comparison with Others; (ref. 209).**

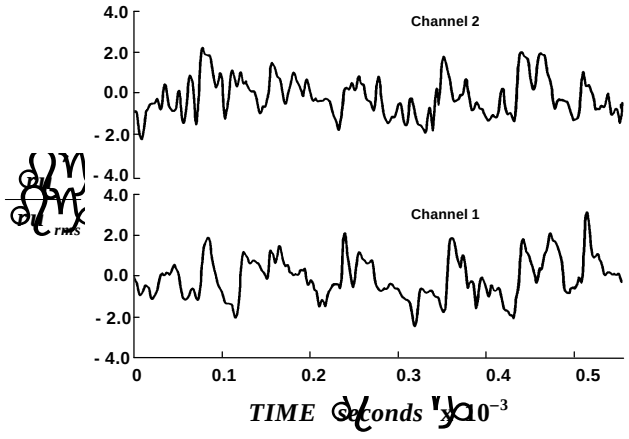


**Figure 64. Typical Fluctuating Mass Flow Data from Two Hot-Wires Indicating Similarity Between the Signals; (ref. 226).**

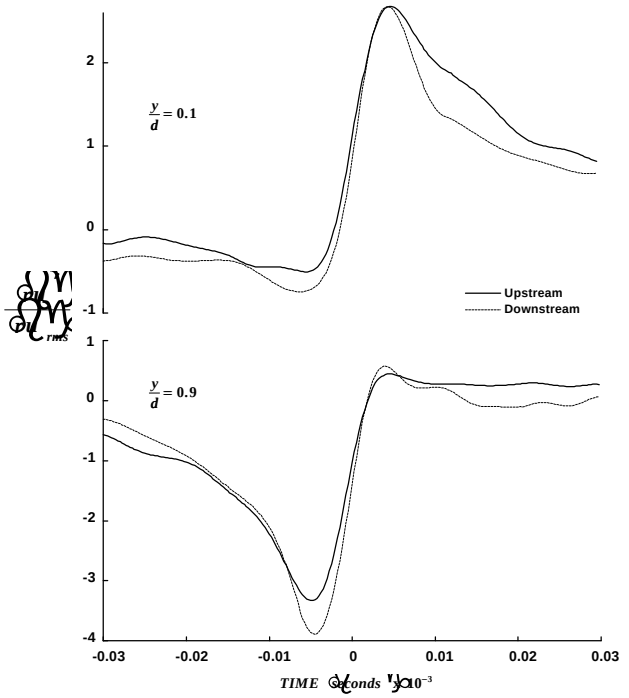


**Figure 65. Ensemble Averaged Positive Events in the Weak Perturbation Case; (ref. 226).**

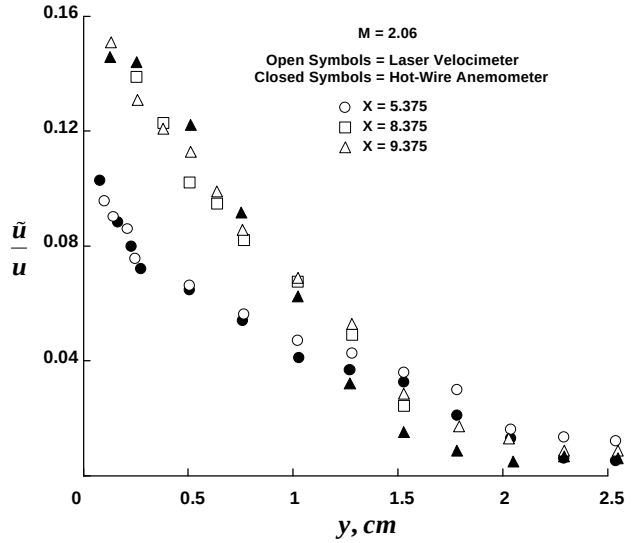


**Figure 66. Comparision of Streamwise Velocity Fluctuations Measured by Hot-Wires and LaserVelocimeter; (ref. 227).**

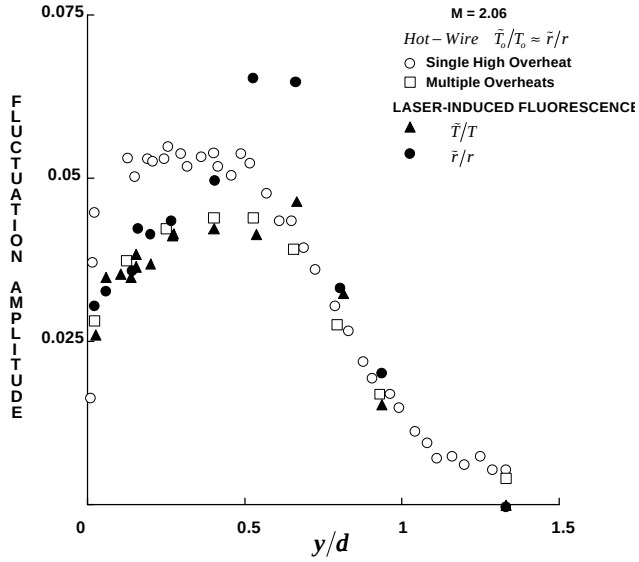


**Figure 67. A Comparison of the Distribution of RMS Fluctuation Amplitudes in Static Temperature and Density within the Boundary-Layer obtained using a Hot-Wire at Single and Multiple Overheat Ratios with Direct Measurements Obtained using Laser-Induced Fluorescence (LIF). The LIF data have been Corrected for Instrument Noise; (ref. 229).**

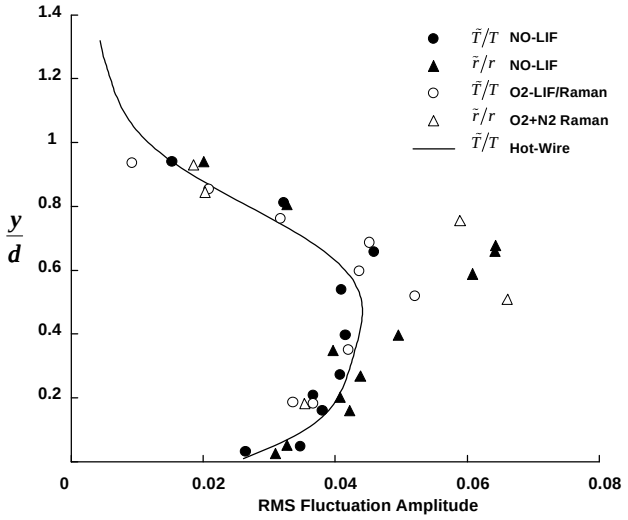


**Figure 68. Comparisons of Temperature and Density RMS Fluctuation Amplitudes Obtained with LIF Techniques or Implied by Hot-Wire Anemometer Data. Flow Conditions are the Same as in Figure 66. For Each Variable, the Fluctuation Amplitude is Normalized by the Local Time-Averaged Value; (ref. 230).**